



Silesian University of Technology
Faculty of Automatic Control, Electronics and Computer Science
Institute of Automatic Control

Active control of sound with a vibrating plate

Doctoral Dissertation

by

Krzysztof Mazur

Supervisor

dr hab. inż. Marek Pawełczyk, prof. Pol. Śl.

November 2013

Gliwice, POLAND

Contents

Acknowledgements	vi
1 Introduction	1
1.1 Sound	1
1.2 Active Noise Control	3
1.3 Structural control	4
1.3.1 Introduction to structural control	4
1.3.2 Vibrating plates	4
1.3.3 Double wall structures	5
1.3.4 Complex structures	5
1.4 Actuators and Sensors	5
1.4.1 Actuators	5
1.4.2 Sensors	6
1.5 Control of sound transmitted through a plate	7
1.5.1 Active control	7
1.5.2 Passive/semi-active control	7
1.6 Overview of classical active control algorithms	8
1.6.1 Feed-forward control	8
1.6.2 Feedback control	9
1.6.3 Notch filters	11
1.6.4 RST controller	12
1.7 Motivation for the research	13
1.8 Objective and Thesis of the dissertation	13
1.9 Contents of the dissertation	13
2 Adaptive linear control	15
2.1 Introduction	15
2.2 Single-channel feed-forward control	16

2.3	Acoustic feedback path neutralization	18
2.4	Multiple outputs	18
2.4.1	Distribution of the control signal to multiple actuators	19
2.5	Experimental verification	22
2.5.1	Laboratory setup	22
2.5.2	Plate and actuators	23
2.5.3	Control system	23
2.5.4	Results of artificial noise reduction	24
2.5.5	Results of Recorded real-world noise reduction	25
2.6	Error signals	27
2.6.1	Multiple-error LMS	27
2.6.2	Selection of error signals	29
2.7	Virtual Microphone Control	32
2.7.1	Experimental verification	34
2.8	Enlarging the zone of quiet	34
2.9	Summary	36
3	Control of sound radiation	40
3.1	Control system	41
3.1.1	Optimal fixed-parameter feed-forward control	41
3.2	Adaptive control with sound radiation measurement	42
3.2.1	Experimental results	44
3.3	Adaptive control with plate vibration measurement	46
3.4	Actuator placement optimization	49
3.5	Summary	50
4	Nonlinear control	54
4.1	Nonlinearity problems in plate control	54
4.2	Internal Model Control	57
4.2.1	Experimental verification	58
4.3	Nonlinear filters	58
4.3.1	NARMA filters	58
4.3.2	Artificial Neural Networks	59
4.3.3	Nonlinear FIR filters	60
4.3.4	Nonlinear FIR filters linear with respect to parameters	60

4.3.5	Hammerstein models	61
4.4	Nonlinear feed-forward control	62
4.4.1	Artificial neural networks	62
4.4.2	Volterra FXLMS	62
4.4.3	FSLMS	62
4.4.4	Nonlinear control with the Hammerstein-like structure	64
4.5	Selection of nonlinear functions	65
4.5.1	Polynomials	65
4.5.2	Chebyshev polynomials	66
4.5.3	Trigonometric expansion	67
4.6	Adaptation of control filter weights	68
4.6.1	Filtered-reference structure	68
4.6.2	Filtered-error structure	68
4.7	Control of sound generation	69
4.8	Application to ANC	71
4.8.1	Experimental verification	71
4.9	Summary	72
5	Two-layer adaptive control	75
5.1	Two-layer active noise controller	76
5.2	Experimental results	78
5.3	Nonlinear ANC with plate controller	79
5.3.1	Experimental verification	82
5.4	Computational complexity analysis	83
5.4.1	Nonlinear control	83
5.5	Summary	83
6	Temperature influence	86
6.1	Introduction	86
6.2	Plate temperature control	86
6.3	Temperature influence on the plate response	88
6.4	Control algorithm	88
6.4.1	FXLMS algorithm convergence	88
6.5	Adaptation of secondary paths	91
6.5.1	On-line secondary path identification	91

6.5.2	Temperature-based gain scheduling	91
6.6	Experimental results	92
6.6.1	Tonal noise reduction	92
6.6.2	Coal mills noise reduction	95
6.7	Summary	96
7	Summary	98
7.1	Conclusions	98
7.2	Author's contribution	99
A	Definitions	100
A.1	Noise reduction level	100
A.1.1	Total noise reduction level	100
A.1.2	A-weighted total noise reduction level	100
A.1.3	Band limited noise reduction level	101
A.1.4	Total Harmonic Distortion	101
	Bibliography	102
	Glossary	113
	Index	115

Acknowledgements

The author would like to thank Professor Marek Pawełczyk for his supervision, guidance and excellent support.

The author would also like to thank members of the Measurement and Control Systems Division for precious comments and friendly atmosphere.

The research has been partially supported by the National Science Centre, under the Grants no. N N514 232037 and DEC-2012/07/B/ST7/01408.

The greatest thanks are to my family for patience and huge support.

Chapter 1

Introduction

1.1 Sound

Sound is a longitudinal, mechanical wave (Halliday *et al.*, 2010). It is usually limited to frequencies that human ear can detect, usually from 20 Hz to 20 kHz. However, the exact frequency range differs between individuals and it also changes with age and adults seldom hear sounds above 10 kHz (Northern & Downs, 2002). Sound propagates through any medium: gas, liquid, solid and plasma. However, due its mechanical vibrations nature, sound cannot propagate through vacuum.

A human ear is sensitive to the sound (acoustic) pressure. In addition to a wide range of frequencies that are heard by a human ear, humans can hear sound with a very wide range of power of dynamics higher than 10^{12} (120 dB). Because the dynamic range of sound is so large the logarithmic SPL (*Sound Pressure Level*) is employed to measure the effective sound pressure. The SPL scale is referenced to the sound pressure $20 \mu\text{Pa}$ (0 dB), which is a typical threshold of human hearing at 1 kHz. The threshold of pain is equal to 63.2 Pa (130 dB). Both the hearing threshold and the perceived loudness depends on the frequency. The dependency is complex and for simplicity a few standardized weighing curves A, B, C, and D have been defined for measurement of the SPL. The A-weighting curve is close to the 40 phone equal loudness curve (SPL 40 dB at 1 kHz) and it is appropriate for measurement of pure tones up to 55 dB SPL. However, it is also widely used for higher SPL and complex signals, and it is commonly used for measurement of industrial and environmental noise and evaluation of a potential hearing damage (Talbot-Smith, 2001).

For humans, sound provides a large amount of useful information about the environment, especially for blind people (Wiciak *et al.*, 2013). It is used for spoken

communication and alerts. Sound, like a music may also provide also enjoyable experience. Because sound is so important, humans since the beginning built devices for generating sound. The important step of evolution of devices, which focus on sound, was the invention of a phonograph in the 1877 by Thomas Edison (Thompson, 1995). The phonograph is a device that records and reproduces sound recordings. Modern systems use loudspeakers for reproduction of sound. To cover a whole frequency range of sound, for high fidelity reproduction multiple speaker drivers are applied to build a common multi-way loudspeaker. Each speaker driver is responsible for reproduction of a limited frequency band. In such systems, the single input signal must be split to multiple control signals, one for each speaker driver. This is usually performed by crossover analog filters. Such classical loudspeakers, however, cannot be used in some harsh environments, common in industry.

In addition to devices, which have been created to generate sound, there are many devices, for which generation of sound is a side-effect. In most cases such sound is unwanted and considered as noise. Low levels of noise are unpleasant and higher levels may cause health problems including permanent damage of hearing ability.

There are many noise reduction methods. Noise can be reduced at a source by modifying devices. However, after some reduction level is obtained, further modifications are very expensive or even unfeasible. Such techniques frequently require significant redesign of the device and may degrade its other parameters. In some cases no other methods can be employed, e.g. for jet engines, where a high bypass ratio allows for using much lower exhaust velocities, which significantly decrease noise emission for the same thrust, at the cost of a significantly larger diameter and weight (Hünecke, 1997).

When noise emission from a device cannot be lowered, passive methods can be employed. Such methods incorporate noise barriers or sound absorbing materials. However, they are ineffective for lower frequencies (Nelson & Elliott, 1993). Additionally, noise barriers might be expensive for some applications.

Another possibility is to employ active control methods. If no other method can be used, the personal hearing protectors can be employed. The classical passive personal hearing protectors have a big disadvantage that the wanted sound is also reduced, but it can be fixed by using active personal hearing protectors that supports verbal communication (Latos, 2011).

1.2 Active Noise Control

In case of linear systems the active control uses superposition of sound to control selected output—sound or vibration.

One of the first documented solutions is a patent granted to Paul Lueg in 1936 (Lueg, 1936). This patent describes a classical one-dimensional ANC (*Active Noise Control*) system for reduction of sound propagated in an acoustic duct. It is a classical feed-forward system. The noise is measured in advance by a microphone and it is later processed by an electronic controller and drive a loudspeaker. The loudspeaker acts as a secondary sound source and generates a wave that interferes with the primary noise. If the control system operates correctly the destructive interference occurs. Lueg also considered active reduction of sound radiated from the primary source in three dimensional space. There are also other justifications to ANC (Nelson & Elliott, 1993).

In 1953, Olson and May proposed an electronic sound absorber that used a feedback control to reduce the sound pressure in the vicinity of a microphone (Olson & May, 1953). The feedback loop consist of a microphone, an amplifier and a loudspeaker. In 1955, sound cancellation was proposed to reduce noise from a transformer (Conover & Ringlee, 1955).

Modern methods for Active Noise Control were developed in the 1980s and 1990s starting with the introduction of an adaptive digital filter (Burgess, 1981) and the FXLMS (*Filtered-reference Least Mean Squares*) algorithm (Morgan, 1980; Burgess, 1981; Widrow & Stearns, 1985).

Active noise reduction in acoustic ducts was widely studied (Zawieska, 1991; Bismor, 1999) and successfully applied to HVAC (*Heating, Ventilation and Air Conditioning*) systems (Larsson *et al.*, 2009b). Another popular application of ANC systems are headphones and earplugs with active noise reduction (Engel *et al.*, 2001; Latos, 2011). Application of active methods were also studied for vehicle cabin noise (Bullmore *et al.*, 1990; Elliott *et al.*, 1990).

ANC systems become also researched in Poland. Initially the research started at the AGH University of Science and Technology in Kraków by a group of scientists around Prof. Zbigniew Engel (Kowal, Gołaś, Sapiński, Batko, Cieślik, Wiciak, Kozupa). Later, research and also development of ANC applications started at the Central Institute for Labour Protection, Warsaw (Zawieska, Makarewicz, Morzyński, Górski), the Silesian University of Technology, Gliwice (Niederliński, Ogonowski,

Mościński, Pawełczyk, Bismor, Figwer, Czyż, Michalczyk, Latos), and the University of Rzeszów (Leniowska, Rdzanek).

1.3 Structural control

1.3.1 Introduction to structural control

Because sound also propagates in structures and frequently it is also generated in structures, control of sound in structures is very important. The field of knowledge, concerned with all vibration and acoustic research is called „vibroacoustics” (Engel, 2010) or „structural acoustics” in the US (Fahy & Gardonio, 2007).

There are three basic topics in the structural control related to reduction of noise:

- reduction of sound generated by the structure. Vibrations are generated in the structure, or transmitted from other structures. This topic is related to the reduction of sound generated by devices.
- reduction of sound transmitted through the structure. The structure can be used as a sound barrier or a casing of the device.
- generation of desired secondary sound for classical Active Noise Control.

This dissertation focuses on control of sound transmitted through the structure. However, the same algorithms can be applied also for other applications, e.g. the problem of generation of desired sound is discussed.

1.3.2 Vibrating plates

The simplest and widely investigated structures are vibrating plates. Plates of different shapes were investigated, including rectangular (Zawieska & Rdzanek, 2007), circular plates (Leniowska, 2006; Rdzanek *et al.*, 2011), triangular plates (Brański & Szela, 2008). Also different sizes of plates were investigated, for instance microplates by Lizhong & Zhentong (2009).

Vibrating plates can be used either as sources of secondary sound for classical active noise control applications, or actuators for active noise-vibration control, or active structural acoustic control (ASAC). Different control strategies can be employed (Hansen & Snyder, 1997; Fahy & Gardonio, 2007; Elliott, 2001; Pietrzko, 2009).

1.3.3 Double wall structures

The acoustic isolation of walls can be improved by employing multiple parallel plates or panels. A typical application of such structures is multiple-glazed windows (Tadeu & Mateus, 2001). A double-wall system can be controlled like two single plates, but additional possibilities exist. Helmholtz resonators can be placed in the cavity between plates (Mao & Pietrzko, 2005). For active control a loudspeaker can be placed between plates (Pietrzko, 2009).

1.3.4 Complex structures

More complex structures are also investigated in literature. The most popular structures are built from multiple plates, e.g. joined rectangular plates (Wiciak, 2008) or a box built from plates (Liu *et al.*, 2010; Pawełczyk, 2013). Such simple shapes allow for easier analysis, but they also are commonly used in real devices casings (Rdzanek & Zawieska, 2003). However, also applications for more complex shapes, such as car engines (Ringwelski *et al.*, 2011a,b), have been recently investigated.

1.4 Actuators and Sensors

1.4.1 Actuators

Figure 1.1 presents popular actuators for plate vibrations control: piezoelectric actuators (PZT and MFC) and electrodynamic actuators. The main advantage of piezoelectric actuators is a high power-to-weight ratio.



Figure 1.1: Different type of actuators, EX-1 electrodynamic actuators (left), PZT patches (center) and MFC patches (right).

MFC actuators

Recently, a new type of piezoelectric actuators, Macro-Fiber Composites (MFC) (Material, 2010), is gaining scientific interest (Staniek & Pawełczyk, 2008; Górski & Kozupa, 2012). MFC actuators have smaller thickness and mass, than PZT actuators, with the same blocking force.

MFC actuators utilize one of two effects: d31 or d33. The d31-effect MFCs are contractors. They operate in the voltage range of -60 V to 360 V and contract up to 750 ppm (Material, 2010). The d33-effect MFCs are elongators. They elongate up to 1800 ppm. They provide higher a power-to-weight ratio, but at cost of much higher power supply voltage and nonlinear response. They operate in the voltage range of -500 V to 1500 V.

Because the d33-effect actuators provide a better power-to-weight ratio, they are usually employed as actuators. Typical applications of d31-effect MFCs are strain sensors and energy harvesters.

The d33-effect MFC actuators are employed for most of experiments in this dissertation.

EX-1 actuators

Because applied MFCs actuators have nonlinear response (Stuebner *et al.*, 2009) for some experiments EX-1 electrodynamic actuators are employed to verify that the problems are not specific to MFC actuators. Table 1.1 presents basic parameters of EX-1 actuators.

Table 1.1: Parameters of EX-1 electrodynamic actuators.

Parameter	Value	Unit
Diameter	70	mm
Thickness	19	mm
Mass	115	g
Power	5	W

1.4.2 Sensors

In AVC and AVC applications microphones and accelerometers are commonly used. However, recently, for vibration control, piezoelectric sensors, e.g. PVDF (Pietrzko,

2009; MEAS, 2008), MFC (Material, 2010), are becoming more popular. Such sensors measure strain and are more sensitive for low frequencies than accelerometers. They also measure average over a larger area, not only at single point, which provides advantages for some control strategies.

1.5 Control of sound transmitted through a plate

1.5.1 Active control

Different methods can be employed for active control of sound transmission through a plate (Hansen & Snyder, 1997; Fahy & Gardonio, 2007; Elliott, 2001).

The basic method for reduction of sound transmitted through a plate is AVC (*Active Vibration Control*). The goal of the control system is to minimize the measured plate vibrations.

The goal of the ANVC (*Active Noise/Vibration Control*) control systems is to minimize the error signal from microphones by using actuators mounted on a plate (Fahy & Gardonio, 2007). In this dissertation such systems will be called ANC systems.

1.5.2 Passive/semi-active control

The plate vibrations can also be reduced passively by mechanical vibration absorbers (Carneal *et al.*, 2004) or shunt systems (Tawfik & Baz, 2004; Pietrzko, 2009). In shunt systems the vibration energy is converted into electrical energy, which is later dissipated in resistors. The performance can be improved by using RLC circuits tuned for a specific frequency band. Further improvements can be made by employing semi-active control by switching specific circuits with semiconductor keys.

Semi-active methods are usually applied for AVC systems (Kowal, 1990). However, in recently developed systems with energy recovery (Kowal & Kot, 2007; Kowal *et al.*, 2008), recovered power could also be employed for active noise control.

1.6 Overview of classical active control algorithms

1.6.1 Feed-forward control

Amplitude and phase adjuster

ANC applications usually employ the feed-forward structure (Figure 1.2). P stands for the primary path representing the acoustic space between the reference signal and the error microphone. The primary noise $x(i)$ is filtered by the primary path resulting in the primary noise at the point of interest $d(i)$. The primary noise is measured by the control system, usually by the reference microphone and later processed by the controller. The result is the control signal $u(i)$. S is the secondary path with the control signal being the input and the error signal as the output. The secondary path output $y(i)$ interferes with the primary noise $d(i)$ at the point of interest, resulting in $e(i)$. When the desired sound is silence the $e(i)$ is the error signal.

This structure was used by Lueg in the first ANC-related patent (Lueg, 1936). In early applications the signal from the microphone was filtered by a carefully designed analog continuous-time filter, and then used to drive a loudspeaker. The amplitude gain and the phase delay for each frequency must be set appropriately to obtain destructive interference with the primary noise.

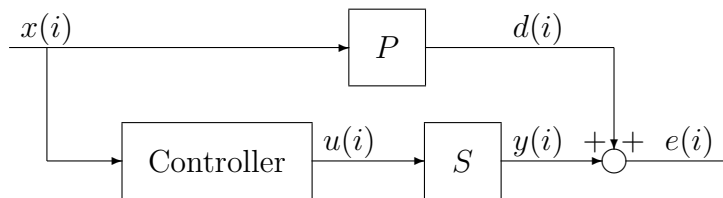


Figure 1.2: Feed-forward system structure.

For simple applications, where the secondary path can be approximated with pure delay and gain, or for tonal signals simple amplifier with phase delay can be employed for the feed-forward control.

The big advantage of non-adaptive feed-forward control is that, when the plant is stable and the controller is stable (easy to achieve for non-adaptive controllers) the control system is always stable.

Optimal feed-forward control

When models of the primary and secondary paths are known, an optimal filter can be designed. Such filter is usually designed as a discrete-time filter using the Wiener

approach.

When the Power Spectral Density (PSD) of noise is not known or noise is non-stationary the idea of the generalized disturbance can be applied (Latos & Pawełczyk, 2009; Latos, 2011). The spectrum of the noise signal can be assumed and the optimal filter can be designed.

Adaptive feed-forward control

When the plant is non-stationary, which is common for ANC, the adaptive control can be utilized.

The adaptive feed-forward system may also provide better performance compared to the fixed-parameter system for non-stationary noise. Because the adaptive control filters have predictive properties improvements are huge for predictive signals, e.g. tonal or multi-tonal.

1.6.2 Feedback control

Classical feedback control

Classical feedback control theory can also be employed for active control. Classical feedback systems can be effective, when the delay in the secondary path is small, e.g. in vibration control, or when the distance between loudspeaker and the point of interest is small (Olson & May, 1953).

When compared to the feed-forward control system, the feedback system uses the error signal instead of the reference signal, so during operation the number of required sensors is the same (Figure 1.3). However, in the feed-forward system the model of the secondary path must be precisely known. Because feedback systems use a real error signal they are more robust, and small plant changes are compensated by the negative feedback loop. For larger changes, special care must be taken to ensure stable operation.

In AVC systems the optimal LQG (*Linear-Quadratic-Gaussian*) control is very popular (Leniowska, 2005, 2006). The LQG control is based on the state-space representation of the system (e.g. Athans, 1971):

$$\begin{cases} \frac{d\mathbf{x}(t)}{dt} = \mathbf{A}\mathbf{x} + \mathbf{B}\mathbf{u}(t) + \mathbf{G}w(t) \\ \mathbf{y}(t) = \mathbf{C}\mathbf{x}(t) + v(t) \end{cases}, \quad (1.1)$$

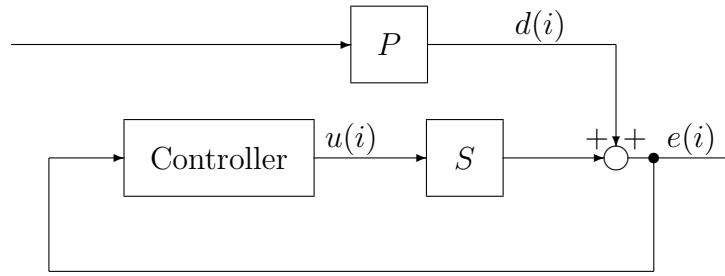


Figure 1.3: Feedback system structure.

where $\mathbf{G}w(t)$ stands for the state noise, and $v(t)$ is the measurement noise. It is assumed that both are stationary white processes.

The LQG controller minimizes the expected value of the following cost function (Athans, 1971):

$$J = \mathbf{x}^T(T)\mathbf{F}\mathbf{x}(T) + \int_t^T [\mathbf{x}^T(\tau)\mathbf{Q}\mathbf{x}(\tau) + \mathbf{u}^T(\tau)\mathbf{R}\mathbf{u}(\tau)] d\tau, \quad (1.2)$$

where \mathbf{F} , \mathbf{Q} and \mathbf{R} matrices are parameters of the LQG regulator, and the T is the final time (horizon). The final time is usually infinite, and the cost related to the final state (\mathbf{F} matrix) is ignored.

Very important application of simple feedback algorithms in AVC is smart panels, where very simple decentralized SISO (*Single-Input Single-Output*) controllers are employed for control of sound transmission (Gardonio *et al.*, 2004). For typical case, when the sensors and actuators are collocated, a simple velocity feedback can be applied. More complex feedback must be employed for non-collocated case. The performance of the system with a large number of simple feedback controllers can be comparable to the optimal MIMO (*Multiple-Input Multiple-Output*) LQG controller (Petitjean & Legrain, 1996).

IMC

IMC (*Internal Model Control*) is a structure of the feedback control system that can be used for plants with high delays, like ANC systems (Figure 1.4). This structure can be used with different control algorithms, including algorithms used for adaptive feed-forward control, because such system estimate the reference signal (Pawelczyk, 2005).

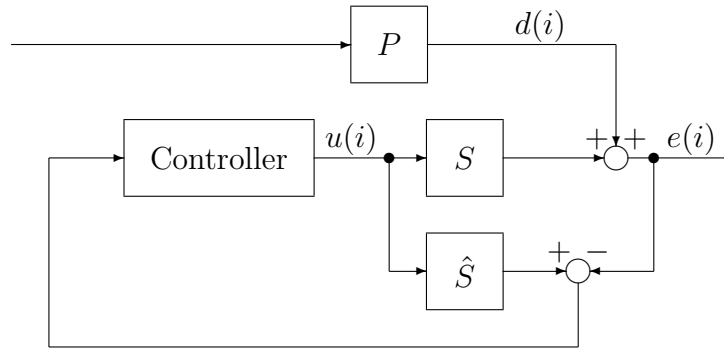


Figure 1.4: Internal Model Control system structure.

1.6.3 Notch filters

In many applications, e.g. most rotary machines, the noise is tonal or multi-tonal. For such applications the virtual reference from a generator can be used. For instance Notch filters, which operate on two sinusoidal signals with a shifted phase, can be applied (Kuo & Morgan, 1996). The phase shift is usually equal to $\frac{\pi}{2}$.

In the simplest case for a single tone, two reference signals are generated by the generator:

$$\begin{cases} x_1(t) = \sin(2\pi ft + \varphi_0) \\ x_2(t) = \cos(2\pi ft + \varphi_0) \end{cases}, \quad (1.3)$$

where f is the frequency of the tonal disturbance, and φ_0 is the initial phase, which can be utilized for phase synchronization in a non-adaptive version. For an adaptive version the initial phase is not needed.

The control signal from the controller is a weighted sum of reference signals:

$$u(t) = w_1 x_1(t) + w_2 x_2(t). \quad (1.4)$$

Because the output is linear with respect to parameters w_i , the LMS algorithm or its modifications can be employed for adaptive control. Such approach can successfully be applied for reduction of sound transmission through a plate (Górski & Kozupa, 2012).

For applications, where the frequency of the signal is not constant or not known, a modified notch filter can be employed (Górski & Morzyński, 2013):

$$u(t) = w_1 \sin(w_3 t) + w_2 \cos(w_3 t). \quad (1.5)$$

The modified Notch filter is nonlinear with respect to the parameter w_3 . More com-

plex adaptation algorithms must be employed to update its parameters, e.g. genetic algorithms.

1.6.4 RST controller

Another popular group of algorithms employs a generalized linear discrete-time RST controller (Figure 1.5) (Niederliński *et al.*, 1995). In this figure $\frac{B(z^{-1})}{A(z^{-1})}$ is a plant model, where z^{-1} is the one-sample delay operator. $R(z^{-1})$, $S(z^{-1})$ and $T(z^{-1})$ are polynomials, $w(i)$ is the desired output. For ANC and AVC the desired output is usually equal to zero, $w(i) = 0$.

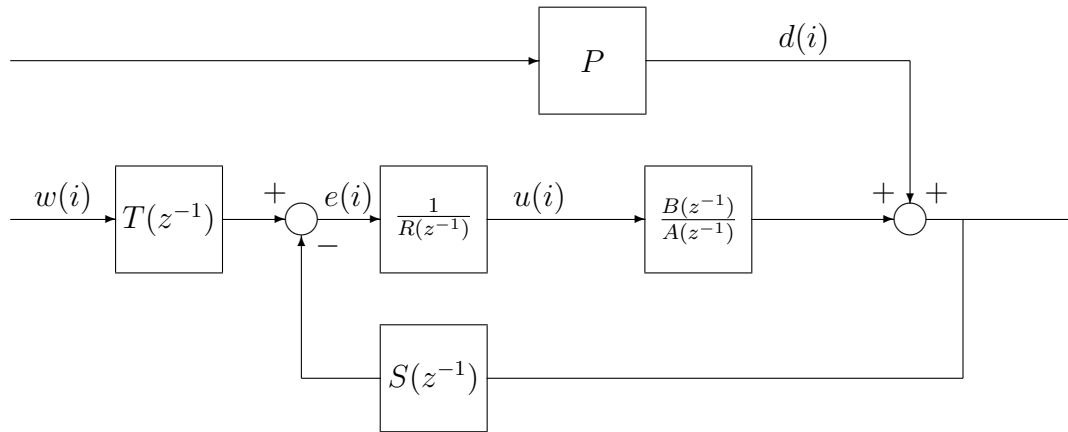


Figure 1.5: RST control system structure.

There are many different control algorithms that utilize the RST control system structure, including MVC (*Minimal Variance Control*), PP (*Pole Placement*) and PZP (*Pole-Zero Placement*).

There are two possibilities for adaptation of RST controllers. $R(z^{-1})$, $S(z^{-1})$ and $T(z^{-1})$ polynomials can be directly estimated, or the plant model can be identified, and then $R(z^{-1})$, $S(z^{-1})$ and $T(z^{-1})$ can be calculated from the model using an appropriate algorithm. The calculation of regulator polynomials from the model usually is performed by solving a controller Diophantine equation. For greater speed, required for AVC systems, a symbolic solution can be utilized (Leniowska, 2011).

Because such algorithms have a higher complexity than the FXLMS algorithm, they are not popular in ANC applications. However, they can be employed for AVC, e.g. vehicle suspension (Konieczny & Kowal, 2005), vibrating plates (Leniowska, 2011), where the number of required coefficients in control filters is smaller.

1.7 Motivation for the research

Because of many unsolved problems, the number of applications of ANC systems, especially in an industrial environment, is still small. Classical loudspeakers are bulky, heavy and cannot be applied in harsh industrial environments. For such applications the sound source is subject to dust, high temperature, high humidity or precipitation. In most cases, the sound source cannot be moved to a less harsh area and more resistant sound sources are needed. Vibrating plates are one of potential alternatives. Such resistant sound sources can also be useful for other problems including the generation of voice messages and alarms in an industrial environment.

Vibrating plates are also useful as active sound barriers. Such applications have been discussed in literature, but the number of applications is still small. One of the interesting potential application of plates as barriers is device casings.

A single vibrating plate can also operate both as an active barrier and a sound source for cancellation of other noise sources. Such operation mode might be useful in industrial halls, where the number of devices is high and adding an active barrier around every noisy device is unfeasible or when some holes in the casing must exist, because of technological limitations.

1.8 Objective and Thesis of the dissertation

The objective of the dissertation is to develop control algorithms for active control of sound with a vibrating plate. The main thesis is formulated as:

Nonlinear adaptive control of plate vibrations, together with equalization of frequency response, compensation of temperature influence and with control signal distribution to multiple actuators allows for increasing the reduction level of noise propagating through the plate, when compared to classical linear active control systems.

1.9 Contents of the dissertation

This dissertation consist of seven chapters. The first chapter contains the introduction.

In Chapter 2 adaptive feed-forward algorithms are applied for active control. Different control strategies, including minimization of plate vibrations, and minimization

of acoustic signal from error microphones, are compared. To minimize the SPL at a selected area, without using error microphones, the idea of VMC (*Virtual Microphone Control*) is applied.

In Chapter 3 the problem of sound radiation control for a plate is discussed. Adaptive feed-forward control algorithms are applied, based on the measurement of radiated sound or measurement of plate vibrations. A simple experimental method, similar to VMC, is applied to provide sound radiation control based on accelerometer sensors.

In Chapter 4 a plate nonlinearity is discussed and adaptive feed-forward algorithms with nonlinear control filters are presented. Algorithms are applied both for Active Noise Control and control of sound radiation from a plate.

In Chapter 5 the idea of two-layer adaptive control is presented. Slightly modified algorithms for control of sound radiation from a plate are applied to change vibrating plate into a simplified SISO (Single-Input Single-Output) plant, and then algorithms for ANC are applied to the new plant.

In Chapter 6 the influence of the temperature of a plate, on the plate response and the performance of ANC systems is investigated. The problem of the convergence of the FXLMS adaptive algorithm is discussed.

In Chapter 7 conclusions and author's contribution are presented.

In Appendix A contains definitions of various performance indices.

Chapter 2

Adaptive linear control

2.1 Introduction

ANC systems for noise reduction in rooms usually exhibit high delays in the secondary path. This significantly reduces the obtained reduction of broadband noise in feedback systems, so the feed-forward structure is commonly used.

Feed-forward systems are very sensitive to changes of plant parameters. For vibroacoustical systems one of the primary source of changes are changes of the acoustic environment geometry, objects can be moved and change the boundary conditions. In such case, adaptive algorithms, e.g. FXLMS, should be used. Additionally, if the goal of the control system is to create zones of quiet around moving objects, further problems arise. If the area, where object may move is very small, the FXLMS algorithm might be sufficient, but for larger changes the FXLMS algorithm with on-line secondary path estimation can be used (Michalczyk, 2004).

In practical applications, even a higher level of adaptation that can be implemented in a higher layer might be useful. In some systems, the number of objects may change in time and the system must be able to adapt to such conditions (Watrás & Pawełczyk, 2011b). Additionally, if objects move over very large areas like in industrial halls, the system must adapt its structure (Pawełczyk, 2012).

There are also other sources of changes of plant parameters, including changes of environmental conditions, such as temperature, humidity or pressure. The change causes a change in wave propagation, e.g. the speed of sound, but also a change in the properties of secondary sound sources and analog electrical elements.

For some ANC applications such as active earplugs, the changes are small enough, so fixed-parameter feed-forward systems can be successfully used (Pawełczyk *et al.*,

2011c; Latos, 2011). However, even in such applications some kind of adaptation, e.g. adaptation to the direction of primary sound (Latos, 2011; Pawełczyk *et al.*, 2011b) might be beneficent.

2.2 Single-channel feed-forward control

The Filtered-reference Least Mean Squares (FXLMS) algorithm is the most popular adaptive feed-forward algorithm used for active noise control. The classical single-channel FXLMS control system is presented in Figure 2.1. In this figure, $x(i)$ is the reference signal, $r(i)$ is the filtered-reference signal, $e(i)$ is the error signal, W is the control filter, X is the reference path, and the symbols with hats stand for models of respective paths.

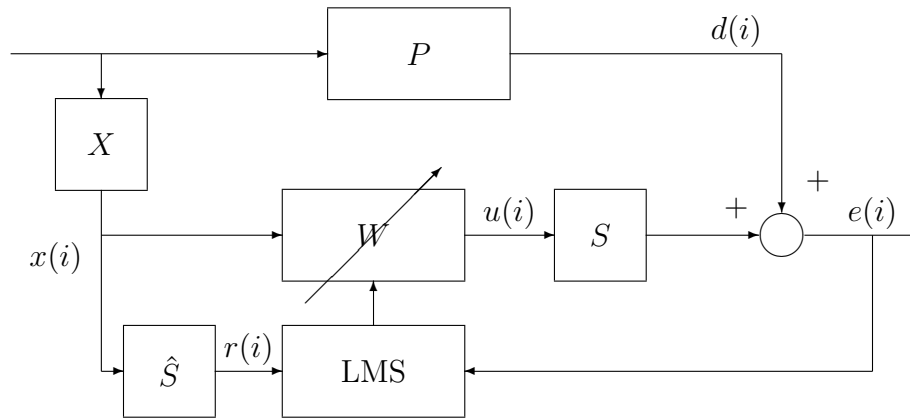


Figure 2.1: A single-channel FXLMS ANC system.

The control signal at the $(i + 1)$ -th sample, $u(i + 1)$, is equal to:

$$u(i + 1) = \mathbf{w}(i)^T \mathbf{x}_u(i), \quad (2.1)$$

where $\mathbf{w}(i) = [w_0(i), w_1(i), \dots, w_{N-1}(i)]^T$ is a vector of parameters of the Finite Impulse Response (FIR) control filter and $\mathbf{x}_u(i) = [x(i), x(i - 1), \dots, x(i - (N - 1))]^T$ is a vector of regressors of the reference signal.

The plain LMS algorithm assumes that the filter output is directly added to the error signal. It is true when the LMS algorithm is used for adaptive filtering, for instance for speech enhancement (Pawełczyk *et al.*, 2011a), and not for controlling a plate. However, for control, an additional path, the secondary path, is present between the output of the adaptive filter and the error signal. To provide convergence,

the algorithm must be modified. The FXLMS algorithm is a popular modification. In FXLMS the reference signal is filtered by a model of the secondary path:

$$r(i) = \hat{\mathbf{s}}(i)^T \mathbf{x}(i), \quad (2.2)$$

where $\hat{\mathbf{s}}(i) = [\hat{s}_0(i), \hat{s}_1(i), \dots, \hat{s}_{M-1}(i)]$ is a FIR model of the secondary path and $\mathbf{x}(i) = [x(i), x(i-1), \dots, x(i-(M-1))]^T$ is a vector of regressors of the reference signal.

There are also alternative methods to provide convergence. The Filtered-Error LMS (FELMS) is also commonly used. For tonal or narrowband signals also other methods that adjust phase by monitoring the ANC system performance can be used (Kurczyk & Pawełczyk, 2013).

The control filter parameters are updated using the Least Mean Squares (LMS) algorithm. In the basic FXLMS algorithm the control weights are updated according to:

$$\mathbf{w}(i+1) = \mathbf{w}(i) - \mu_{LMS} \mathbf{r}(i) e(i), \quad (2.3)$$

where μ_{LMS} is the LMS algorithm step size and $\mathbf{r}(i) = [r(i), r(i-1), \dots, r(i-(M-1))]^T$ is a vector of regressors of the filtered-reference signal.

This basic FXLMS algorithm have one parameter μ_{LMS} that must be set to an appropriate value. Too small value results in slow adaptation, and too high value results in the lack of convergence. In practical implementations Variable Step LMS (VS-LMS), is commonly used:

$$\mathbf{w}(i+1) = \mathbf{w}(i) - \mu_{LMS}(i) \mathbf{r}(i) e(i), \quad (2.4)$$

A large number of methods were proposed to select good value of $\mu_{LMS}(i)$ step size. One of the most popular method is the Normalized LMS algorithm, which selects $\mu_{LMS}(i)$ in each sample using the power of the reference signal:

$$\mu_{LMS}(i) = \frac{\mu}{\mathbf{r}^T(i) \mathbf{r}(i) + \zeta} \quad (2.5)$$

where μ is a constant convergence coefficient, and the ζ is a parameter protecting against division by zero in case of lack of excitation. When the Normalized LMS algorithm is used without the secondary path, the μ for stable operation should be positive and considered smaller than 2.

Another popular variation of the LMS algorithm is the Leaky LMS algorithm:

$$\mathbf{w}(i+1) = \alpha \mathbf{w}(i) - \mu_{LMS} \mathbf{r}(i) e(i), \quad (2.6)$$

where $0 \ll \alpha < 1$ is the leakage coefficient. Usually both a leak and a normalization is used:

$$\mathbf{w}(i+1) = \alpha \mathbf{w}(i) - \mu \frac{\mathbf{r}(i)}{\mathbf{r}^T(i) \mathbf{r}(i) + \zeta} e(i), \quad (2.7)$$

There are many variations of the LMS algorithm. Some of them, such as AutoLMS (Bismor, 2012) focus on a fast adaptation. To provide faster adaptation also other adaptation algorithms are used in Active Noise/Vibration Control systems, such as Affine Projection (Michalczyk & Wiczorek, 2011) or Recursive Least Squares (RLS) (Leniowska & Kos, 2009).

2.3 Acoustic feedback path neutralization

In many active systems the control signal have influence on the reference signal (Figure 2.2). This adds unwanted additional feedback path, F , which might destabilize the system. In ANC systems, such acoustic feedback is common. Different techniques can be applied to eliminate this feedback or neutralize it (Makarewicz, 1993; Engel, 1993). A frequently used solution to this problem, is to subtract a predicted influence from the raw reference signal $x_r(i)$. The influence can be predicted by employing a linear model of the feedback path \hat{F} .

Because the need of the feedback path neutralization depends on the application, and can be added if necessary, in all control system structures the existence of the feedback path was skipped.

2.4 Multiple outputs

The FXLMS algorithm can also be used for systems with multiple outputs. For the c -th channel, the control signal value is equal to (Figure 2.3):

$$u_c(i+1) = \mathbf{w}_c(i)^T \mathbf{x}_u(i), \quad (2.8)$$

where $\mathbf{w}_c(i) = [w_{c,0}(i), w_{c,1}(i), \dots, w_{c,N-1}(i)]^T$ is a vector of parameters of the c -th FIR control filter and $\mathbf{x}_u(i) = [x(i), x(i-1), \dots, x(i-(N-1))]^T$ is a vector of

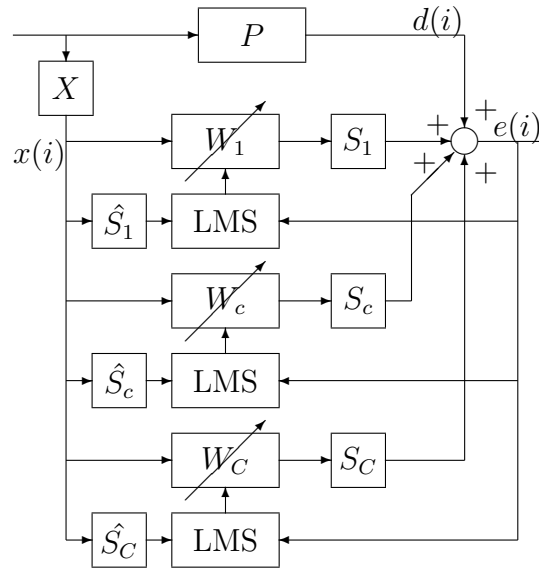


Figure 2.3: ANC system with multiple control signals.

many different control signals. A single solution can be obtained by adding additional constraints. The minimization of the control signal power is one of possible constraints.

In the case of the FXLMS algorithm another problem exists. When the control signal is limited in value, as for real systems, the algorithm may no longer converge to the optimal solution, when some signals reach saturation. This problem was observed in experiments, but for better illustration simulation results will be presented.

Figure 2.4 presents the power of the error signal in time for a simulated simple ANC system with two secondary sources and a 200 Hz tonal disturbance. All signals are normalized to $[-1, 1]$ range. The disturbance power is smaller than the possible power generated by both secondary sources. So this system, when used in simulation, should be able to ideally cancel that disturbance except for numerical errors. The FXLMS works as expected if the control signal is not saturated, but when the saturation was added the FXLMS algorithm no longer converges to the optimal solution and reduces noise by 22 dB only. This is caused by the saturation of one of control signals (see Figure 2.4).

The simplest solution is to introduce some kind of reduction of the control signal power. This, can be achieved by using the Leaky FXLMS algorithm. This, however, comes with a cost of degraded performance. The degradation can be controlled by setting the leak coefficient. By using the leak coefficient α close to 1, the degrada-

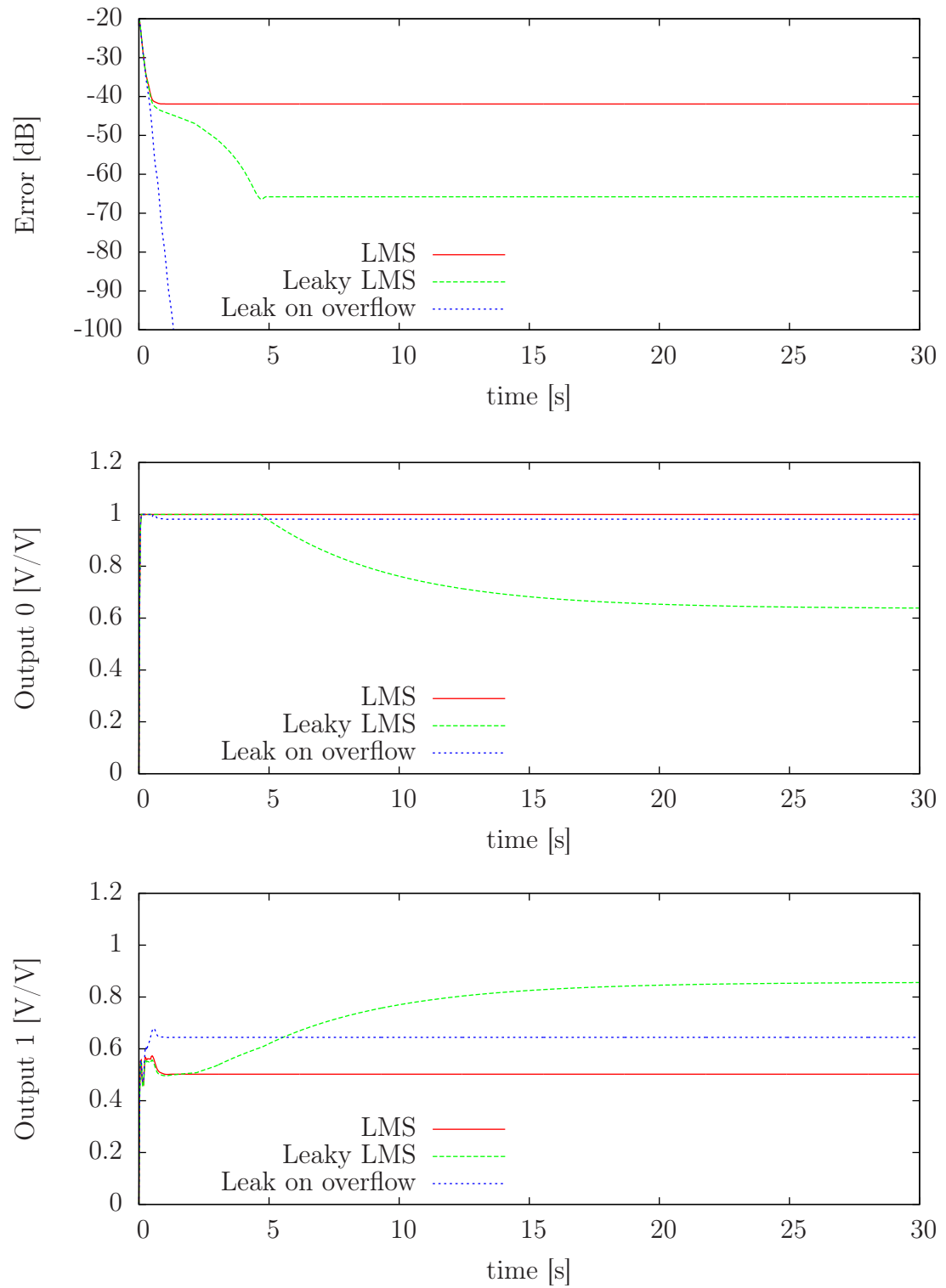


Figure 2.4: Convergence in case of saturation for 200 Hz tonal signal (simulation).

tion can be small. Figure 2.4 shows the Leaky FXLMS algorithm with $\alpha = 0.99999$. However, with a small leak the convergence is slow, and the control system needs approximately 5 seconds (10000 samples at 2 kHz sampling frequency). The convergence speed can be improved by setting smaller α , at the cost of a worse performance.

The problem can be reduced by using a smaller α , when the output reaches saturation (Mazur & Pawełczyk, 2012b). When the control signal limit was reached the leak coefficient was set to $\alpha = 0.999$ for next 16 samples.

2.5 Experimental verification

2.5.1 Laboratory setup

Figure 2.5 shows a simple application of Active Noise Control for reduction of noise transmitted from a small-dimensional enclosure. The enclosure is acoustically isolated, except the area, where a fully clamped aluminum plate is placed.

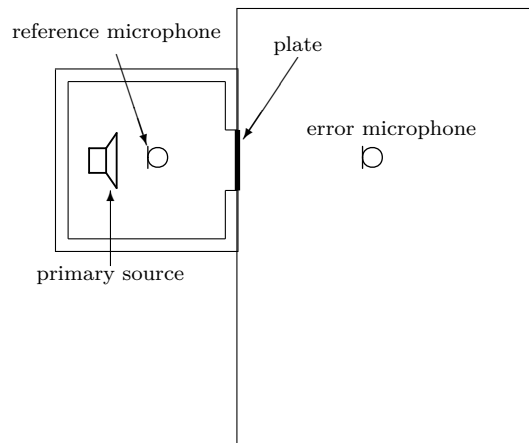


Figure 2.5: Laboratory setup for testing active noise control.

Noise is generated by a loudspeaker placed in the enclosure. An advantage of such approach is that the noise signal is reproducible, what allows for testing different control systems with the same noise. This is especially important for stochastic noise, for which using a real machine would lead to different test signals.

For feed-forward control the reference signal is needed. In this example an acoustic reference was used. The reference microphone is placed in the enclosure. The signal from this microphone, after amplification, filtration by analog anti-aliasing low-pass filters and conversion to sampled digital signal, is the $x(i)$ reference signal for the control algorithm.

For adaptation the error signal is needed. This is the signal that will be minimized by the control system. In this simple example the acoustical error signal measured by the error microphone placed in the laboratory room is used.

2.5.2 Plate and actuators

The aluminum plate that separates the enclosure and the laboratory room used in this dissertation, is of dimensions $400\text{ mm} \times 500\text{ mm} \times 1\text{ mm}$. Nine MFC patches were mounted on the plate (Figure 2.6). However, only three patches 1, 2 and 3 were used. Those three patches were selected experimentally based on the amplitude response.

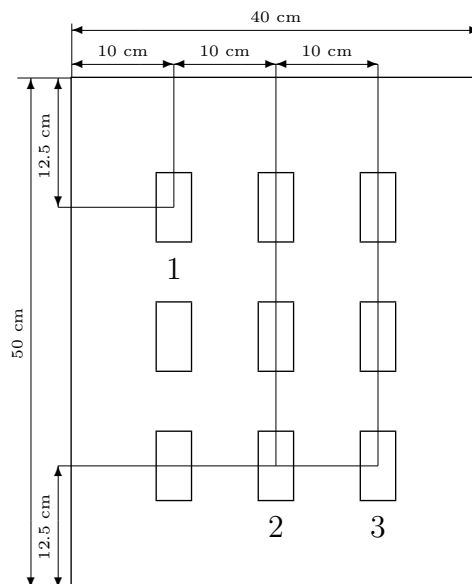


Figure 2.6: MFC actuators on the plate.

2.5.3 Control system

The Normalized Leaky Filtered-reference LMS algorithm is applied for on-line adaptation of three FIR control filters used to drive three secondary paths, each containing an MFC actuator.

The structure of the control system is presented in Figure 2.7. The inputs are connected to 16-bit ADC with synchronous sampling by using microphone amplifiers and 8th order Butterworth low-pass anti-aliasing analog filters. The sampling frequency was set to 2 kHz (0.5 ms sampling period). For this frequency 3 dB cut-off frequency of analog filters was set to 600 Hz. 16-bit ZOH DACs with synchronous sampling

were used to control loudspeaker in the enclosure and all actuators. As reconstruction filters, 8th order Butterworth low-pass filters with 600 Hz cut-off frequency were used. The DACs and ADCs sampling processes were not fully synchronous—the DAC outputs were updated just after ADC conversion, i.e. $1.44 \mu\text{s}$. This delay is, however, marginal.

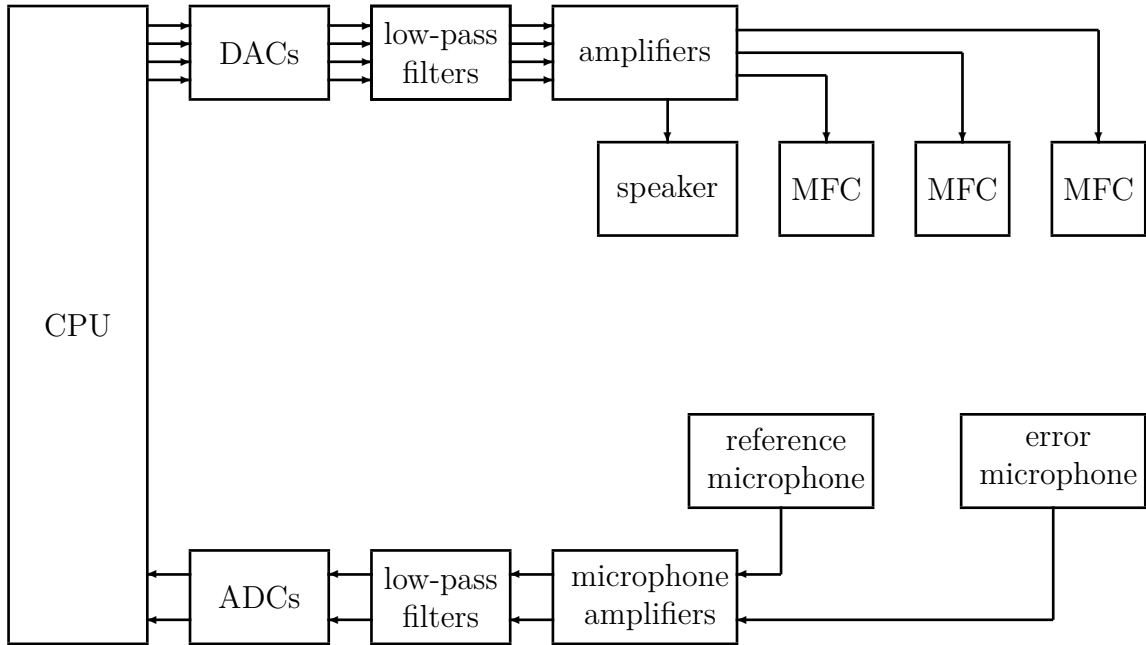


Figure 2.7: Implementation of the ANC system.

2.5.4 Results of artificial noise reduction

Acoustic feedback paths neutralization has been used in all experiments. The length of feedback path FIR models has been set to 128. Secondary paths have been modeled using 255 order FIR filters. The order has been chosen based on impulse response analysis. The length of FIR control filters has been set to $N = 640$.

Figure 2.8 shows the Power Spectral Density (PSD) of the signal from the error microphone for a 180 Hz tonal noise without and with ANC system. The tonal noise reduction is the simplest case for adaptive ANC systems, because the predictive properties of the adaptive filters can be used. The tonal signal can be easily predicted and the performance is not limited by delays in the secondary path and the reference path.

The 180 Hz tone was reduced to the noise floor level, as expected. However, 360 Hz and 540 Hz harmonics of the primary tone are clearly visible. Those harmonics are

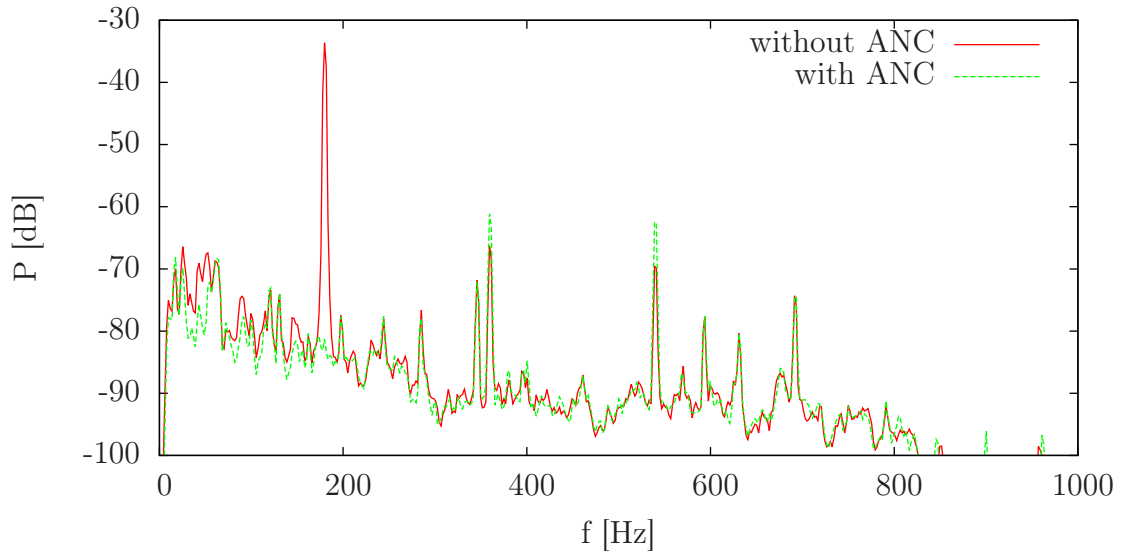


Figure 2.8: PSD of error microphone signal without and with Active Noise Control for 180 Hz tonal noise.

also visible without ANC. This problem will be discussed in Chapter 4. The reduction of primary tone is equal to 47 dB, but the reduction in the whole frequency band is equal to 18.0 dB.

For multi-tonal primary signals the results are similar—the primary tones are reduced to the noise floor.

In another experiment, stochastic signals were considered. They were generated by bandpass filtration of the uniformly distributed white noise. The 4th order Butterworth bandpass filter was used. Figure 2.9 presents results for reduction of narrowband noise. Because in this system the sum of delays in the reference path, X , and the secondary path, S , is larger than the delay in the primary path, the system performance for random signals is much worse. This problem is caused by too small distance between the reference microphone and the plate. The reduction in the whole frequency band is equal to 7.0 dB.

For a wider band (Figure 2.10) the results are even worse. The reduction in the whole frequency band is decreased to 3.8 dB, and the reduction in the 350–450 Hz band is equal to 5.2 dB.

2.5.5 Results of Recorded real-world noise reduction

Figure 2.11 shows results for noise recorded in a coal mill hall, near the fan. The reduction is equal to 3.1 dB. The tonal disturbance at 330 Hz related to the fan is

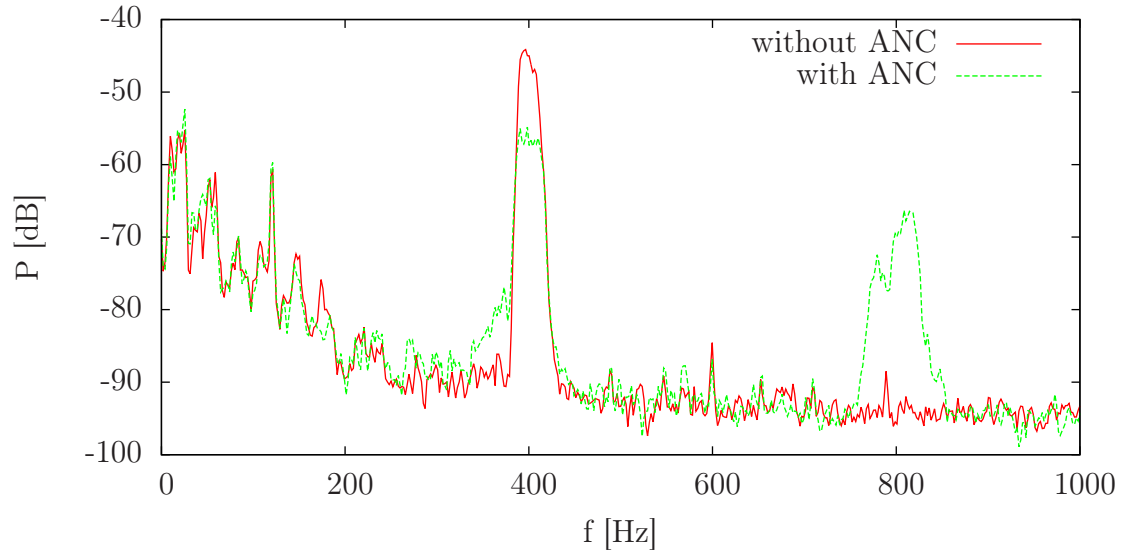


Figure 2.9: PSD of error microphone signal without and with Active Noise Control for 390-410 Hz narrowband random noise

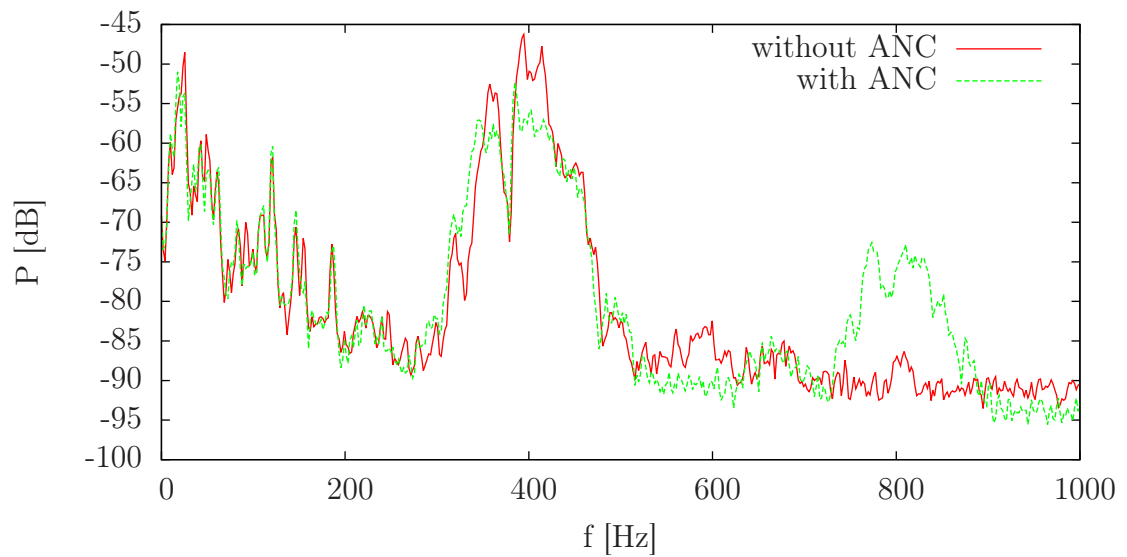


Figure 2.10: PSD of error microphone signal without and with Active Noise Control for 350-450 Hz random noise.

reduced to the level of the wideband noise component. Figure 2.12 shows results for the noise recorded in the same hall, but near the mill.

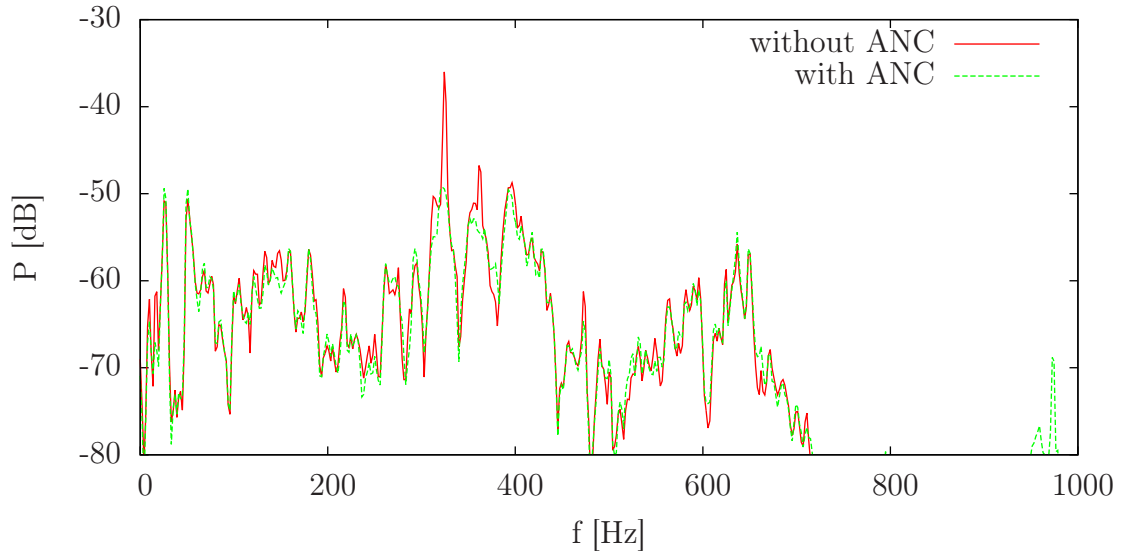


Figure 2.11: PSD of error microphone signal without and with Active Noise Control for noise recorded in the coal mills hall near the fan.

Figure 2.13 presents results for noise recorded in a turbo-generators hall. The ANC was able to reduce most tonal disturbances present in the noise related to turbo-generators.

2.6 Error signals

2.6.1 Multiple-error LMS

The FXLMS algorithm can be extended to multiple errors (Elliott *et al.*, 1987). Figure 2.14 shows a structure of the ANC system with three secondary sources and two error signals using the FXLMS algorithm.

The output signals are calculated using (2.8), as in the single-error case. The difference is only in filter weights adaptation. When multiple errors are used the parameters of the c -th control filter are updated according to:

$$\mathbf{w}_c(i+1) = \alpha \mathbf{w}_c(i) - \mu \frac{\sum_{l=1}^L e_l(i) \mathbf{r}_{c,l}(i)}{\sum_{j=1}^C \sum_{l=1}^L \mathbf{r}_{j,l}^T(i) \mathbf{r}_{j,l}(i) + \zeta}, \quad (2.11)$$

where L is the number of error signals. In this equation $\mathbf{r}_{c,l}(i) = [r_{c,l}(i), r_{c,l}(i -$

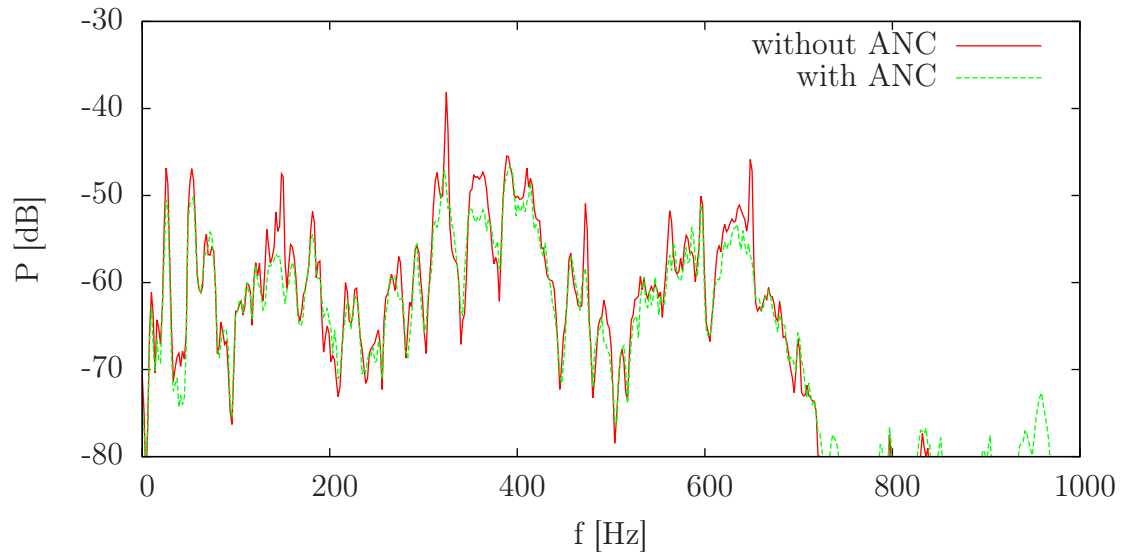


Figure 2.12: PSD of error microphone signal without and with Active Noise Control for noise recorded in the coal mills hall near the pulverizer.

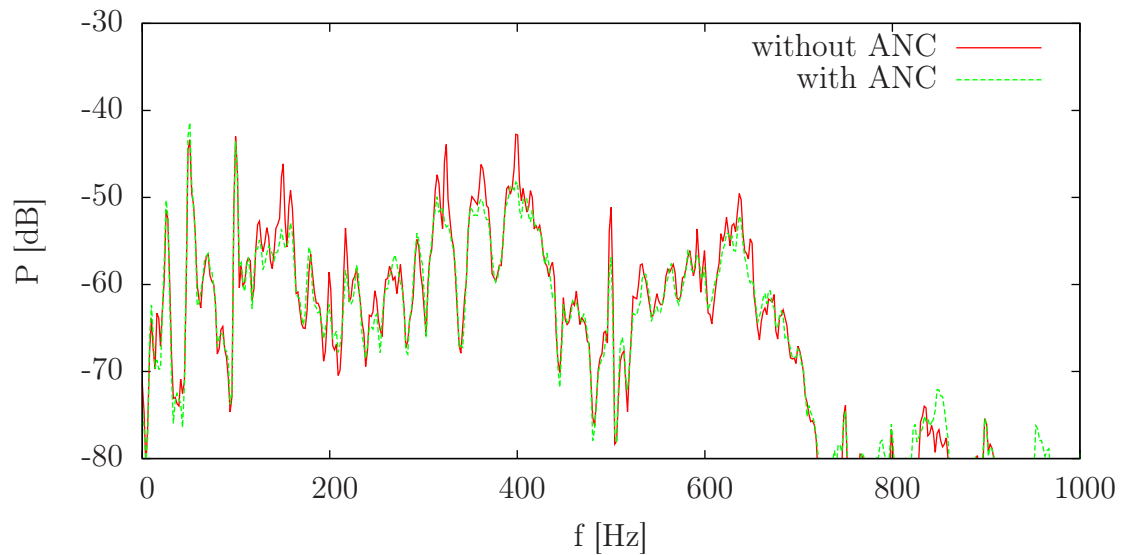


Figure 2.13: PSD of error microphone signal without and with Active Noise Control for noise recorded in the turbo-generators hall.

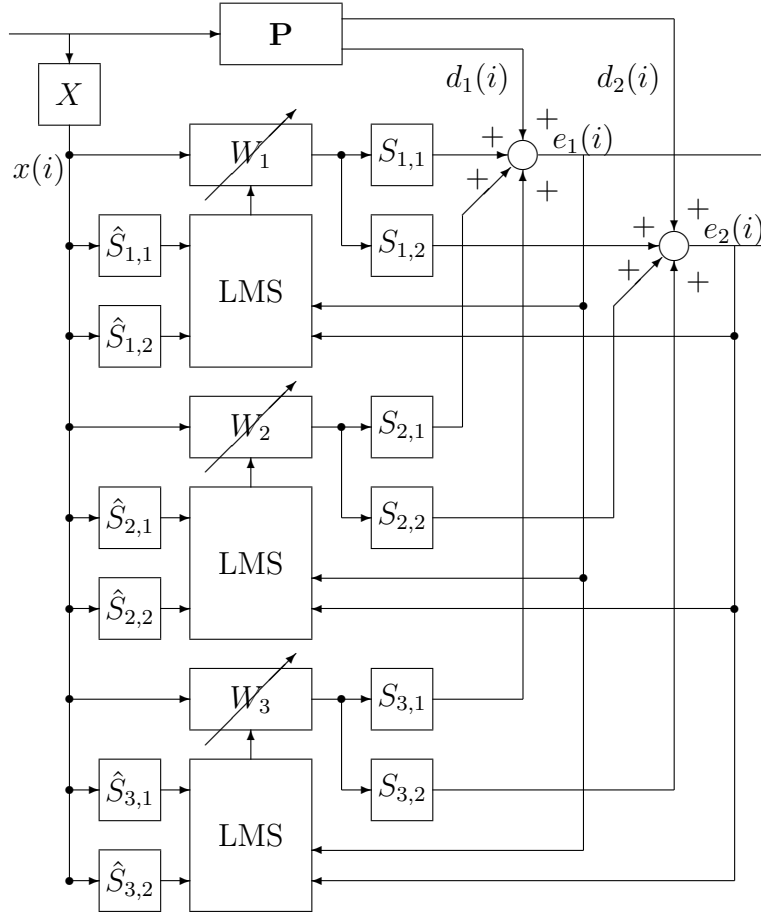


Figure 2.14: ANC system with multiple error signals.

$1), \dots, r_{c,l}(i - (N - 1))\}^T$ is a vector of regressors of the filtered-reference signal, with elements obtained as:

$$r_{c,l}(i) = \hat{\mathbf{s}}_{c,l}(i)^T \mathbf{x}(i), \quad (2.12)$$

where $\hat{\mathbf{s}}_{c,l}(i) = [\hat{s}_{c,l,0}(i), \hat{s}_{c,l,1}(i), \dots, \hat{s}_{c,l,M-1}(i)]$ is a model of the c -th secondary path filter impulse response, $\mathbf{x}(i) = [x(i), x(i - 1), \dots, x(i - (M - 1))]^T$ is a vector of regressors of the reference signal.

2.6.2 Selection of error signals

For reduction of sound transmitted through a vibrating plate two types of error signals are usually used: acoustic signals usually measured by microphones and vibration signals usually measured by accelerometers. For acoustic measurement also sound intensity probes can be used (Watras & Pawełczyk, 2011a). By using also acoustic kinetic energy the acoustic pressure gradient is reduced and the size of zone of quiet

can be increased (Pawełczyk, 2013). There are also other vibration sensors, such as piezoelectric PVDF (Pietrzko, 2009), PZT or MFC sensors.

In this dissertation only microphones and accelerometers are used. The length of control filters was set to $N = 512$, and the length of secondary path models was set to $M = 256$. Two MFC actuators and two accelerometers were used (Figure 2.15). For the system with the acoustic error signal, only one error microphone was used.

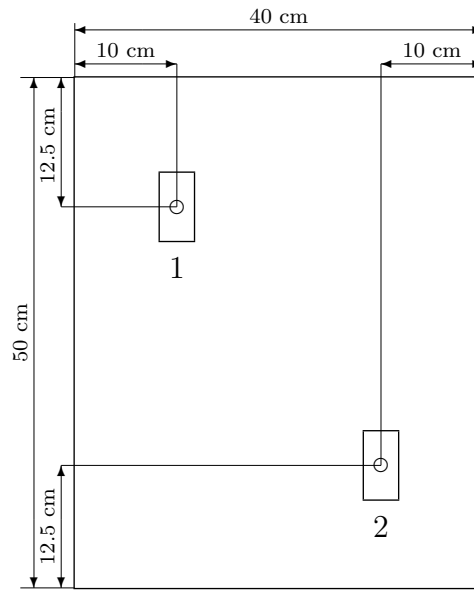


Figure 2.15: Placement of MFC actuators (rectangular patches) and accelerometers (circles).

The ANC system was tested for a 300–550 Hz wideband noise (see Figure 2.16). The noise was generated by bandpass filtration of a uniformly distributed white noise. The 4th order Butterworth bandpass filter was used.

Figure 2.17 presents the PSD of the error signal acquired by a microphone for two control strategies. The ANC system used the error microphone as the error signal. The AVC system minimized plate vibrations in locations, where accelerometers were placed. Because the ANC system minimizes directly the error signal, it provides a better performance, when compared to the AVC system. The AVC system is effective only for frequencies close to plate resonance frequencies and it cannot be used for effective reduction of a wideband noise (Hansen & Snyder, 1997).

However, the AVC systems have advantages. Firstly, they do not have a tendency to create local zones of quiet. They usually provide smaller reduction of noise, but over a wider area than typical ANC systems. The second big advantage is that the control

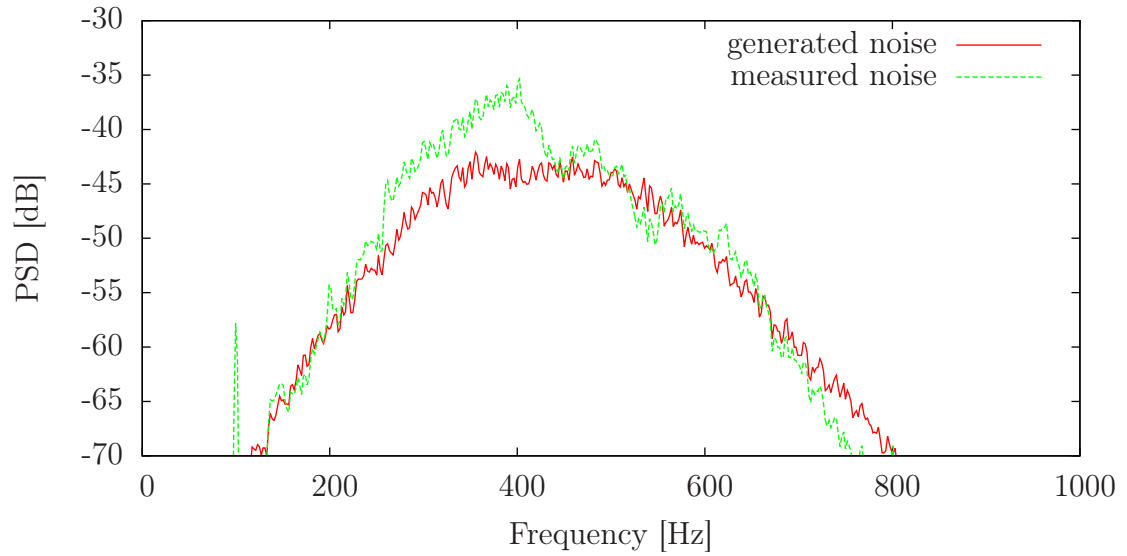


Figure 2.16: PSD of the test signal.

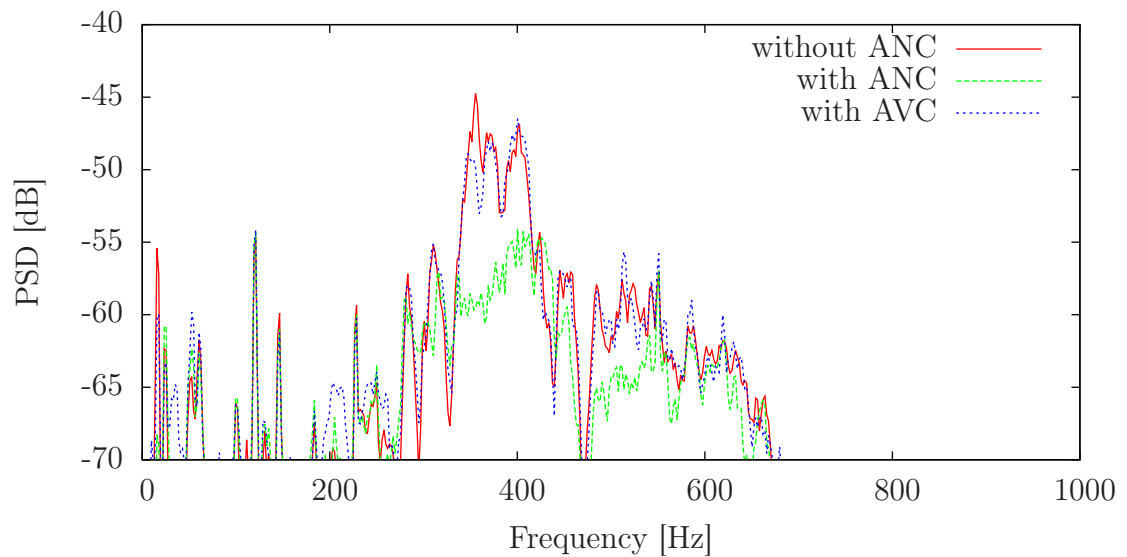


Figure 2.17: PSD for ANC and AVC systems.

system with accelerometers is more compact—error microphones are not needed.

2.7 Virtual Microphone Control

Where creation of local zones of quiet is acceptable, the ANC system may provide better performance than the AVC system. However, the adaptive ANC system needs an error microphone, which cannot be used for some applications. This problem can be solved by using a fixed-parameter feed-forward ANC system, where after initial adaptation or identification of primary and secondary paths with use of an error microphone the parameters of control filters are frozen.

Another possibility that keeps a limited adaptation is to use Virtual Microphone Control (VMC) (Mazur & Pawełczyk, 2012a). Figure 2.18 and Figure 2.19 show a block diagram of one of such systems (Pawełczyk, 2004). The symbol S^a stands for the secondary path defined to an accelerometer. This system uses an experimental approach to identify the path K that models the transfer function between reference signal and the virtual microphone sensor—accelerometer—during operation of the reference system. In this case the reference system is the ANC system that use the error microphone for adaptation.

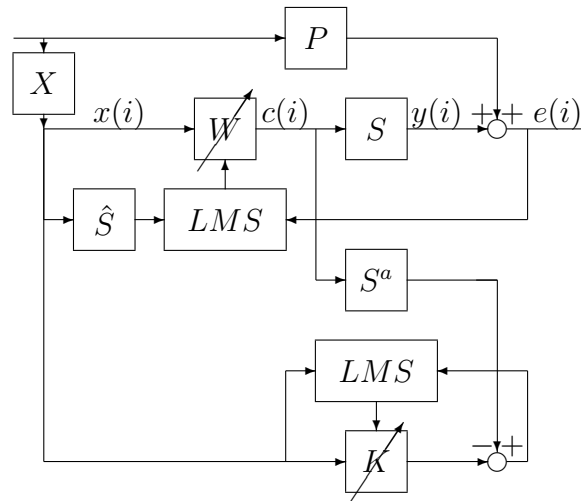


Figure 2.18: Single-channel Virtual Microphone Control system—tuning phase.

During that phase the K model is identified as a FIR filter. Its parameters, $\mathbf{k} = [k_0, k_1, \dots, k_{N_K}]$, are obtained with the Normalized LMS algorithm:

$$\mathbf{k}(i+1) = \mathbf{k}(i) - \mu \frac{\mathbf{x}_k(i)}{\mathbf{x}_k^T(i)\mathbf{x}_k(i) + \zeta} e(i), \quad (2.13)$$

where $\mathbf{x}_k(i) = [x(i), x(i-1), \dots, x(i-(N_K-1))]^T$ is a vector of regressors of the input signal, and $e(i)$ is the current error:

$$e(i) = y^a(i) - \mathbf{k}^T(i)\mathbf{x}_k(i). \quad (2.14)$$

where $y^a(i)$ is the output signal of the accelerometer.

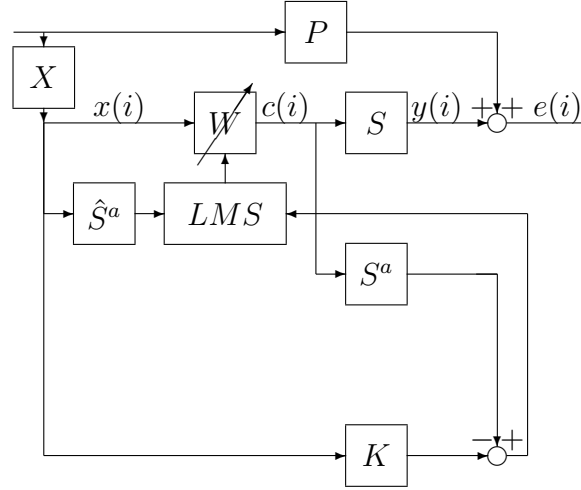


Figure 2.19: Single-channel Virtual Microphone Control system—operation phase.

During the operation stage (Figure 2.19) the control filter weights are updated according to formula:

$$\mathbf{w}_c(i+1) = \alpha \mathbf{w}_c(i) - \mu \frac{\mathbf{r}_c^a(i)}{\sum_{j=1}^C (\mathbf{r}_j^a(i))^T \mathbf{r}_j^a(i) + \zeta} e^a(i), \quad (2.15)$$

where $e^a(i)$ is a plate vibration error signal:

$$e^a(i) = y^a(i) - \mathbf{k}^T \mathbf{x}_k(i). \quad (2.16)$$

The input signal is now filtered by secondary paths to accelerometers:

$$\mathbf{r}_c^a(i) = \hat{\mathbf{s}}_c^a(i)^T \mathbf{x}(i), \quad (2.17)$$

where $\hat{\mathbf{s}}_c^a(i) = [\hat{s}_{c,0}^a(i), \hat{s}_{c,1}^a(i), \dots, \hat{s}_{c,M-1}^a(i)]$ is a model of the c -th secondary path to accelerometer filter impulse response.

2.7.1 Experimental verification

The same system as previously described in Section 2.6.2 was used for verification of VMC control with accelerometers. Two separate filters K_1 and K_2 were used for each of the two accelerometers. The length of both filters was set to $N_K = 256$.

Figure 2.20 presents the performance of VMC ANC system compared to the reference ANC system and the AVC system. The results are close to ANC system and much better than AVC system. Noise reduction level results are shown in Table 2.1.

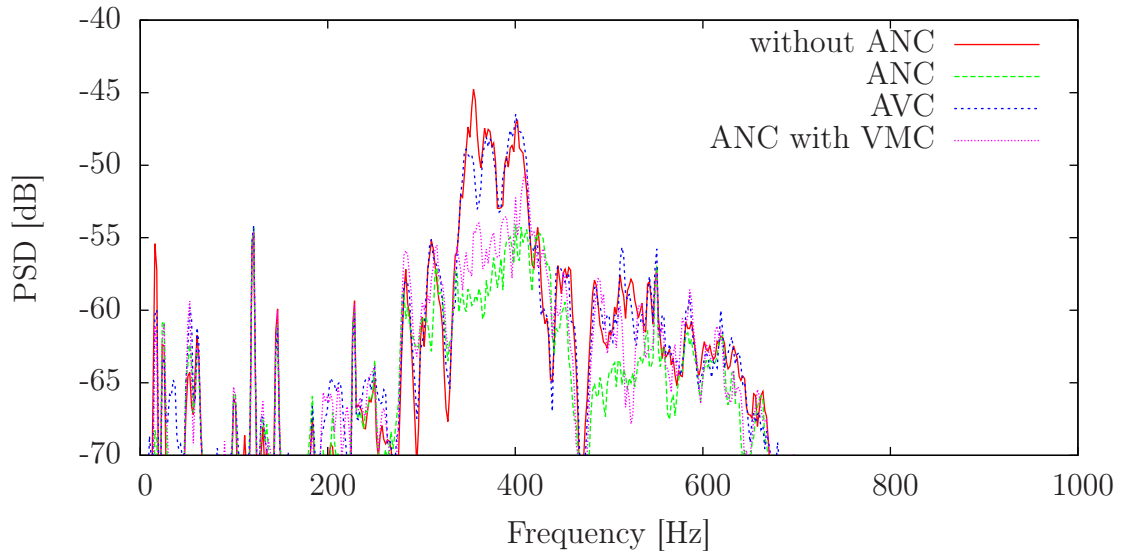


Figure 2.20: Comparison of different control systems.

Table 2.1: Noise reduction level, for wideband noise 300–550 Hz.

System structure	Reduction [dB]
ANC with real microphone	6.1
ANC with virtual microphone	4.1
AVC	0.4

2.8 Enlarging the zone of quiet

The multiple error FXLMS algorithm can be used for enlarging the zone of quiet (Pawelczyk & Watras, 2011; Pawelczyk, 2013). By using multiple error microphones

the ANC system may create one larger zone that contains all error microphones. This technique can be also used for transmission of sound through a vibrating plate, as an alternative to AVC that usually provides global reduction. An interesting approach is also to use mixed ANC/AVC approach by minimization both vibrations and sound pressure at specified points (Mazur & Pawełczyk, 2010b).

For testing the size of the generated zones of quiet the laboratory layout shown in Figure 2.21 was used. The goal of the control systems was to reduce the SPL in $1.2 \text{ m} \times 1.2 \text{ m}$ area. Three different strategies were used. The first concerned a reduction of signals from two error microphones. The second system concerned reduction of signals from two accelerometers. The third system used one accelerometer and one microphone.

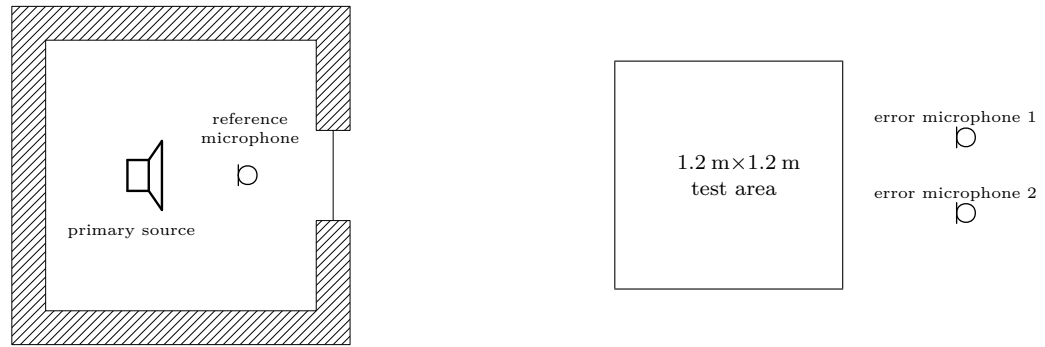


Figure 2.21: Laboratory setup for testing active reduction on area.

When both error signals represented different physical quantities—acceleration from accelerometer and pressure from microphone—additional weights b_l were introduced to (2.11):

$$\mathbf{w}_c(i+1) = \alpha \mathbf{w}_c(i) - \mu \frac{\sum_{l=1}^L b_l e_l(i) \mathbf{r}_{c,l}(i)}{\sum_{j=1}^C \sum_{l=1}^L \mathbf{r}_{j,l}^T(i) \mathbf{r}_{j,l}(i) + \zeta}. \quad (2.18)$$

For experiments the FXLMS algorithm parameters were set to: $\mu = 0.001$, $\zeta = 0.001$ and $\alpha = 0.99999$. A small leakage has been chosen to guarantee or improve algorithm convergence in case of secondary path changes.

For tests, a 500 Hz tonal signal was chosen. This frequency is close to the one of resonant frequencies of the plate. For that frequency the wavelength was smaller than size of the test area, so zones of quiet should be smaller than the area. Figure 2.22 shows obtained noise reduction map. The AVC system provides, as expected, a flat zone with average SPL reduction of 3.5 dB. The ANC system using two microphones

as error sensors generates a very irregular noise reduction zone with average SPL reduction of 0.8 dB. The maximal reduction at some points exceeds 20 dB, but at other points the SPL is increased by more than 10 dB.

For the system employing one microphone and one accelerometer with appropriate weights ($b_1 = 1$ for accelerometer and $b_2 = 0.05$ for microphone) the reduction zone is also irregular, but there are very few regions with increased SPL. The PSDs of error signals without and with active control for this system are shown in Figure 2.24. The reduction of plate vibrations is very high and it exceeds 40 dB, but it is not as high as in the AVC case. Also the reduction of the SPL at the far-field microphone is much lower than in ANC system, and it reaches 4.1 dB. However, because the weight of the signal from accelerometer is higher than the weight of the signal from microphone, this system does not have tendency to just create zones of quiet around error microphones, but provides good average SPL equal to 6.6 dB.

Figure 2.23 shows the Sound Pressure Level for the same experiment. Table 2.2 collects the peak and average SPL reduction for different control systems.

Table 2.2: Comparison of the SPL reduction at test area.

Error sensors	Peak reduction [dB]	Average reduction [dB]
two accelerometers	8	3.5
two microphones	22	0.8
accelerometer + microphone	21	6.6

2.9 Summary

In this chapter the adaptive feed-forward structure, typical for Active Noise Control applications, was used for reduction of sound transmission through a vibrating plate. Such technique is effective both for simple tonal noises, and narrowband and wideband stochastic noises. However, for signals, where very high reduction of primary noise was obtained such as tonal signals, the performance was limited by harmonics. This problem will be discussed in Chapter 4.

AVC is effective only for frequencies close to resonant frequencies, and ANC provides much better noise reduction at specific points. However, ANC also has disadvantages. It creates only local zones of quiet around error microphones. However, the control of sound transmission through a plate has the capability of global reduction.

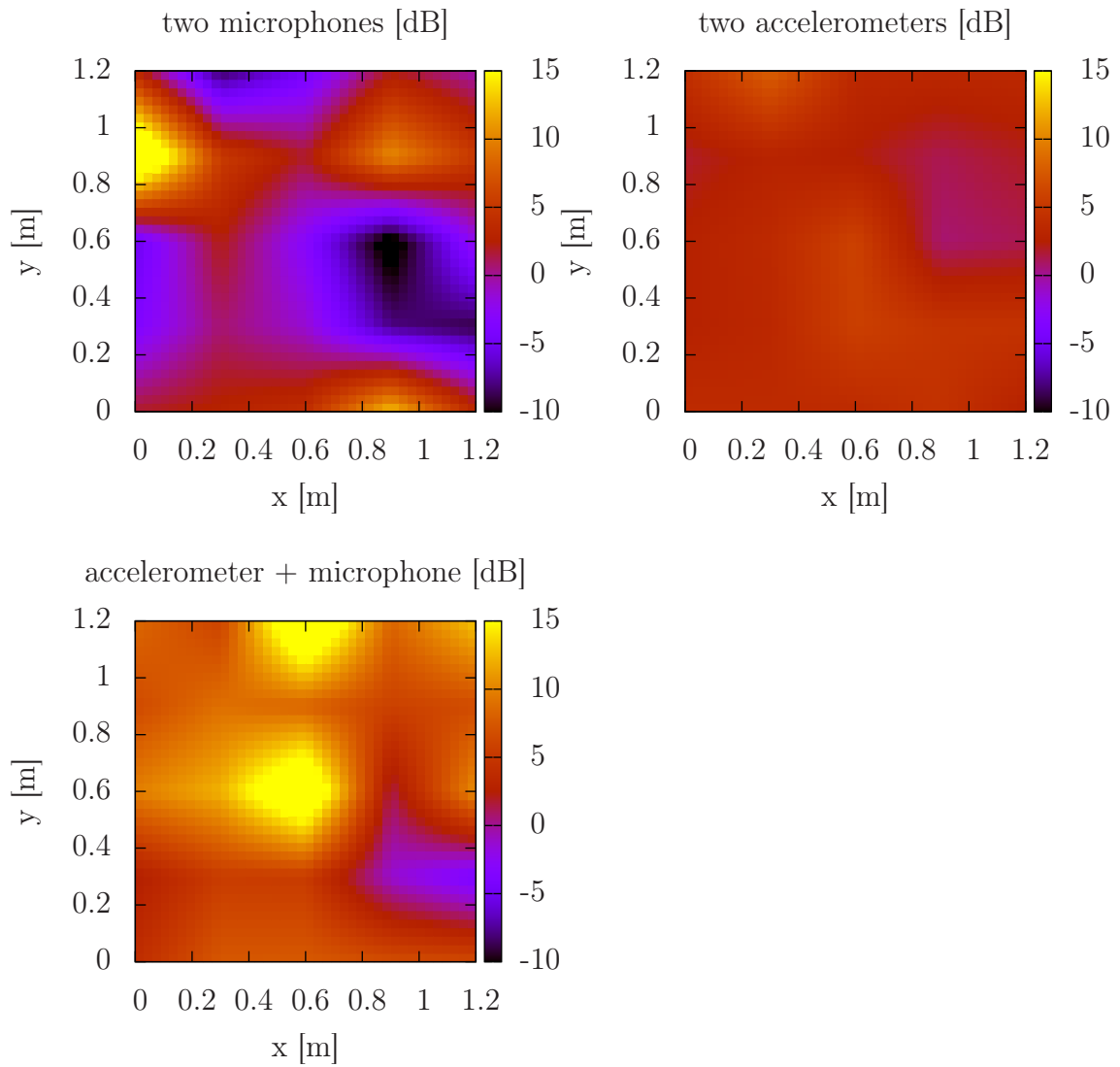


Figure 2.22: Noise reduction map for a 500 Hz tone.

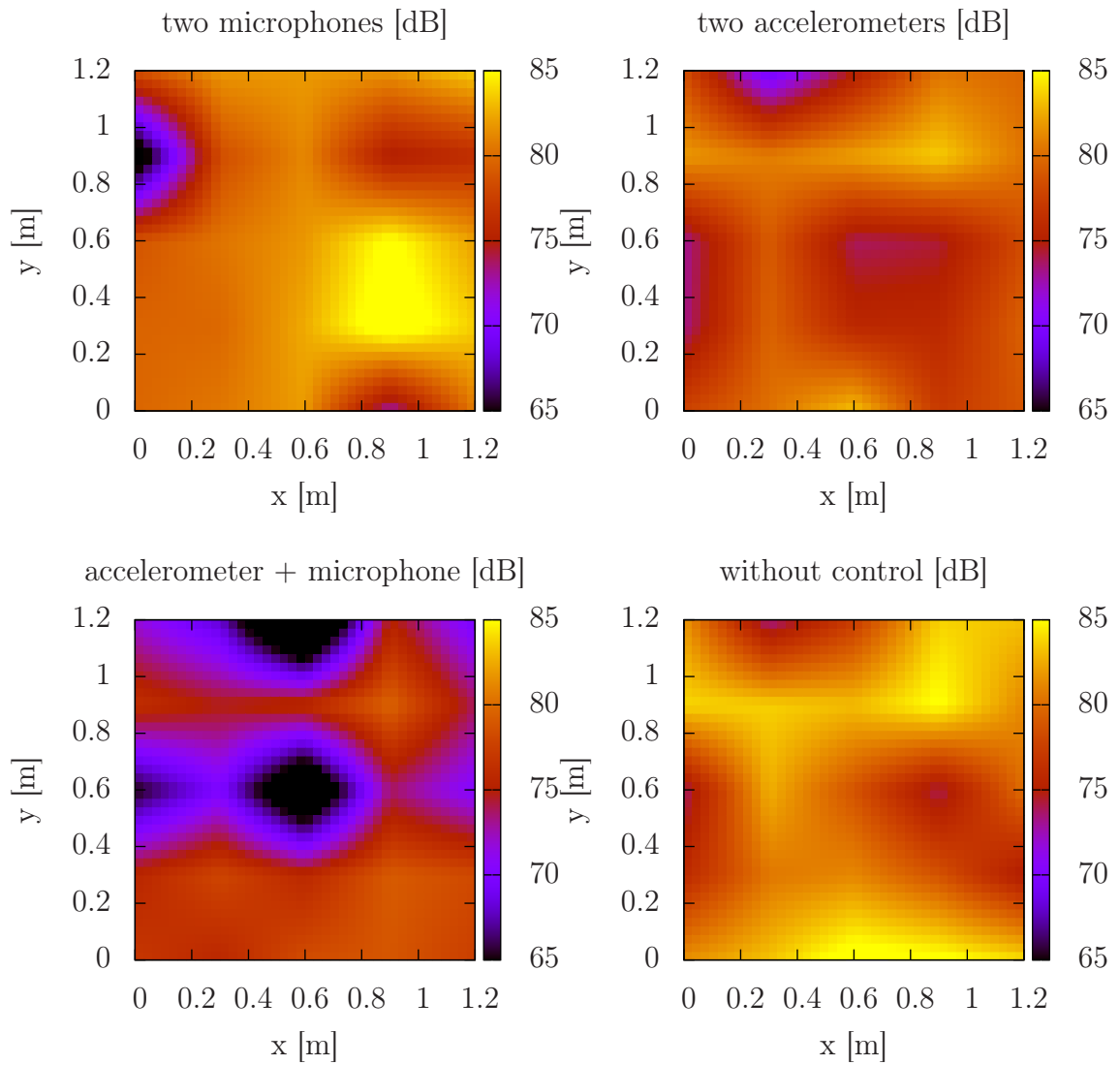


Figure 2.23: Sound Pressure Level map for a 500 Hz tone.

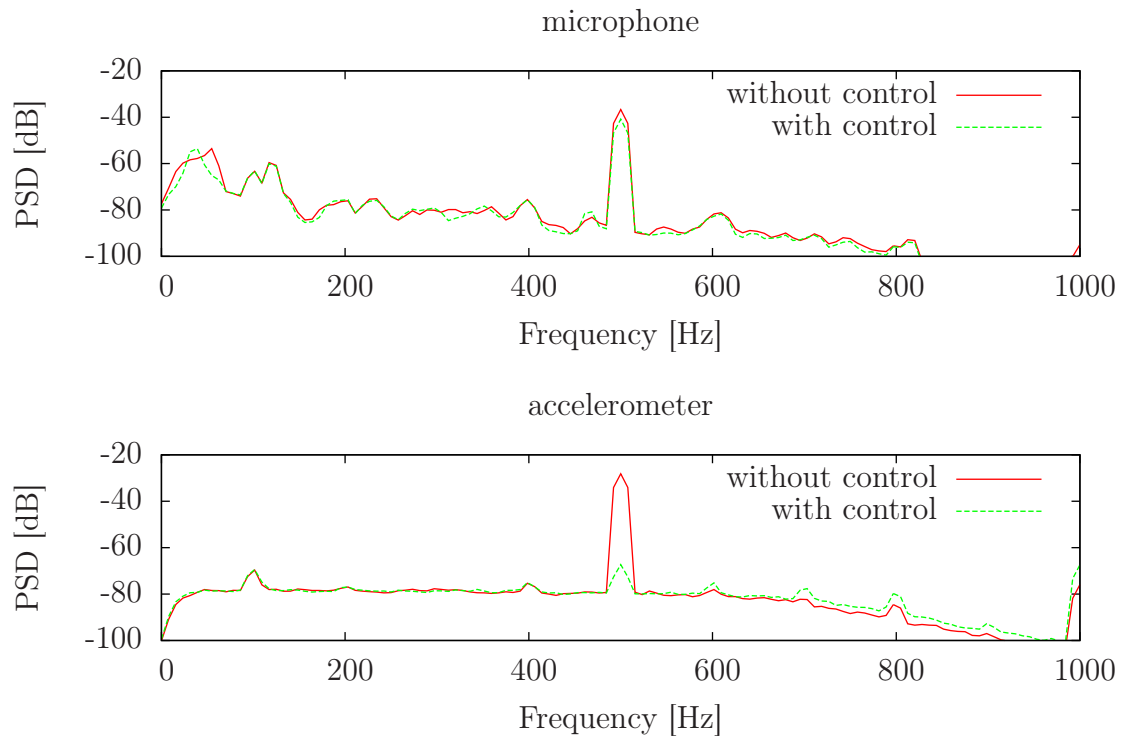


Figure 2.24: PSD of minimized error signals in the system employing the accelerometer ($b_1 = 1$) and the microphone ($b_2 = 0.05$)

This problem can be solved by using many error microphones. Another solution that combines AVC and ANC was also proposed and in the tested case provided much better average SPL reduction for a test area larger than the wavelength.

The second disadvantage of ANC is that the error microphones must be placed at the points where noise should be reduced or near that points and VMC should be used. Another idea of using accelerometer sensors for the VMC system was tested and results were close to those obtained with the reference ANC system.

Chapter 3

Control of sound radiation

Introduction

Vibrating plates can also be used as sound sources. They can be convenient for applications, which require operation in harsh industrial environments, when the sound source is subject to high temperature, high humidity or dust. In such environments, classical loudspeakers cannot be directly installed.

As sound sources, vibrating plates have worse response, when compared to loudspeakers. The sound radiation from a vibrating plate is still of scientific interest (Rdzanek, 2000; Zawieska *et al.*, 2007; Cieřlik & Bochniak, 2010). Figure 3.1 presents the amplitude response for three MFC actuators mounted on a plate (see also Figure 2.6). High variations in the amplitude response caused by multimodal response are clearly visible.

The first problem is that such a system has three inputs, instead of one. The simplest solution is to use only one actuator, but because different actuators are most effective for different frequencies, such approach leads to significant decrease of possible controlled bandwidth. The second possible solution is to use the same input signal directly to drive all actuators. However, in this case destructive interference may occur, because of differences in phase responses. The simplest solution to eliminate the destructive interference is to use a bank of band-pass filters for each actuator. Such solution is used commonly in crossover filters for multi-way loudspeakers.

In this chapter improvements of the sound radiation response from a vibrating plate are investigated. The response can be improved by modifying the plant or by adding an additional controller. First, possible benefits by application of a controller for the plate with three MFC actuators will be investigated. Later, optimization of

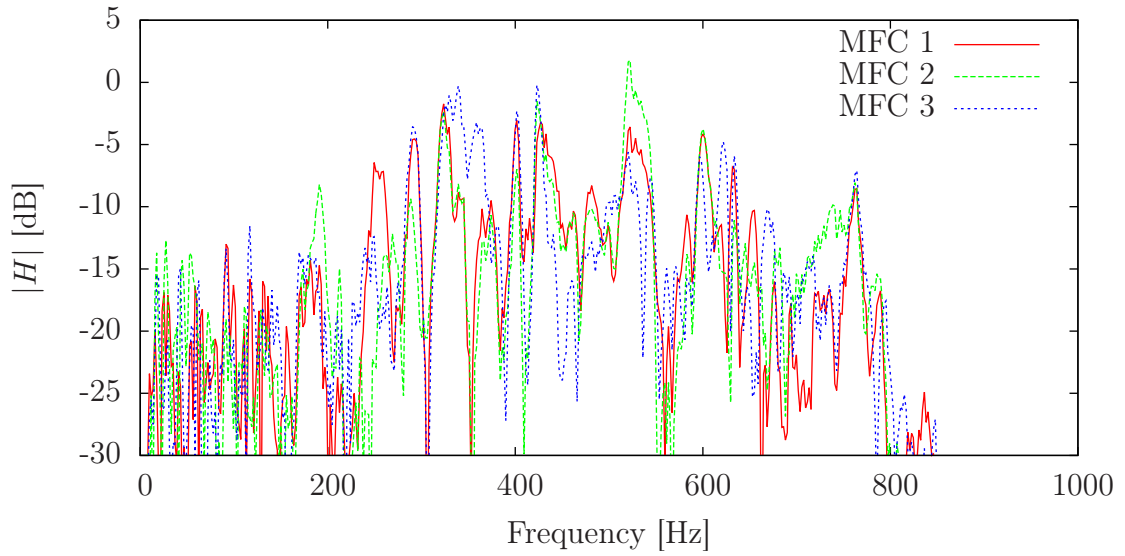


Figure 3.1: Sound radiation from an uncontrolled plate.

actuator placement will be concerned.

3.1 Control system

3.1.1 Optimal fixed-parameter feed-forward control

The simplest approach for control of sound radiation is to filter the input signal by fixed-parameter filters, one for each actuator (Figure 3.2).

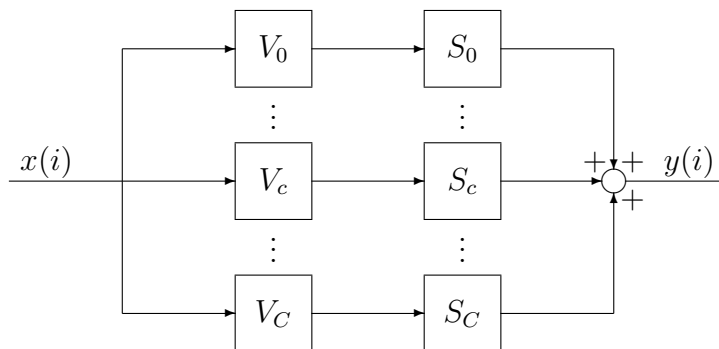


Figure 3.2: Fixed-parameter feed-forward sound radiation control system.

The c -th control signal value is equal to input signal, $x(i)$, filtered by a FIR control filter V_c :

$$u_c(i+1) = \mathbf{v}_c(i)^T \mathbf{x}_v(i), \quad (3.1)$$

where $\mathbf{v}_c(i) = [v_{c,0}(i), v_{c,1}(i), \dots, v_{c,N_V-1}(i)]^T$ and $\mathbf{x}_v(i) = [x(i), x(i-1), \dots, x(i-(N_V-1))]^T$

The goal for designing control filters is that the whole transfer function from input signal and radiated sound is equal to the desired transfer function $H(z^{-1})$. For real applications this is impossible, and the difference between the actual transfer function and the desired one should be minimized. When the H_2 norm is used, V_i filters can be obtained by minimizing the following cost function:

$$L = E \{ e^2(i) \}, \quad (3.2)$$

where $e(i)$ is the error signal equal to:

$$e(i) = \left(\sum_{c=1}^C V_c(z^{-1}) \hat{S}_c(z^{-1}) x(i) \right) - H(z^{-1}) x(i), \quad (3.3)$$

In (3.3) V_c is the control filter for the c -th actuator, and \hat{S}_c is the model of the secondary path. For multiple actuators, $C > 1$, and a single error signal, this problem have an infinite number of solutions, and some additional requirements, like minimization of control power, should be added. For a single actuator the Wiener solution can be used.

3.2 Adaptive control with sound radiation measurement

The fixed-parameter feed-forward solution have many advantages: the control system is always stable and no additional sensors are needed. This solution, however, assumes that each secondary path is stationary. In case of secondary path changes the response of the whole plate with the control system will also change. In case of vibrating plates, huge changes can be caused by temperature changes (Mazur & Pawełczyk, 2011a). Such changes can be compensated by gain-scheduling. However, this comes with a cost of additional sensors and a need to design control filters for the whole range of parameter changes.

An alternative to gain-scheduling adaptation is to govern the adaptation by sound radiation measurement. In the simplest case, the sound radiation can be measured at a single point or at many points with microphones. When the expectation operator

is discarded from (3.2) the optimization problem can be solved by using the FXLMS algorithm.

The structure of the single-channel adaptive control system is presented in Figure 3.3 (Mazur & Pawełczyk, 2012b, 2011e). The input signal, $x(i)$, is filtered by control filter, F , and then it drives the plant, S . The radiated sound is compared with the input signal filtered by the reference path, H . The difference is used by the FXLMS algorithm with leakage to adapt parameters of control filter, F (Mazur & Pawełczyk, 2012b). This system can be easily extended to multiple secondary paths and error signals—the differences between measured radiated sound by microphones and the desired sound at specified points.

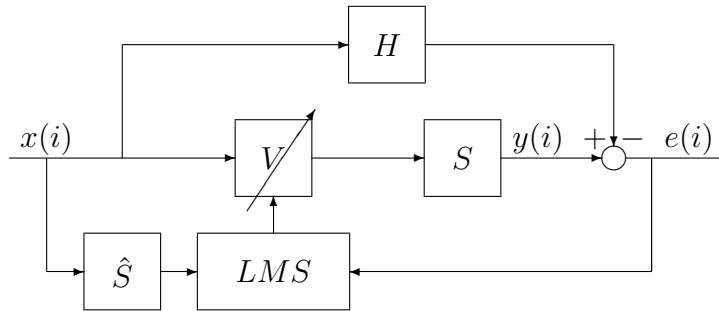


Figure 3.3: Adaptive sound radiation control system.

When using the Normalized Leaky FXLMS algorithm, the control filter parameters are then updated using the following formula:

$$\mathbf{v}_c(i+1) = \alpha \mathbf{v}_c(i) - \mu \frac{\mathbf{r}_c(i)}{\sum_{j=0}^C \mathbf{r}_j^T(i) \mathbf{r}_j(i) + \zeta} e(i), \quad (3.4)$$

where $e(i)$ is the acoustic error signal:

$$e(i) = y(i) - \mathbf{h}^T \mathbf{x}_H(i), \quad (3.5)$$

$\mathbf{h} = [h_0, h_1, \dots, h_{N_H-1}]^T$ is a vector of parameters of the desired model impulse response, and $\mathbf{x}_H(i) = [x(i), x(i-1), \dots, x(i-(N_H-1))]^T$ is a vector of regressors of the reference signal. The desired path model is used only in this equation for filtration of the reference signal, and also the infinite impulse response desired path model can be used without increase of algorithm complexity.

The filtered reference signal $\mathbf{r}_c(i) = [r_c(i), r_c(i-1), \dots, r_c(i-(N_V-1))]^T$ from

(3.4) is a vector of regressors with elements obtained as:

$$r_c(i) = \hat{\mathbf{s}}_c(i)^T \mathbf{x}(i), \quad (3.6)$$

where $\hat{\mathbf{s}}_c(i) = [\hat{s}_{c,0}(i), \hat{s}_{c,1}(i), \dots, \hat{s}_{c,M-1}(i)]$ is a model of the j -th secondary path filter impulse response, $\mathbf{x}(i) = [x(i), x(i-1), \dots, x(i-(M-1))]^T$ is a vector of regressors of the input signal.

When compared to typical application of the FXLMS algorithm for ANC, the primary path is replaced by an arbitrary chosen desired path model, and the output of the model H is subtracted from the plant output (not added as for classical ANC systems, where sound interference is concerned).

3.2.1 Experimental results

The desired response of the plate with control filter was set to:

$$H(z^{-1}) = z^{-D}. \quad (3.7)$$

Thus, the plate should have unity magnitude and a linear phase response. The control filter length was set to $N_V = 256$. The order of models of the secondary paths were set to $M = 256$.

Figure 3.4 presents the amplitude response of the previously used system with three MFC actuators for different values of delay, D , in the desired response, $H(z^{-1})$. The system was tested for a white noise, i.e. the worst case for an adaptive system. Higher delays allow for better results. For all cases the variations in amplitude response are much lower than in case of driving actuators directly (see Figure 3.1).

The control system, for the assumed gain, was unable to compensate for the very low radiation of the vibrating plate, because it would require driving actuators above control signal limits. The phase response is very close to the desired one, even for small delays (see Figure 3.5).

Figure 3.6 presents the impulse response of the plate with the control system. The response is close to the desired one. Because of physical nature of the system, the gain for a constant signal must be equal to zero, so the sum of the impulse response must also be equal to zero. This caused additional high negative peaks around the positive desired peak.

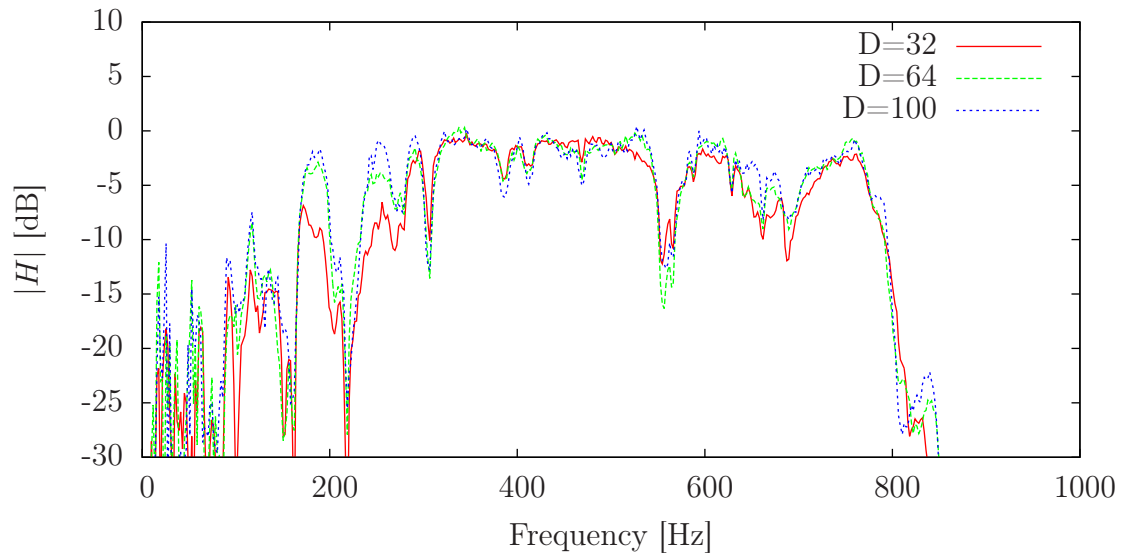


Figure 3.4: Sound radiation from the plate amplitude response with the FXLMS control algorithm.

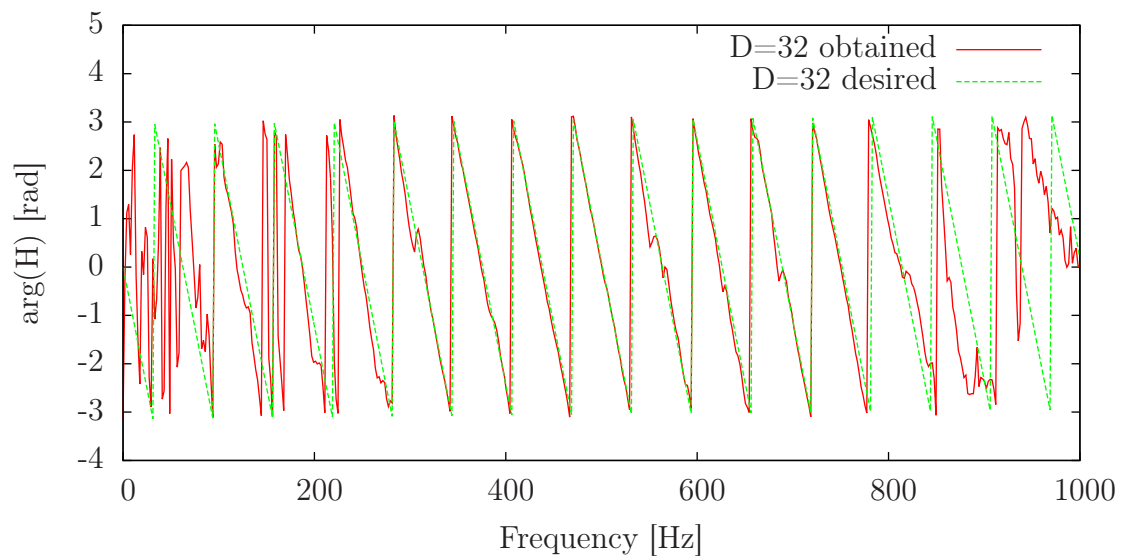


Figure 3.5: Plate phase response with FXLMS control algorithm.

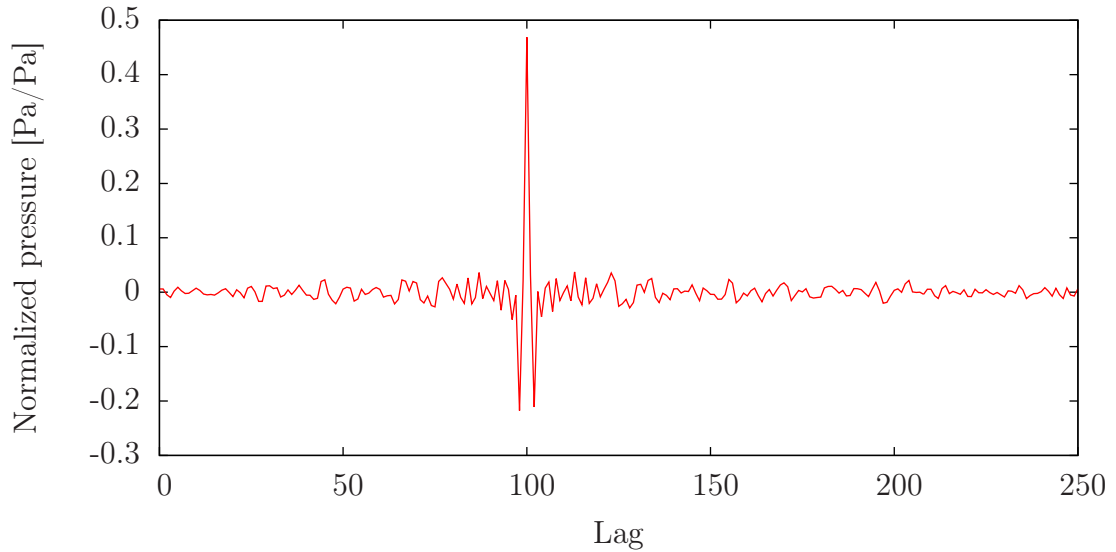


Figure 3.6: Plate impulse response with the FXLMS control algorithm.

Figure 3.7 shows the PSD of a generated 180 Hz tone. Additionally to the 180 Hz tone, the harmonics were also generated. This shows that the system is nonlinear. The level of nonlinearity is quite high. For the first four harmonics the Total Harmonic Distortion THD_R (Shmilovitz, 2005) was equal to 10% at this experiment.

Because the system is nonlinear, even without adaptation, the amplitude response (Figure 3.4) and phase response (Figure 3.5) cannot be used to describe it, because they are valid only for linear systems. The linearity of the system was also tested by the spectral coherence (Figure 3.8). The spectral coherence shows the linearity of the system for specific frequencies, it is the spectral equivalent of the correlation. If the coherence function is equal to 1 the system the linear model fully explains the behavior of the system. If the coherence is equal to 0 the linear model does not explain anything. For most frequencies the coherence function is close to 1 indicating that the linear model explains most of the system behavior. The values smaller than 1 indicate the existence of nonlinearity in the system or presence of disturbances.

3.3 Adaptive control with plate vibration measurement

For the adaptive system directly using sound radiation measurement, error microphones must be used. In many cases such microphones cannot be placed due to

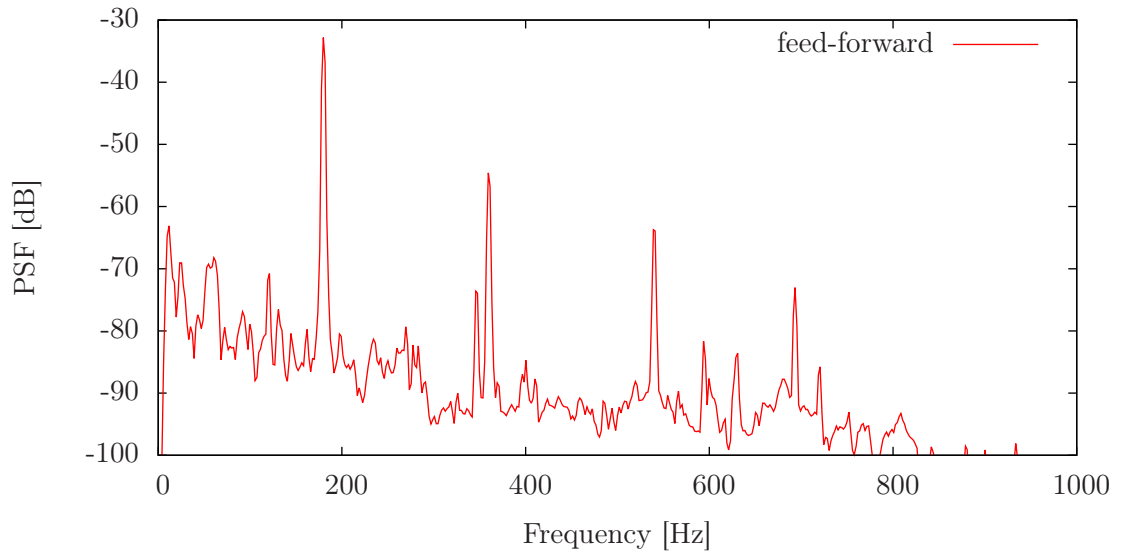


Figure 3.7: The PSDs of generated a 180 Hz tone for linear feed-forward sound radiation control system.

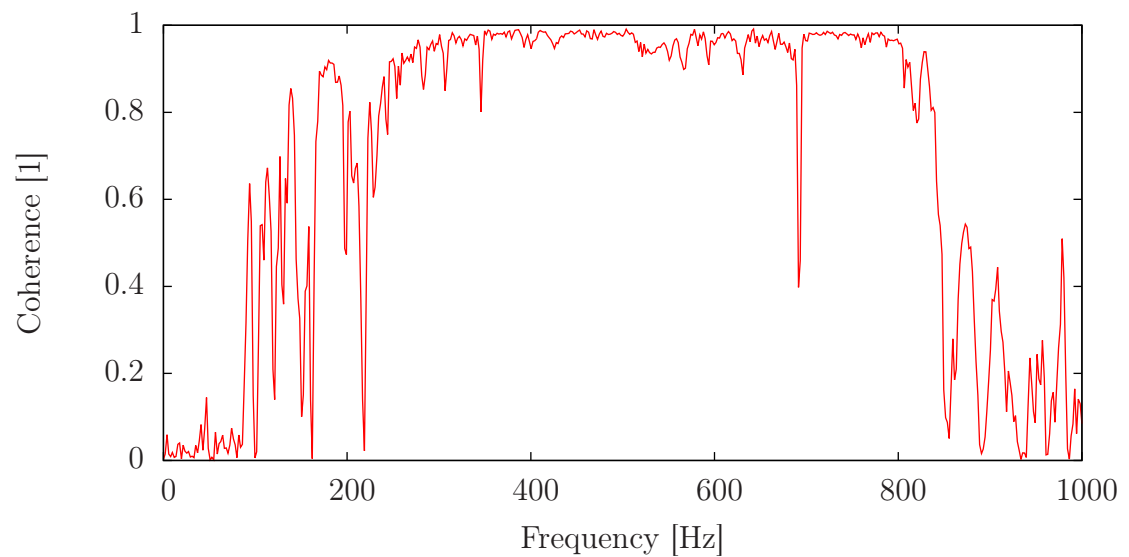


Figure 3.8: Plate spectral coherence with the FXLMS control algorithm.

technological or ergonomic reasons, and different signal for adaptation must be then required. The measurement of plate vibrations is a good alternative. Plate vibrations can be easily measured using accelerometer sensors. Such sensors are suitable for difficult environmental conditions, and they do not occupy extra physical space (they are mounted on the plate).

Acceleration sensors, however, cannot be directly used for adaptation, because the relation between plate acceleration at specified points and radiation of sound is not trivial. Using a simple arbitrary desired transfer function between input signal and plate acceleration or plate velocity will not provide the same desired transfer function between the input signal and radiated sound. The needed desired transfer function between input signal and accelerometer sensors must be chosen with consideration of transfer function between accelerometer and radiated sound. It can be done by accurate modeling of plate radiation. However, it is usually difficult. The desired transfer function can also be obtained with identification of this path during operation of the reference system, which provides the desired transfer function between the input signal and sound radiation. The adaptive system that uses the sound radiation measurement can be used for this purpose. The control system structure during identification of the needed path between input signal and accelerometer sensor is presented in Figure 3.9 (Mazur & Pawełczyk, 2011b).

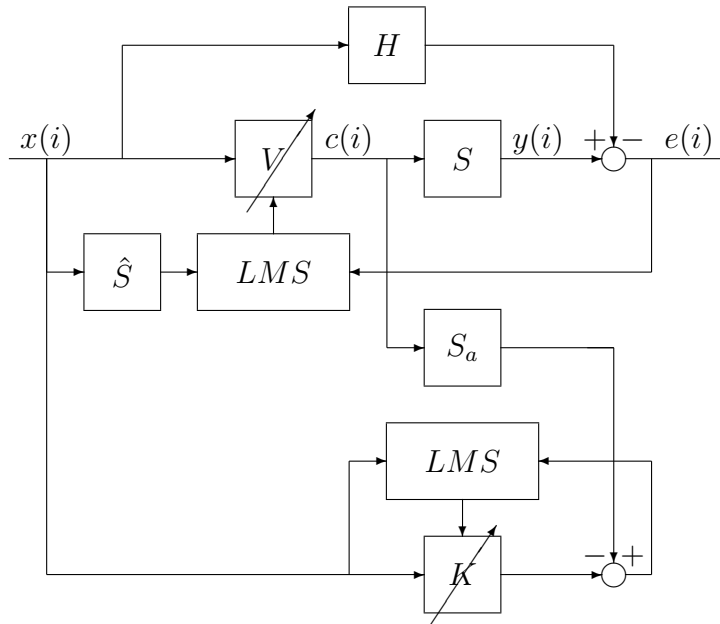


Figure 3.9: Adaptive sound radiation control system with vibration measurement—tuning stage.

This control system is similar to the previously used VMC ANC system described in Section 2.7. However, the idea used for the plate sound radiation control involves a simpler system, because the control system structure for the operating and tuning stages is exactly the same (Figure 3.10). The K filter represents the new desired path. It is identified during operation of the reference system that use the real microphone.

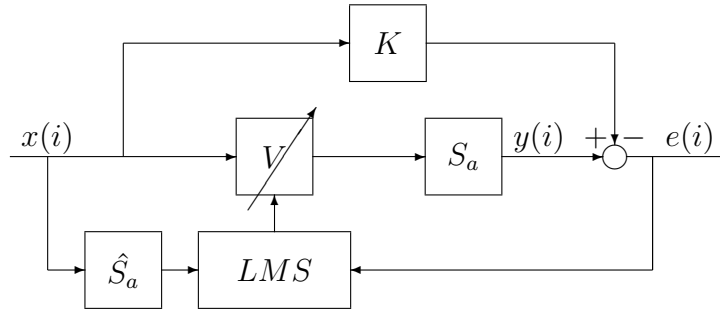


Figure 3.10: Adaptive sound radiation control system with vibration measurement—operating stage.

3.4 Actuator placement optimization

Assuming classical Kirchhoff-Love plate theory for thin plates the equation of transverse displacement η of thin plate subject to a distributed transverse force per unit area f is (Fahy & Gardonio, 2007):

$$D \left(\frac{\partial^4 \eta}{\partial x^4} + 2 \frac{\partial^4 \eta}{\partial x^2 \partial y^2} + \frac{\partial^4 \eta}{\partial y^4} \right) + m \frac{\partial^2 \eta}{\partial t^2} = f, \quad (3.8)$$

where $m = \rho h$ is the mass per unit area, D is the bending stiffness per unit length equal to:

$$D = \frac{Eh^3}{12(1 - \nu^2)}. \quad (3.9)$$

In these equations E is the Young's modulus, ν is the Poisson's ratio, ρ is the density of plate and h is the plate thickness.

The biharmonic equation (3.8) can be solved using the Ritz method or Finite Element Method (FEM), and the plate model can be rewritten as second order differential equation (Wrona & Pawełczyk, 2013a):

$$\mathbf{M} \frac{d^2 \mathbf{q}}{dt^2} + \mathbf{K} \mathbf{q} = \mathbf{Q}, \quad (3.10)$$

where \mathbf{q} is the vector of generalized displacements, \mathbf{M} is the mass matrix, \mathbf{K} is the stiffness matrix and \mathbf{Q} is the vector of generalized forces.

Shapes of first 25 modes are collected in Figure 3.11. The optimization goal was to minimize the minimal eigenvalue of the controllability Gramian matrix for the first 25 plate model modes. The optimal solution was obtained by employing a memetic algorithm (Figure 3.12) (Wrona & Pawełczyk, 2013a).

Figure 3.13 presents the obtained sound radiation without control. The amplitude response of the plate with the FXLMS equalization system is shown in Figure 3.14. The delay was set to $D = 16$. The same method can be also used for placement of sensors (Wrona & Pawełczyk, 2013b).

3.5 Summary

In this chapter the control of sound radiation from a plate was investigated. The adaptive feed-forward FXLMS algorithm was proposed for control generation of sound by a plate with measurement of generated sound by microphones. With appropriate control and allowed high delay the plate amplitude response could be successfully equalized for a quite large frequency band. For carefully chosen actuator placement, good results were obtained also for smaller delays, comparable to delays already existing in the secondary path.

Additionally, the adaptive control of radiation, based on signal from accelerometers instead of microphones, was investigated. Because the dependency between the plate vibration and the measured sound radiation is not simple, especially when the room acoustics must be taken into account, the plate accelerometers mounted on a plate cannot be simply used for control. The desired path is more complex. An experimental method for obtaining the desired model for path between controller input and the accelerometer sensors based on identification of this path during operation of reference system was proposed and tested.

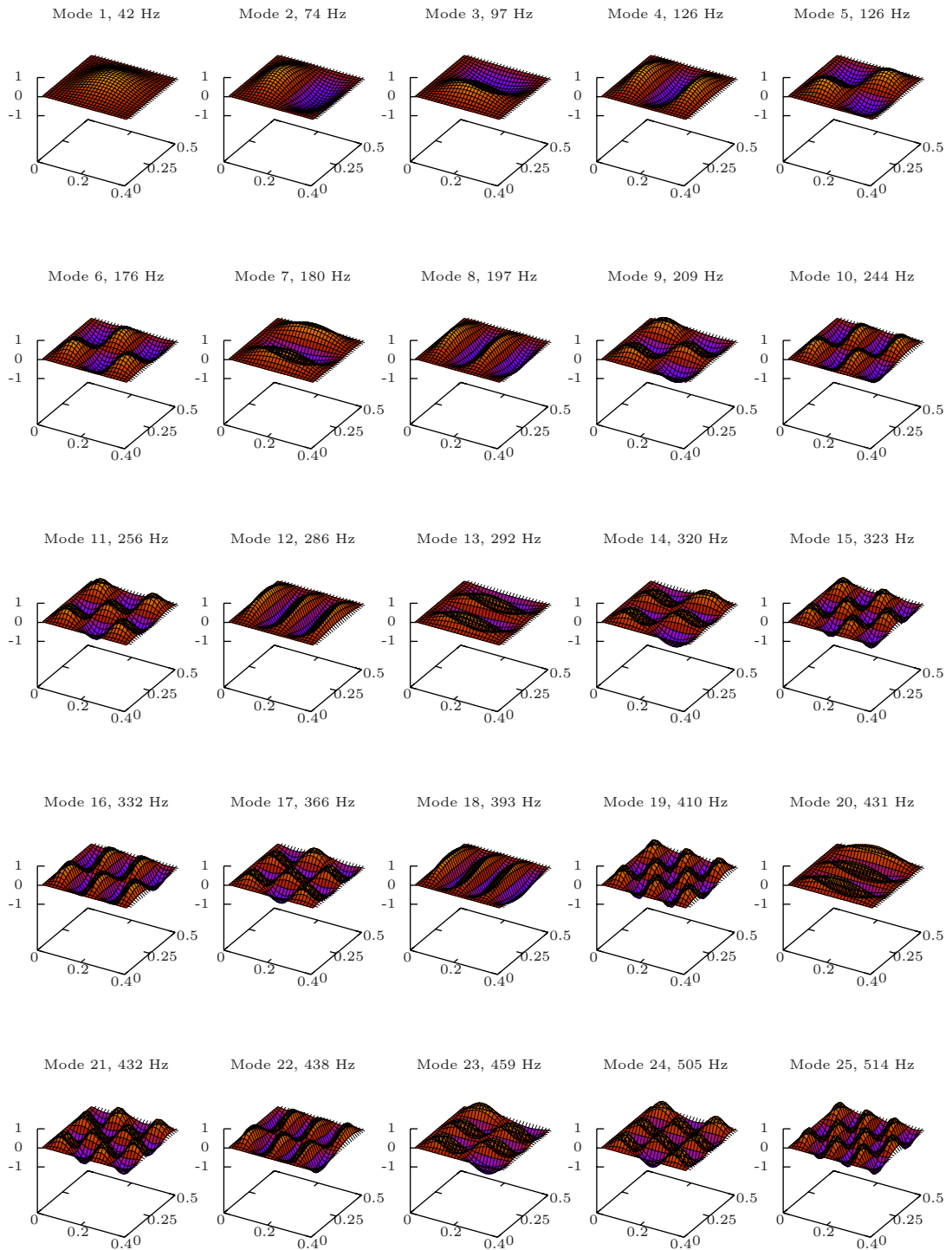


Figure 3.11: First 25 mode shapes for used $0.5 \text{ m} \times 0.4 \text{ m}$ plate. The vertical axis shows the vibration amplitude normalized to $[-1, 1]$ range.

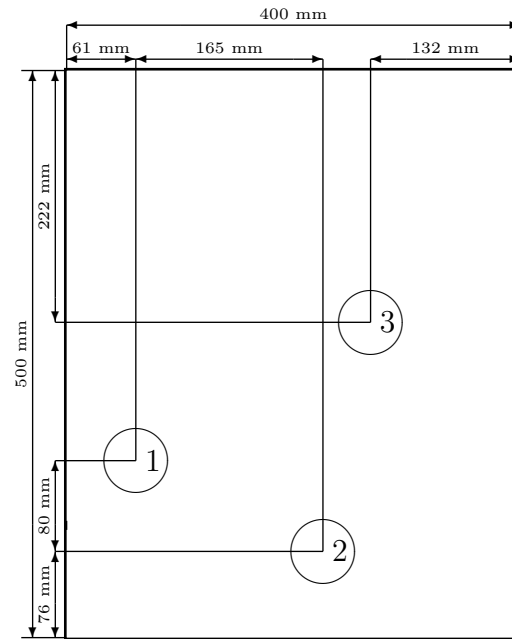


Figure 3.12: Placement of EX-1 actuators.

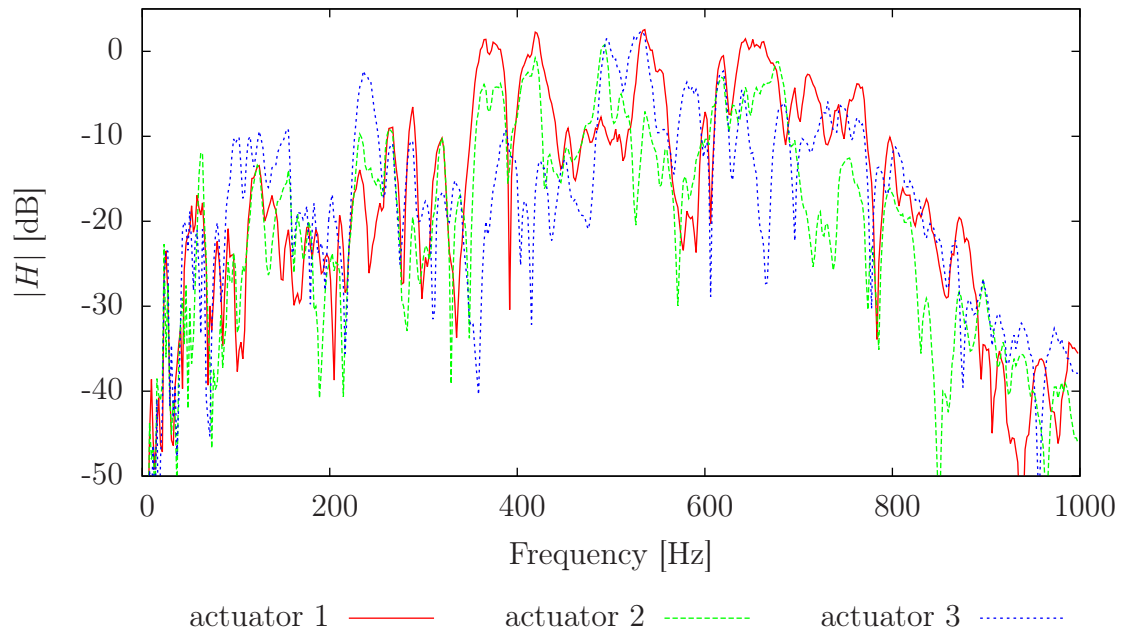


Figure 3.13: Uncontrolled sound radiation from the plate with three optimally placed EX-1 actuators.

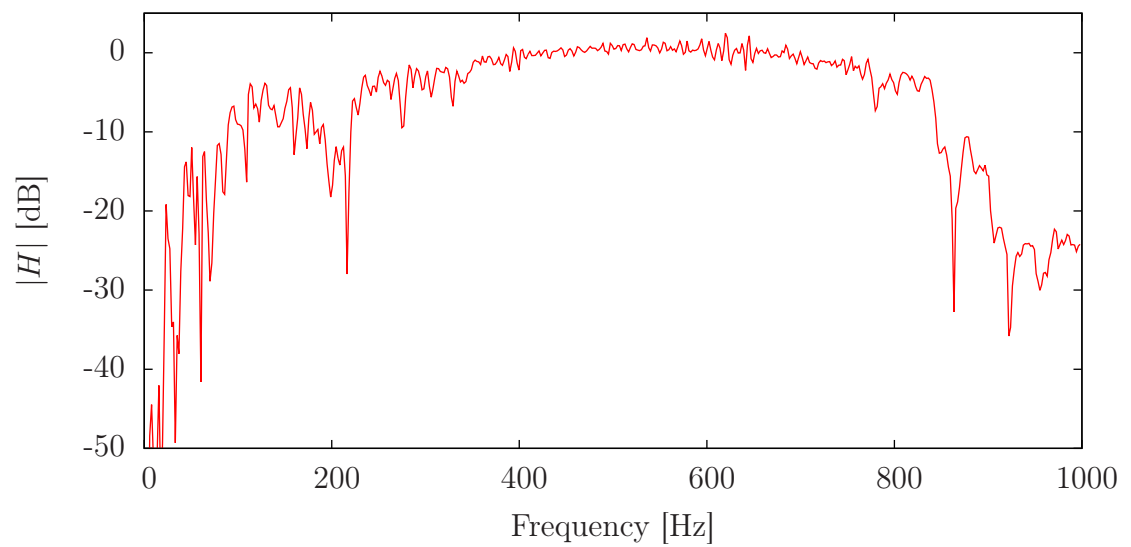


Figure 3.14: Plate phase response with the FXLMS control algorithm for $H = z^{-16}$.

Chapter 4

Nonlinear control

4.1 Nonlinearity problems in plate control

Linear feed-forward systems commonly used for ANC applications assume that the plant is linear. This assumption is usually adequate, and linear systems work satisfactorily, then. However, in case of vibrating plates used as secondary sources, the secondary paths are nonlinear. This is a problem for both sound generation using vibrating plates and for ANC systems. Additionally, if sound transmission through the plates is concerned, the primary paths are also nonlinear.

There are many potential sources of nonlinearities in the ANC systems using plates. Most of them, such as amplifiers, ADCs, DACs or nonlinear acoustic wave propagation in air (Weyna., 2010; Weyna. *et al.*, 2013) exists also in systems that use classical loudspeakers, but they are usually not significant. When vibrating plates are used, two additional sources of nonlinearity usually exists. First, the nonlinearities can be caused by vibrations of clamped plates (Kadiri *et al.*, 1999; Saha *et al.*, 2005). Second, actuators can be nonlinear, e.g. MFC patches utilizing the d33 effect (Stuebner *et al.*, 2009).

To show the impact of nonlinearity on the performance of an ANC system, a simple experiment was performed. The plate with three EX-1 electrodynamic actuators was used, with the same layout as in Section 3.4 (see Figure 3.12). The EX-1 actuators were used instead of MFC piezoelectric actuators because they response is considered linear.

Figure 4.1 shows the performance of a classical linear feed-forward FXLMS ANC system, for different levels of a 155 Hz tonal noise. For comparison, the PSD of the noise floor signal (without the primary noise and with disabled ANC) is included in

each plot. The PSD of the primary noise (without control but with the noise floor) is not plotted for clarity of the figures, but above each plot the power of the 155 Hz tone without ANC is presented.

For small noise powers, nonlinear artifacts are not visible or they have powers comparable to the noise floor power. For higher powers, -30 dB and -36 dB, the harmonics are clearly visible and they significantly limit the noise reduction level. For instance, the 155 Hz tone at the level of -30 dB power is reduced to the floor level, i.e. -80.6 dB, but the second harmonics at 310 Hz is at the level of -53 dB, namely only 23 dB lower than the original dominating tone.

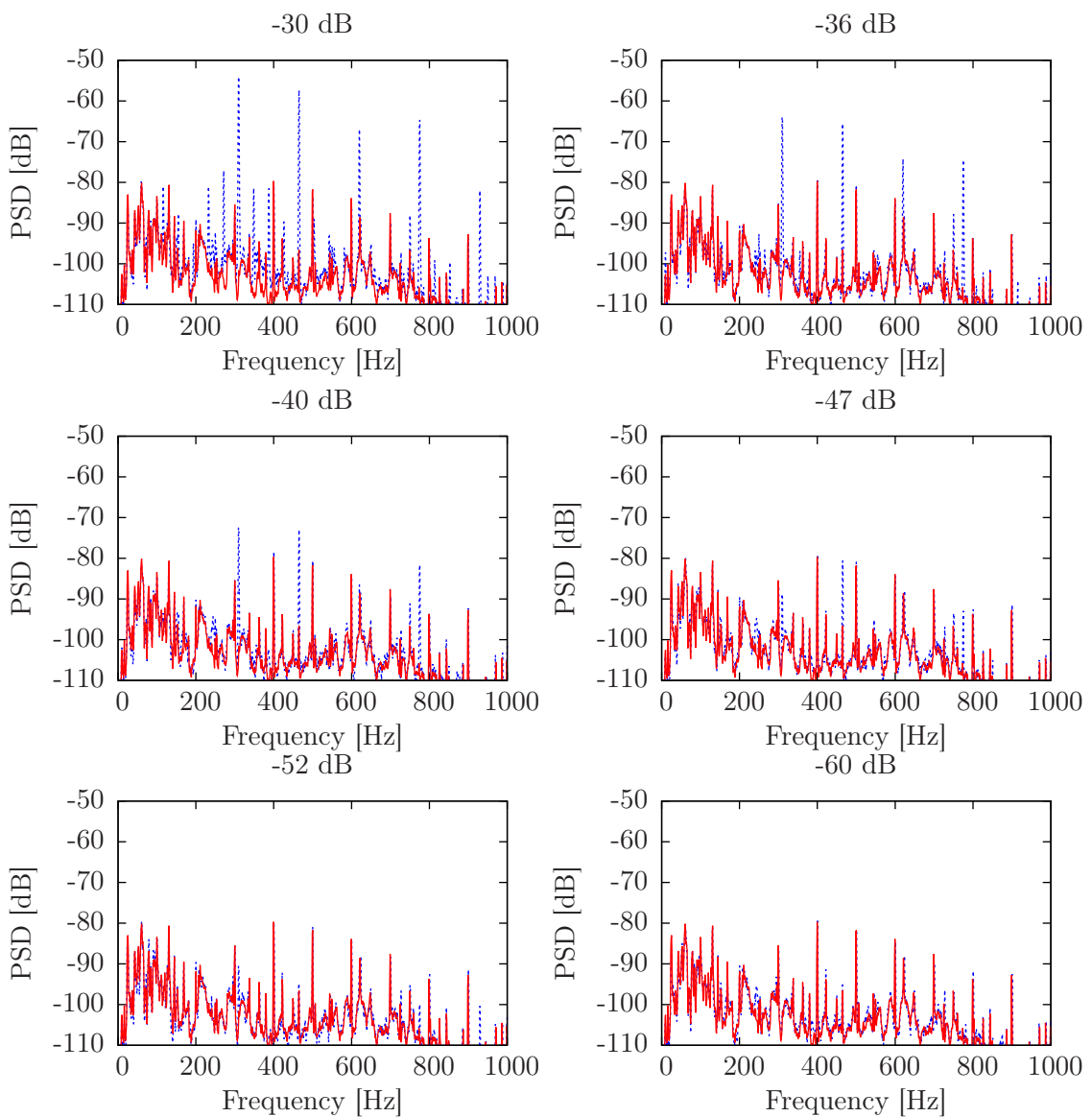


Figure 4.1: PSD of error microphone signal for FXLMS ANC system, for different levels of a 155 Hz tonal noise and noise floor level.

The results are even worse, because below 1 kHz, where the ANC systems are usually used, the human hearing system is much more sensitive to higher frequencies (Bauer & Torick, 1996). With A-weighting, the difference between the power of the primary tone without ANC and secondary harmonics after ANC is even smaller and it is equal to 17 dB (see Figure 4.2).

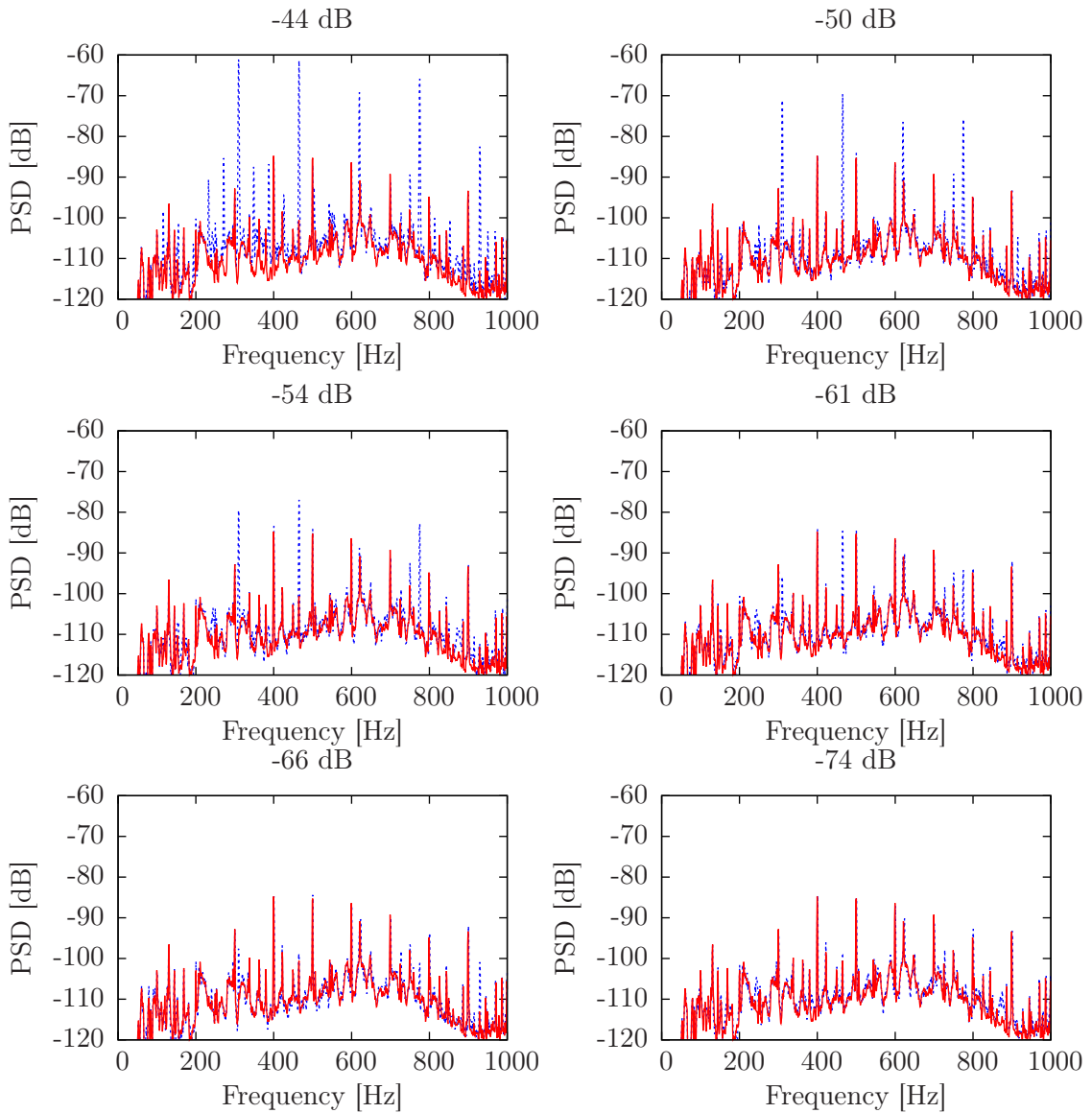


Figure 4.2: PSD of A-weighted error microphone signal for FXLMS ANC system, for different levels of 155 Hz tonal noise and noise floor level.

The feed-forward system with a linear control filter is unable to cope with higher harmonics generated by the nonlinearity. In the ideal case, for a pure tonal signal, the reference signal is sinusoidal and the output of such system with linear control filters will always be a sinusoidal signal of the same frequency as the reference signal.

To allow to cope with plant nonlinearity the system should use feedback control or nonlinear filters.

4.2 Internal Model Control

Because of high delays in the secondary path of ANC systems and sound radiation control systems, the FXLMS algorithm in the Internal Model Control (IMC) structure feedback system can be used (Figure 4.3). The equivalent block diagram for the sound radiation control is presented in Figure 4.4.

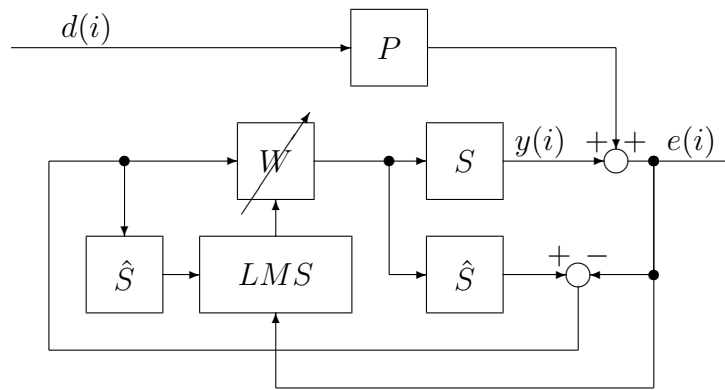


Figure 4.3: Internal Model Control FXLMS ANC system.

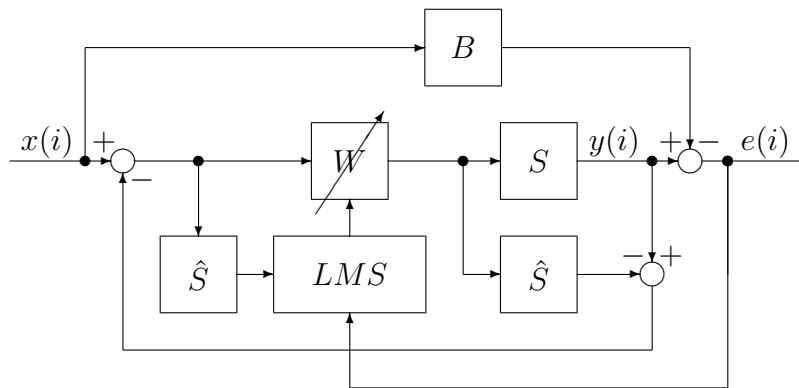


Figure 4.4: Internal Model Control FXLMS sound radiation system.

In the ANC system, the reference signal for the FXLMS algorithm is calculated by subtracting the error signal, $e(i)$, from the control signal filtered by a secondary path model. This subtraction can be also written in reverse order, as in (Pawelczyk, 2005), because when the set point is equal to zero, as in ANC, the positive feedback

loop can be converted to the negative one by just negating parameters of the control filters. However, for the sound radiation control the negative feedback loop must be used.

4.2.1 Experimental verification

The IMC system was applied for control of sound radiation from the plate with three MFC actuators, considered in Section 3.2.1.

Figure 4.5 presents the PSD of a generated 180 Hz tone. The IMC system reduced the second harmonic by 15 dB and the third harmonic by 5 dB, as compared to the linear feed-forward controller. For the first four harmonics the Total Harmonic Distortion THD_R (Shmilovitz, 2005) was improved from 10% to 2%. The results are better, but the harmonic distortion is still significant.

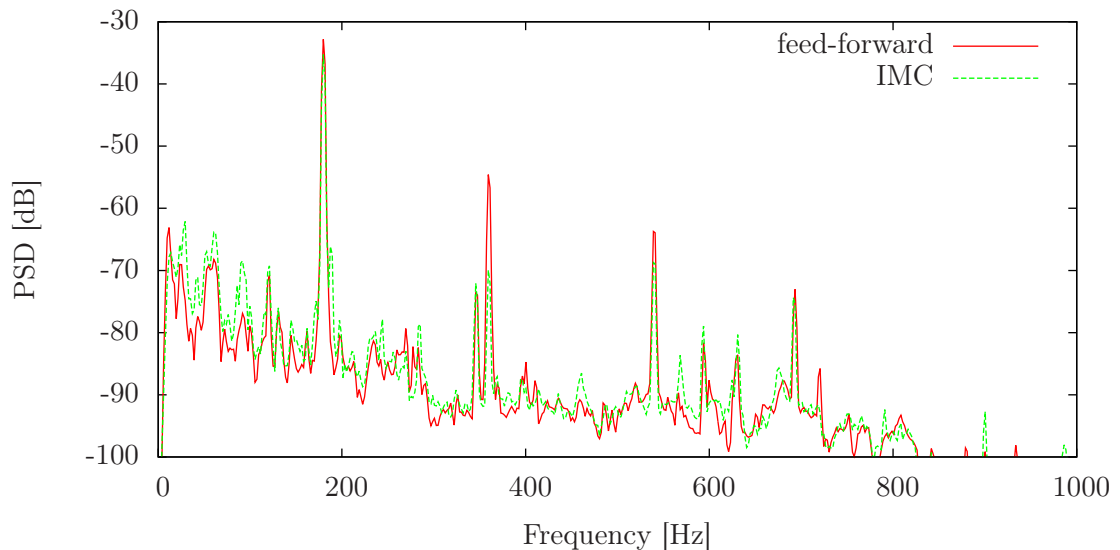


Figure 4.5: Comparison of PSDs of a generated 180 Hz tone for linear feed-forward sound radiation control system and the IMC system.

4.3 Nonlinear filters

4.3.1 NARMA filters

Nonlinear extension of ARMA models, usually used for modeling of linear filters, are NARMA (Nonlinear ARMA) models. The NARMA model can be written as

a general nonlinear function of regressors of the input signal and the output signal (Liao & Sethares, 1995):

$$y(i+1) = f(x(i), x(i-1), \dots, x(i-N_B), y(i), y(i-1), \dots, y(i-N_A), w_0, w_1, \dots, w_k, \dots, w_{K-1}), \quad (4.1)$$

where $y(i)$ is the value of the output signal of the i -th sample, f is an arbitrary nonlinear function, $x(i)$ is the input signal, and w_k is the k -th coefficient. If the f function is linear the model becomes ARMA.

The model can represent the plant with a smaller number of coefficients compared to other simplified models that will be used later, such as Volterra expansion (Liao & Sethares, 1995), but on-line estimation of parameters needed for adaptive control is difficult.

4.3.2 Artificial Neural Networks

Artificial neural networks (ANN) is a subclass of nonlinear models widely used for modeling nonlinear systems. The idea of ANN is inspired by natural neural networks present in animal central nervous systems.

The artificial neural network is built based on artificial neurons (Figure 4.6), which are modeled by the following equation (Haykin, 1994):

$$y = f_a \left(\sum_{j=0}^n w_j x_j \right), \quad (4.2)$$

where x_j are the inputs, except for $x_0 = 1$ (which is used as a bias), w_j are the weights, and the f_a is a nonlinear activation function.

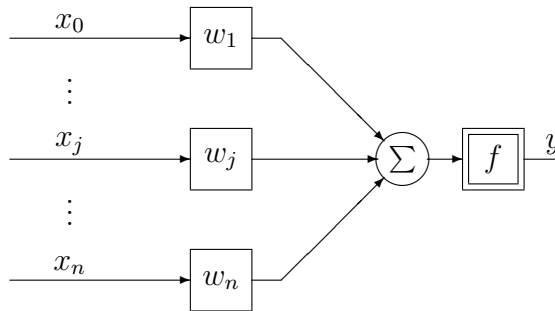


Figure 4.6: Artificial neuron.

Artificial neurons are grouped into networks. Usually simple multilayer topologies are used, where neurons are grouped into layers (Figure 4.7) (Haykin, 1994). The first layer inputs are connected to the artificial neural network inputs. The outputs of each layer are connected to the inputs of all neurons in the next layer, except for the last layer, where the outputs are used as artificial neural network outputs.

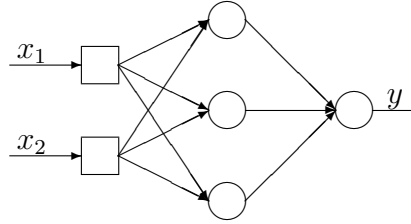


Figure 4.7: Artificial neural network.

4.3.3 Nonlinear FIR filters

For simplicity, for control nonlinear FIR models are usually preferred over nonlinear ARMA models. The general nonlinear FIR filter can be written as:

$$y(i+1) = f(x(i), x(i-1), \dots, x(i-N), w_0, w_1, \dots, w_k, \dots, w_{K-1}). \quad (4.3)$$

Identification of nonlinear FIR filters is still difficult and other simpler models are preferred.

4.3.4 Nonlinear FIR filters linear with respect to parameters

To simplify adaptation, nonlinear filters that are linear with respect to parameters are used. The outputs of such filters can be written as:

$$y(i+1) = \sum_{j=1}^K w_j f_j(x(i), x(i-1), \dots, x(i-N)), \quad (4.4)$$

where w_j are filter parameters and f_j are nonlinear functions.

A large number of filters fall into this category (George & Panda, 2013), including Volterra filters (Tan & Jiang, 1997), FSLMS (Das & Panda, 2004; George & Panda, 2012), Generalized FLANN (Sicuranza & Carini, 2011).

4.3.5 Hammerstein models

The Hammerstein model combines a nonlinear static function with a linear dynamics:

$$y(i+1) = W(z^{-1})F(x(i)), \quad (4.5)$$

where $W(z^{-1})$ is a linear model and F is a nonlinear function.

Much more complex models can be build as a sum of Hammerstein models (Mazur & Pawełczyk, 2011d, 2013c):

$$y(i+1) = \sum_{k=1}^K W_k(z^{-1})F_k(x(i)). \quad (4.6)$$

Figure 4.8 presents the structure of such filter.

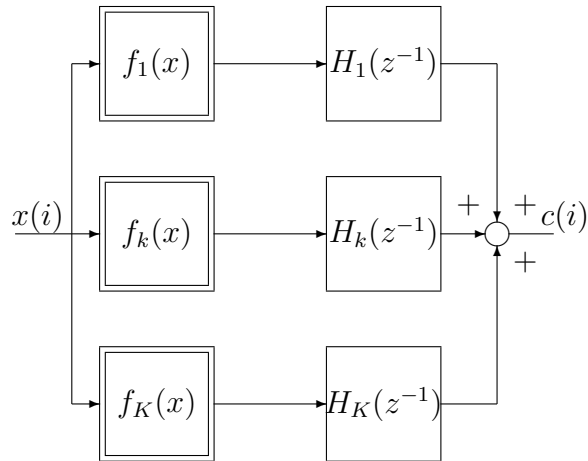


Figure 4.8: Sum of Hammerstein models nonlinear control filters.

This model can also be extended by combining values of the reference signal from different samples:

$$u(i+1) = \sum_{k=1}^K W_k(z^{-1})F_k(x(i), x(i-1), \dots, x(i-(R-1))) \quad (4.7)$$

where R is the number of regressors used by nonlinear function.

4.4 Nonlinear feed-forward control

4.4.1 Artificial neural networks

Employment of artificial neural networks for Active Control was proposed in (Snyder & Tanaka, 1995). The ANN was used both for modeling the secondary path and as the control filter in the Active Vibration Control system. The Filtered-x Back Propagation (FxBP) algorithm was proposed for updating weights of the control ANN.

The ANN has two significant disadvantages: numerical complexity is very high, and the adaptation algorithms are complex. The numerical complexity is a problem especially important for Active Noise Control applications, where the control filter must have a long enough impulse response to be effective.

4.4.2 Volterra FXLMS

Because of complexity of ANNs a large number of simpler, faster nonlinear control structures have been developed. One of early proposed alternatives was to use truncated Volterra series polynomials (Tan & Jiang, 1997, 2001).

The Volterra series is defined as (Schetzen, 1980):

$$y(i) = \sum_{j=1}^N y_j(i). \quad (4.8)$$

In (4.8) N is the filter order, and $y_j(i)$ is equal to:

$$y_j(i) = \sum_{m_0=0}^{M-1} \sum_{m_1=m_0}^{M-1} \cdots \sum_{m_{j-1}=m_{j-2}}^{M-1} w_{j,m_0,m_1,\dots,m_{j-1}} \prod_{k=1}^j x(i - m_k), \quad (4.9)$$

where M is the number of used previous samples.

4.4.3 FSLMS

The FSLMS algorithm was proposed by Das & Panda (2004). It uses Functional Link Artificial Neural Network (FLANN) nonlinear filter structure. Figure 4.9 shows the structure of the FSLMS algorithm. The output of the control filter for single channel

system is defined as (Das & Panda, 2004):

$$u(i) = \mathbf{w}^T(i)\mathbf{s}(i), \quad (4.10)$$

where $\mathbf{w}(i) = [w_1(i), w_2(i), w_3(i), \dots, w_M(i)]^T$, and:

$$\mathbf{s}(i) = [s_{1,1}(i), s_{1,2}(i), s_{1,3}(i), s_{1,2P+1}(i), \dots, s_{2,1}(i), s_{2,2}(i), s_{2,3}(i), s_{2,2P+1}(i), \dots, s_{N,1}(i), s_{N,2}(i), s_{N,3}(i), s_{N,2P+1}(i)]. \quad (4.11)$$

The $s_{j,k}(i)$ element is equal to:

$$s_{j,k} = \begin{cases} x(i-j) & k = 1 \\ \sin(l\pi x(i-j)) & k > 1 \text{ and even} \\ \cos(l\pi x(i-j)) & k > 1 \text{ and odd} \end{cases} \quad (4.12)$$

where $1 \leq k \leq P$.

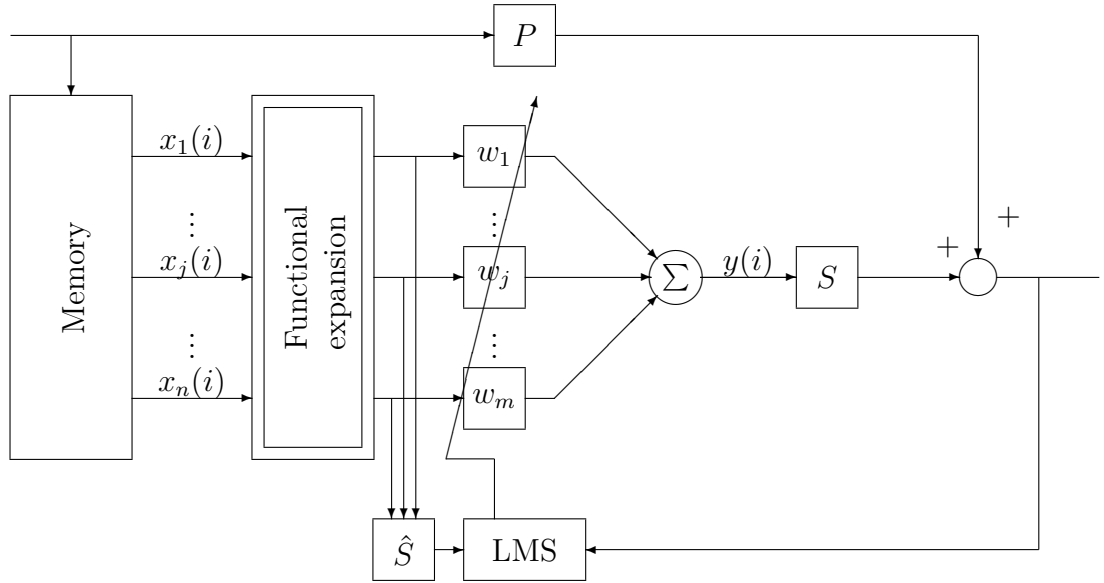


Figure 4.9: FSLMS Active Noise Control system diagram (based on (Das & Panda, 2004)).

4.4.4 Nonlinear control with the Hammerstein-like structure

When multiple secondary paths are used, a separate filter can be employed for each path, c , i.e.:

$$u_c(i+1) = \sum_{k=1}^K W_{c,k}(z^{-1}) F_k(x(i), x(i-1), \dots, x(i-(R-1))). \quad (4.13)$$

To simplify the system, all nonlinear control filters share the same set of nonlinear functions F_k and the same order of $W_{c,k}$ FIR adaptive filters. However, it does not limit the considerations, because for systems with secondary paths of different types, different number and type of nonlinear functions might be used. For instance, for a system, which combines a vibrating plate and a classical loudspeaker, the loudspeaker subsystem might use a linear control filter with single function $F_1 = 1$. In this thesis multiple secondary paths are related to different actuators of the same type mounted on a single plate, so the same structure is used for all actuators.

The structure of the ANC system with such nonlinear filter is shown in Figure 4.10. The bank of F_k nonlinear functions converts reference signal, $x(i)$, into a vector $\mathbf{x}(i) = [x_1(i), x_2(i), x_3(i)]^T$. The rest of the system is a classical linear active control system with multiple reference signals. The reference signals are then filtered by a bank of linear FIR adaptive filters $W_{c,k}(z^{-1})$. These filters can be grouped into a matrix of FIR filters $\mathbf{W}(z^{-1})$:

$$\mathbf{W}(z^{-1}) = \begin{bmatrix} W_{1,1}(z^{-1}) & W_{1,2}(z^{-1}) & \cdots & W_{1,K}(z^{-1}) \\ W_{2,1}(z^{-1}) & W_{2,2}(z^{-1}) & \cdots & W_{2,K}(z^{-1}) \\ \vdots & \vdots & \ddots & \vdots \\ W_{C,1}(z^{-1}) & W_{C,2}(z^{-1}) & \cdots & W_{C,K}(z^{-1}) \end{bmatrix}. \quad (4.14)$$

For such system, (4.13) can be rewritten as:

$$u_c(i+1) = \sum_{k=1}^K W_{c,k}(z^{-1}) x_k(i). \quad (4.15)$$

Outputs of adaptive control filters $W_{c,k}(z^{-1})$ are summed according to (4.15), and form a vector of control signals $\mathbf{u}(i+1) = [u_1(i+1), u_2(i+1), \dots, u_C(i+1)]^T$. These signals are then used to drive a vector of secondary paths $\mathbf{S} = [S_1, S_2, \dots, S_C]^T$.

For the adaptive version, the adaptation algorithm might use the vector of reference signals, $\mathbf{x}(i)$, and the scalar error signal, $e(i)$, to adapt weights of control filters

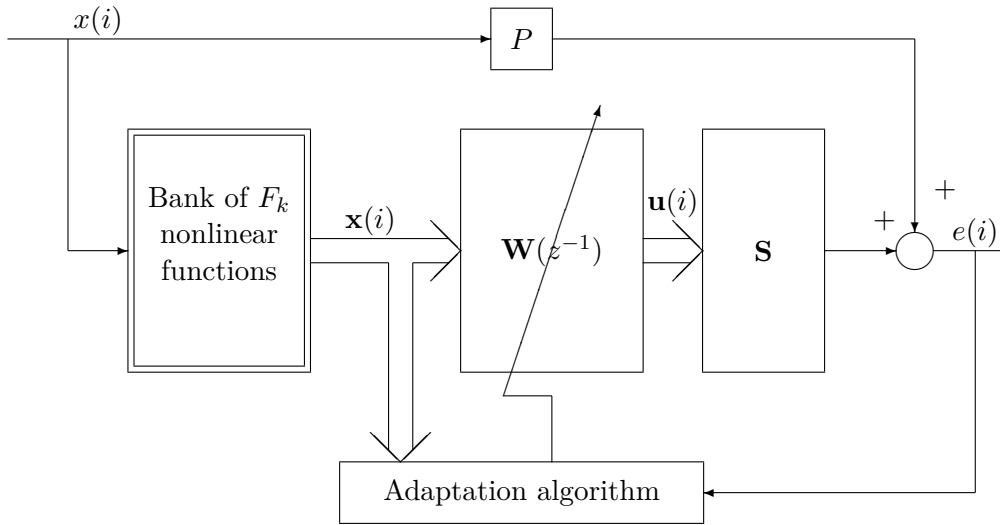


Figure 4.10: Multichannel ANC system with Hammerstein nonlinear control filters.

$\mathbf{W}(z^{-1})$.

4.5 Selection of nonlinear functions

4.5.1 Polynomials

The selection of nonlinear functions is a very important step. The feed-forward ANC system can only reduce noise correlated with the reference signals. In the ideal case the ANC error is orthogonal to the inputs. To yield the unique solution, reference signals for the multichannel FXLMS algorithm should be uncorrelated (Tu & Fuller, 2000; Mazur & Pawełczyk, 2013c). This is, however, hard to satisfy for real applications.

One of the simplest set of nonlinear functions are polynomials. For instance, the following polynomials can be used:

$$\begin{cases} F_1(x) = x^1 \\ F_2(x) = x^2 \\ F_3(x) = x^3 \\ \vdots = \vdots \\ F_n(x) = x^n \end{cases} \quad (4.16)$$

In such case the effects on the spectrum of signal can easily be predicted. The x^n polynomial will generate the n -th harmonic. However, for $n > 1$ lower order harmonics are also generated. This is demonstrated in Figure 4.11. For instance, x^3 generates

not only the 3rd harmonic, but the fundamental frequency as well, and x^4 generates not only the 4th harmonic but also the 2nd harmonic and a constant. Generally, x^n generates the n -th harmonic and also $(n - 2)$ -nd, $(n - 4)$ -th, \dots harmonics.

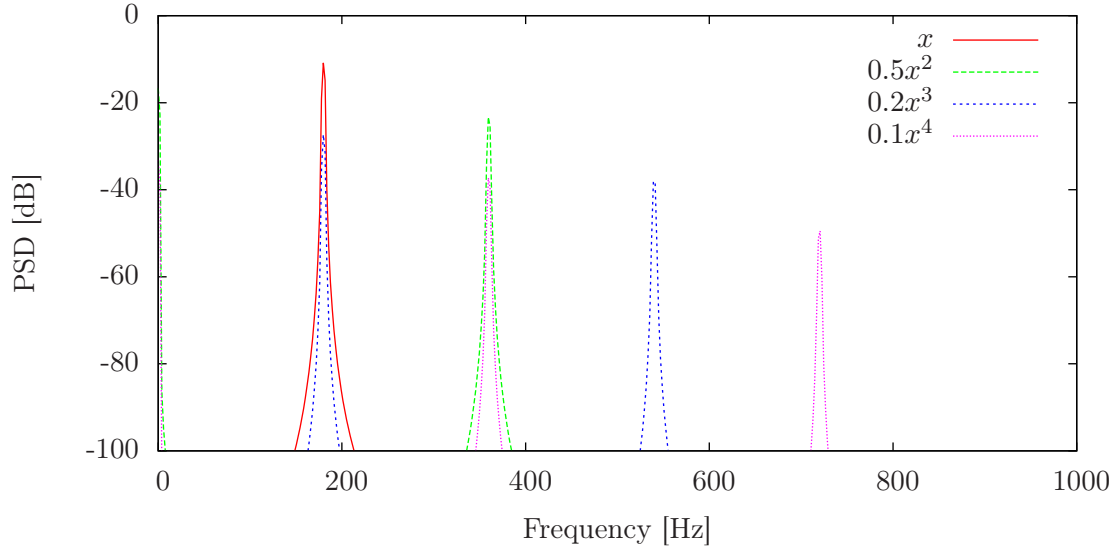


Figure 4.11: PSD of a 180 Hz tone after applying polynomial nonlinear function.

4.5.2 Chebyshev polynomials

For some specific signals it is possible to construct polynomials, which generate orthogonal output signals. For instance, for tonal signals the Chebyshev polynomials can be used (Gil *et al.*, 2007):

$$\begin{cases} F_1(x) = x^1 \\ F_2(x) = 2x^2 - 1 \\ F_3(x) = 4x^3 - 3x \\ F_4(x) = 8x^4 - 8x^2 + 1 \\ \vdots = \vdots \\ F_n(x) = 2xF_{n-1}(x) - F_{n-2}(x) \end{cases} \quad (4.17)$$

In this case, a specific single harmonic can be generated by the appropriate Chebyshev polynomial (see Figure 4.12). Therefore, employment of such polynomials allows for applying an individual linear filter for each harmonic. Unfortunately, such property of the Chebyshev polynomials is not valid for signals other than tones. For other types of input signals, other polynomials, which generate uncorrelated outputs can be found.

For example, for a normally distributed random signal the Hermite polynomials can be appropriate. The Hammerstein structure can also be employed for Volterra series polynomials.

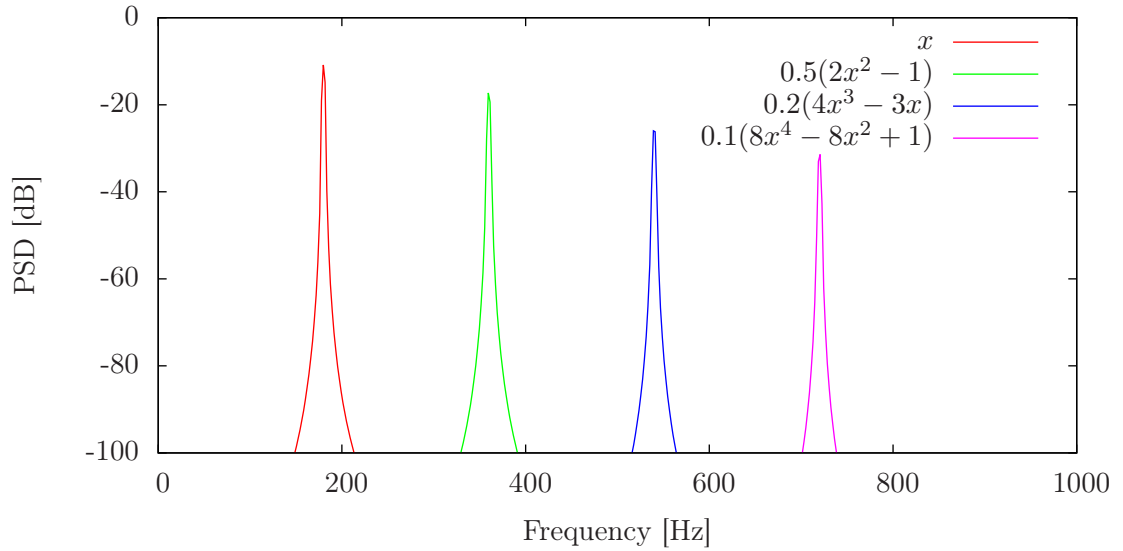


Figure 4.12: PSD of a 180 Hz tone after applying Chebyshev polynomials.

4.5.3 Trigonometric expansion

For the FSLMS algorithm, the following functions are used:

$$\left\{ \begin{array}{l} F_1(x) = x \\ F_2(x) = \sin(\pi x) \\ F_3(x) = \cos(\pi x) \\ \vdots \\ F_{2p}(x) = \sin(p\pi x) \\ F_{2p+1}(x) = \cos(p\pi x) \\ \vdots \\ F_{2P}(x) = \sin(P\pi x) \\ F_{2P+1}(x) = \cos(P\pi x) \end{array} \right. \quad (4.18)$$

4.6 Adaptation of control filter weights

4.6.1 Filtered-reference structure

When the filters are linear with respect to parameters, the classical adaptive control adaptation algorithms, like LMS, Affine Projection or RLS, with appropriate modifications to improve convergence properties can be employed. Otherwise, more complex algorithms such as genetic algorithms (Górski & Morzyński, 2013) or memetic algorithms should be employed.

The Normalized Leaky LMS algorithm takes the form (Elliott, 2001):

$$\mathbf{w}_{c,k}(i+1) = \alpha \mathbf{w}_{c,k}(i) - \mu \frac{\mathbf{x}_{c,k}^*(i)}{\sum_{j=1}^C \sum_{k=1}^K \mathbf{x}_{j,k}^{*T}(i) \mathbf{x}_{j,k}^*(i) + \zeta} e_c^*(i), \quad (4.19)$$

For notation simplicity it is assumed that orders of all secondary paths are the same. The symbol $e_c^*(i)$ stands for the error signal for the c -th secondary path.

In contrary to electrical noise cancellation or speech enhancement (see, e.g. (Latos, 2011)) for active noise/vibration control applications the filter outputs drive the secondary path (acousto-electric or vibro-acousto-electric), the algorithm must be modified to guarantee convergence (Pawełczyk, 2008). The most popular modification is filtration of the reference signal by a model of the secondary path, what results in obtaining the well-known Filtered-x LMS algorithm (Elliott, 2001; Kuo & Morgan, 1996). Figure 4.13 shows a block diagram of the multichannel FXLMS algorithm, when used for adaptation of nonlinear filters as in (4.13). The ANC error signal is then used as the error signal for the LMS algorithm $e_c^*(i) = e(i)$.

4.6.2 Filtered-error structure

Because each reference signal must be filtered by a model of the corresponding secondary path, the Filtered-x structure involves a number of numerical operations, if multiple reference signals are generated from a single reference with a bank of F_k filters. The Filtered-error LMS (FELMS) algorithm is more appropriate in this case (Figure 4.14) (Mazur & Pawełczyk, 2012c, 2013c). In the FELMS algorithm the multiple reference signals are simply delayed, $x_{c,k}^*(i) = x_k(i - (M - 1))$, but the error signal is obtained as:

$$e_c^*(i) = \hat{\mathbf{s}}_c(i)^T \mathbf{e}(i), \quad (4.20)$$

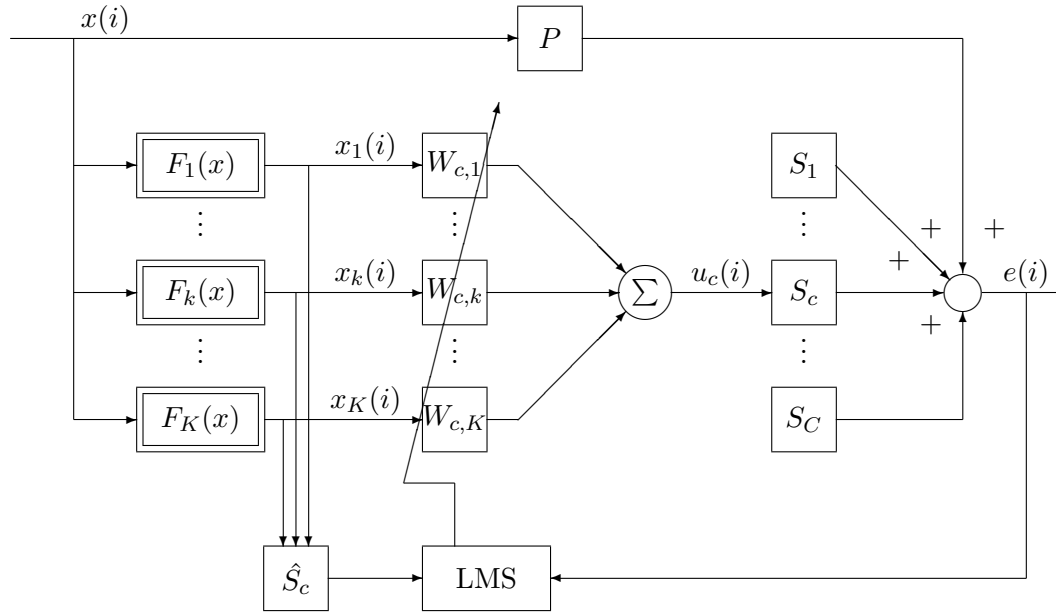


Figure 4.13: An excerpt of the ANC system with Hammerstein nonlinear control filters and multichannel FXLMS algorithm for the c -th control channel.

where $\hat{\mathbf{s}}_c(i) = [\hat{s}_{c,M-1}(i), \hat{s}_{c,M-2}(i), \dots, \hat{s}_{c,0}(i)]$ is a time-reversed model of the c -th secondary path, $\mathbf{e}(i) = [e(i), e(i-1), \dots, e(i-(M-1))]^T$ is a vector of regressors of the error signal.

The FELMS structure can also be used with nonlinear plant model \hat{S}_c . Such idea was tested, but no significant improvements have been observed. The linear secondary path model is sufficient for adaptation.

4.7 Control of sound generation

Figure 4.15 shows a comparison of results obtained for the feed-forward FXLMS control system with linear control filter, IMC FXLMS feedback system, and the feed-forward FXLMS system with nonlinear Hammerstein control filter. Two nonlinear functions were used:

$$\begin{cases} F_1(x) = x^4 \\ F_2(x) = x^5 \end{cases} \quad (4.21)$$

The feed-forward control system with nonlinear control filter was able to reduce all harmonics to the floor level. The THD_R coefficient was improved to 0.2%. Table 4.1 presents values of THD_R for different control algorithms.

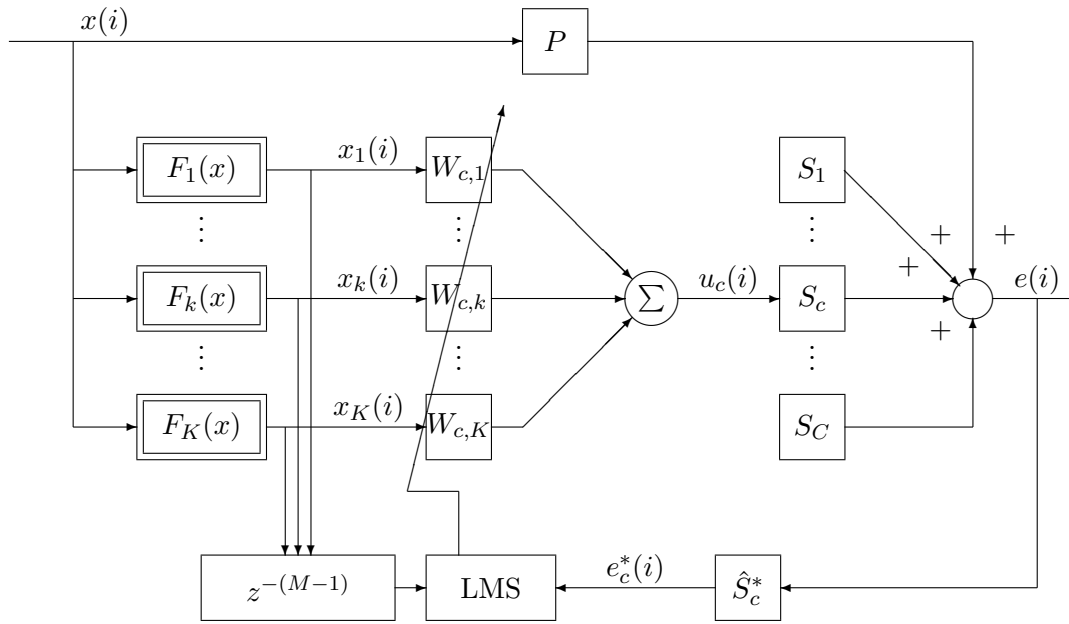


Figure 4.14: An excerpt of the ANC system with Hammerstein nonlinear control filters using FELMS algorithm for the c -th control channel.

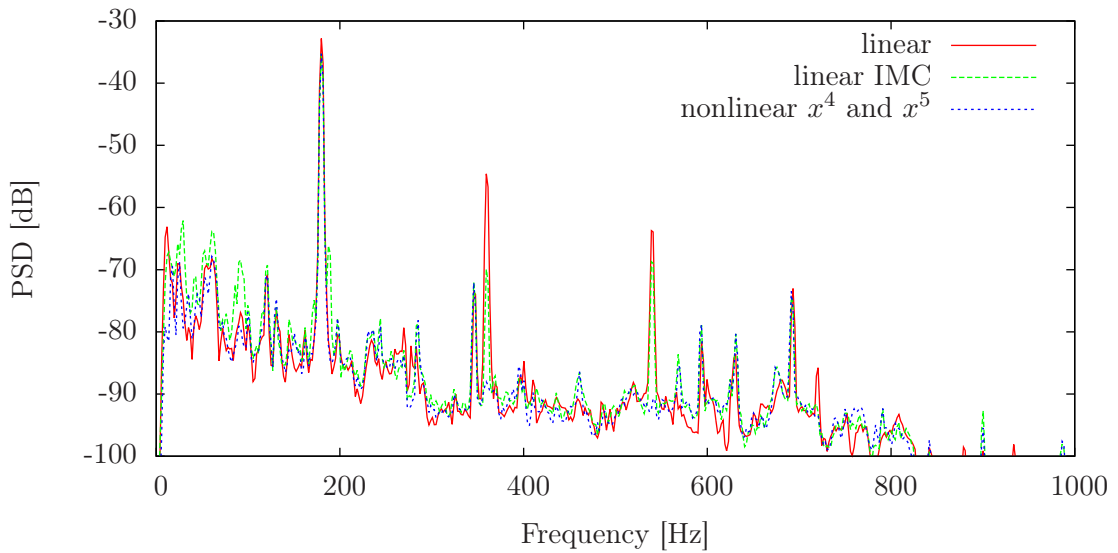


Figure 4.15: Comparison of PSDs of a generated 180 Hz tone for different sound radiation control systems.

Table 4.1: Total Harmonic Distortion, THD_R , for a 180 Hz tone.

Control algorithm	THD_R
linear feed-forward	10%
IMC	2%
non-linear feed-forward	0.2%

4.8 Application to ANC

4.8.1 Experimental verification

For all experiments the sampling frequency has been set to 4 kHz, and 8th order Butterworth low-pass analogue filters with 1200 Hz cut-off frequency have been used as anti-aliasing and reconstruction filters. The order of the FIR path models has been set to $M = 256$ for all experiments. This value has been chosen based on impulse response analysis. The order of the FIR control filters has been set to $N = 256$ for all experiments. Filtered-error structure has been used. For nonlinear control, two functions $F_1 = x$ and $F_2 = x^3$ have been employed.

For tests, two simple deterministic signals, a 382 Hz tone, and a sum of 382 Hz and 504 Hz tones, have been selected. The frequencies for tonal signals have been roughly selected for the secondary path to yield a high gain. The exact choice has been dictated to have a high least common multiple with the other frequency and the sampling frequency, to avoid aliasing of harmonic frequencies. The third signal has been a recorded real-world noise originating from ball-bearing pulverizers.

Figure 4.16 presents the PSD of A-weighted noise measured by the error microphone for the 382 Hz tonal noise. The ANC system with linear control filter is able to reduce the fundamental frequency to the noise floor level. However, some clearly visible harmonic frequencies are generated. The measured sound pressure level reduction is equal to 22.0 dB. However, the dominating third harmonic is in the band of a higher sensitivity of the human hearing system. With the A-weighting, the reduction level drops to 17.3 dB. The ANC system with nonlinear control filters is able to reduce the third harmonic to the noise floor level, and improve the sound pressure level reduction to 28.7 dB, and to 27.9 dB with A-weighting. It is in accordance with the design assumption, because it has been noticed that the highest noise reduction

could be achieved by reducing the third harmonic, and hence the nonlinear function $F_2 = x^3$ has been selected. Further improvements can be obtained by adding more non-linear functions or, for simple signals, by using nonlinear functions, which would generate multiple harmonics.

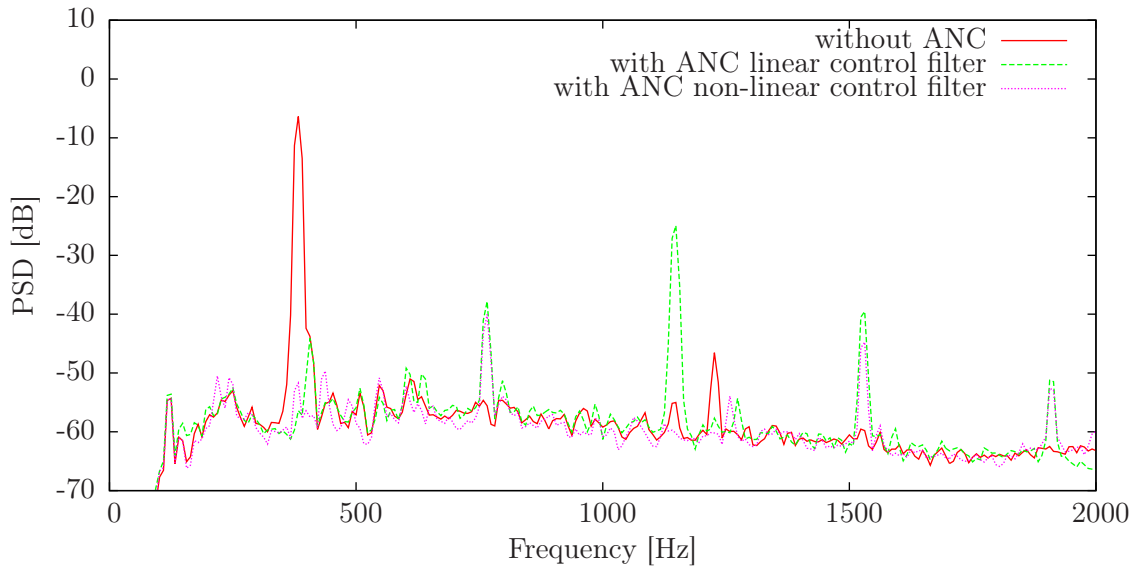


Figure 4.16: PSD of A-weighted error microphone signal for different control strategies and a 382 Hz tonal noise.

Figure 4.17 presents the PSD of A-weighted noise measured by the error microphone for a sum of two tones, 382 Hz and 504 Hz. Similarly to the single tone case, the third harmonic after reduction by the ANC system with linear control filter is dominant. By applying the ANC system with nonlinear control filters, the A-weighted noise reduction level was improved from 15.3 dB to 23.9 dB.

For more complex noise signals such as recorded noise from ball-bearing pulverizers the improvement is much lower (see Table 4.2). In such case nonlinear distortions have lower power than the residue from active reduction of primary noise.

4.9 Summary

Nonlinearity of the vibrating plate significantly degrades performance of the ANC system. The human hearing system is more sensitive to higher harmonics than to fundamental frequencies of the noise usually tackled with by active means.

By using a nonlinear control filter the performance of ANC can be improved, resulting in a high acoustic comfort. The nonlinear control filter, however, comes

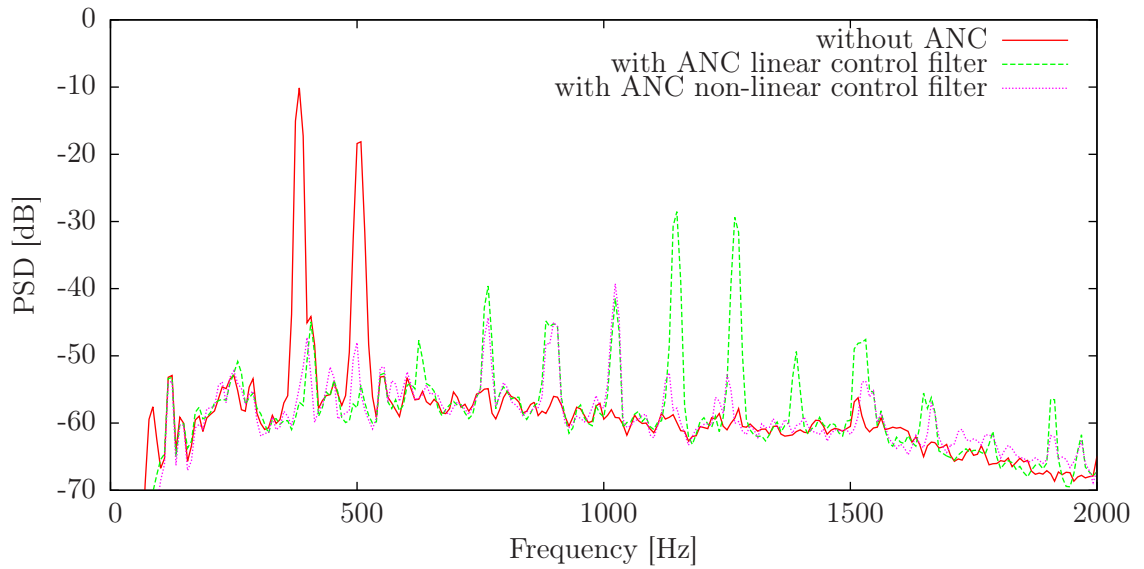


Figure 4.17: PSD of A-weighted error microphone signal for different control strategies for sum of 382 Hz and 504 Hz tones.

Table 4.2: Noise Pressure Levels measured without active control and with different control systems operating (A-weighted).

Noise	without ANC [dB]	FXLMS [dB]	nonlinear FELMS [dB]
382 Hz tone	87.0	69.7	59.1
382 Hz + 504 Hz tones	82.8	67.5	58.9
ball-bearing pulverizers	74.7	64.6	64.1

with the cost of huge increase of computational load. Application of the Filtered-error LMS algorithm instead of the Filtered-reference LMS algorithm is therefore beneficial, because the set of generated reference signals does not need filtering. Significant improvements have been obtained only for simple signals, where noise reduction level was high and nonlinear distortions were dominant.

Chapter 5

Two-layer adaptive control

Introduction

Unfortunately, vibrating plates have worse sound radiation properties than loudspeakers. This causes problems for Active Noise Control systems. Plates have multimodal responses with high variations of the amplitude. To effectively excite multiple vibration modes, multiple actuators are usually needed. Multiple actuators mounted on a single plate significantly increase the total number of control signals to be worked out. ANC systems are then required to have a large number of secondary paths. Some of the secondary paths that share the same vibrating plate are not fully independent, and cannot be used to effectively provide reduction of noise at multiple zones of quiet.

In this chapter, a two-layer control system is proposed, which first controls the plate response using methods described in Chapter 3, and then takes advantage of the system, easier to control, in order to reduce noise more efficiently.

The typical approach for ANC was described in Chapter 2. In case of vibrating plates the secondary paths are not fully independent.

For ANC systems it is convenient to consider a single plate as a single sound source. However, to effectively excite multiple vibration modes multiple actuators are usually needed, what makes the system multichannel. Each channel have a different amplitude response. Similarly, for classical loudspeakers it is important to yield a flat amplitude response for the whole frequency range of acoustic signals, and in many cases multiple speakers are used to build a single multi-way loudspeaker. In case of loudspeakers, each speaker is used to emit sound in a given frequency band. The loudspeaker input signal is filtered by a set of crossover filters to generate control signal for each speaker. In the simplest case, when the amplitude response of each speaker

is equal in passband, the sum of crossover filters must have a flat amplitude response. In case of vibrating plates with multiple actuators, the problem is more complicated. A single actuator must be used to generate sound in multiple bands. Additionally, the amplitude response of each actuator is highly irregular and additional response correction should be performed.

5.1 Two-layer active noise controller

Figure 5.1 presents a two-layer system—active noise control with plate radiation control. The ANC controller drives the plate with only one control signal, or one per plate, in case of a more complex system. The plate radiation controller is, in turn, responsible for driving actuators using this signal. Additionally, the plate radiation controller can improve response of the whole plate, and the number of parameters of the new secondary path model required for adapting the ANC controller may be much smaller.

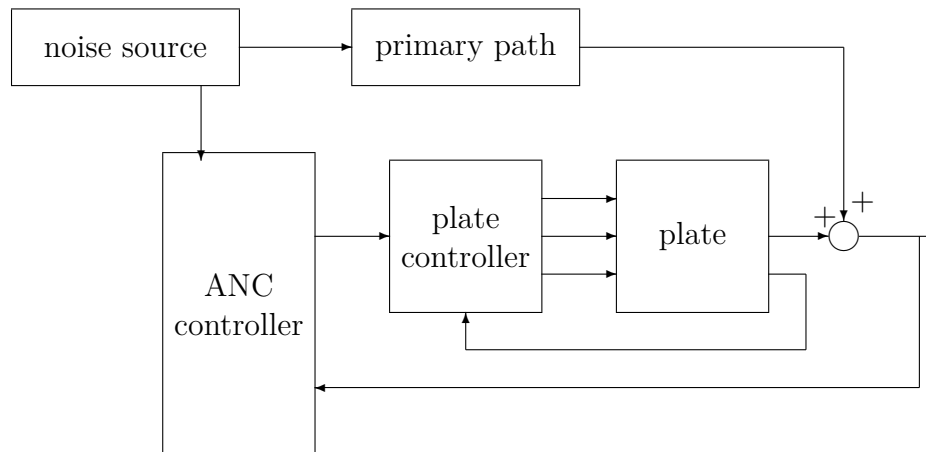


Figure 5.1: ANC system with plate radiation controller.

In the simplest case, a fixed-parameter feed-forward controller can be used as the plate radiation controller. It is placed between the output of the ANC controller and the actuator. If multiple actuators are used, the radiation control filter is necessary for each actuator. Only one ANC adaptive filter is still used. This allows for a faster adaptation.

In case of an ANC system with adaptive plate controller, additional care must be taken to provide convergence of both adaptive filters. A relevant structure is proposed in Figure 5.2.

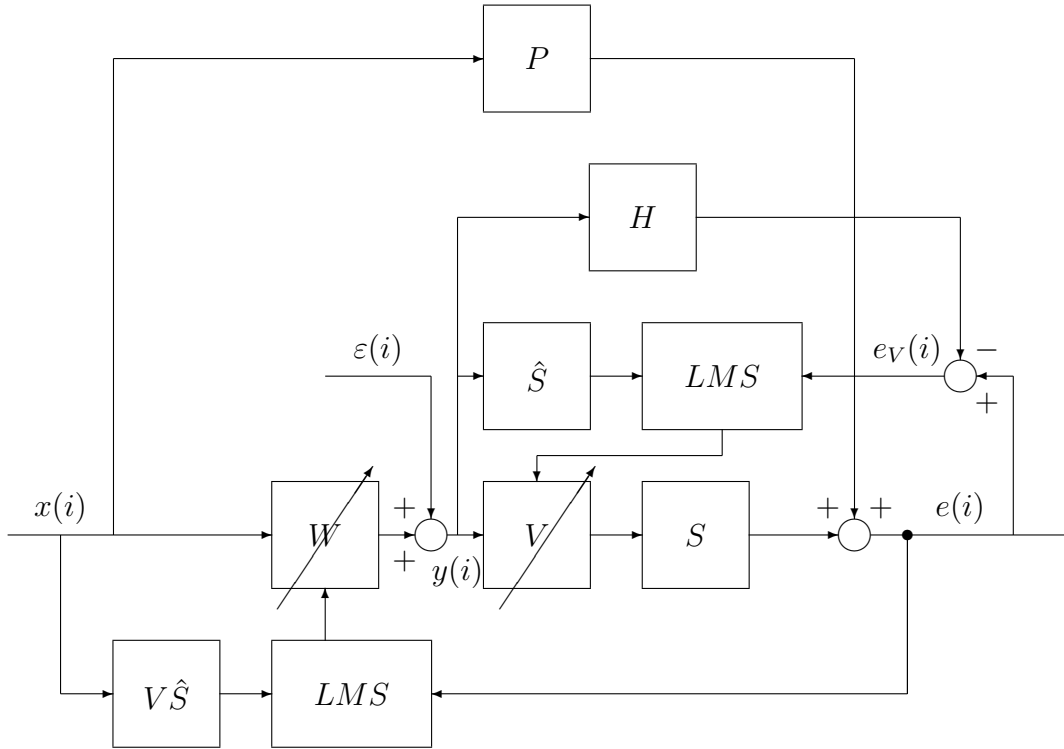


Figure 5.2: ANC with adaptive plate controller.

The error signal yielded during operation of the ANC system is equal to:

$$e(i) = P(z^{-1})x(i) + W(z^{-1})V(z^{-1})S(z^{-1})x(i) + V(z^{-1})S(z^{-1})\varepsilon(i). \quad (5.1)$$

The adaptive plate controller adds additional noise $\varepsilon(i)$ to the output of the ANC controller, $c(i)$:

$$y(i) = c(i) + \varepsilon(i) = W(z^{-1})x(i) + \varepsilon(i). \quad (5.2)$$

The secondary path control error signal $e_v(i)$ is equal to:

$$e_v(i) = P(z^{-1})x(i) + \left(V(z^{-1})S(z^{-1}) - H(z^{-1})\right)y(i), \quad (5.3)$$

and it can also be written as:

$$\begin{aligned} e_v(i) = & P(z^{-1})x(i) + \left(V(z^{-1})S(z^{-1}) - H(z^{-1})\right)W(z^{-1})x(i) + \\ & + \left(V(z^{-1})S(z^{-1}) - H(z^{-1})\right)\varepsilon(i). \end{aligned} \quad (5.4)$$

In this structure, the reference signal, $x(i)$, cannot be used for adaptation of both filters W and V , because only the product of those filters can directly be estimated. Because of this problem, the additional signal $\varepsilon(i)$ was introduced and the adaptation of filter V uses $\varepsilon(i)$. When the ANC filter converges, the term $P(z^{-1})x(i) + W(z^{-1})V(z^{-1})S(z^{-1})x(i)$ should be minimized in appropriate sense, and the effect of $x(i)$ signal on adaptation of V filter should be small.

In this system the ANC controller is exactly the same as described in Chapter 2, but the plate sound radiation controller must be modified as in Figure 5.2. In this case, the error signal required for adaptation of V is expressed as:

$$e_V(i) = e(i) - \mathbf{h}^T \mathbf{y}_H(i), \quad (5.5)$$

where $\mathbf{y}_H(i) = [y(i), y(i-1), \dots, y(i - (N_H - 1))]^T$ is a vector of regressors of the introduced noise $\varepsilon(i)$. If the radiation control filter were designed to control radiation to the same point in the acoustic field, the difference between $V(z^{-1})\hat{S}(z^{-1})$ and the desired model $H(z^{-1})$ should be small, and the desired model $H(z^{-1})$ could be used for reference signal filtration in the FXLMS algorithm. For different points, a model of the whole cascade $V(z^{-1})S(z^{-1})$ can be identified.

5.2 Experimental results

Figure 5.3 shows the amplitude response of secondary paths for different EX-1 actuators, and the combined amplitude response of plate with sound radiation controller with desired path $H = z^{-16}$. The goal of the control system is to reduce sound pressure level around the error microphone placed in the laboratory room.

The order of the FIR path models has been set to $M = 256$. The order of the FIR control filters for ANC controller and plate controller has been set to $N = 256$. For the higher-level ANC controller, the desired model H was used as secondary path model in FXLMS.

The plate controller introduces additional delay to the secondary path. This delay is tuned by the desired path model H . It can decrease performance of the ANC system for broadband disturbances if the reference signal is not available sufficiently well in advance. Figure 5.4 presents the PSD of a pulverizer noise used as one of test signals. It is a broadband noise with a dominating 330 Hz tonal component due to fan operation. The plate controller adds a small delay to the secondary path. This

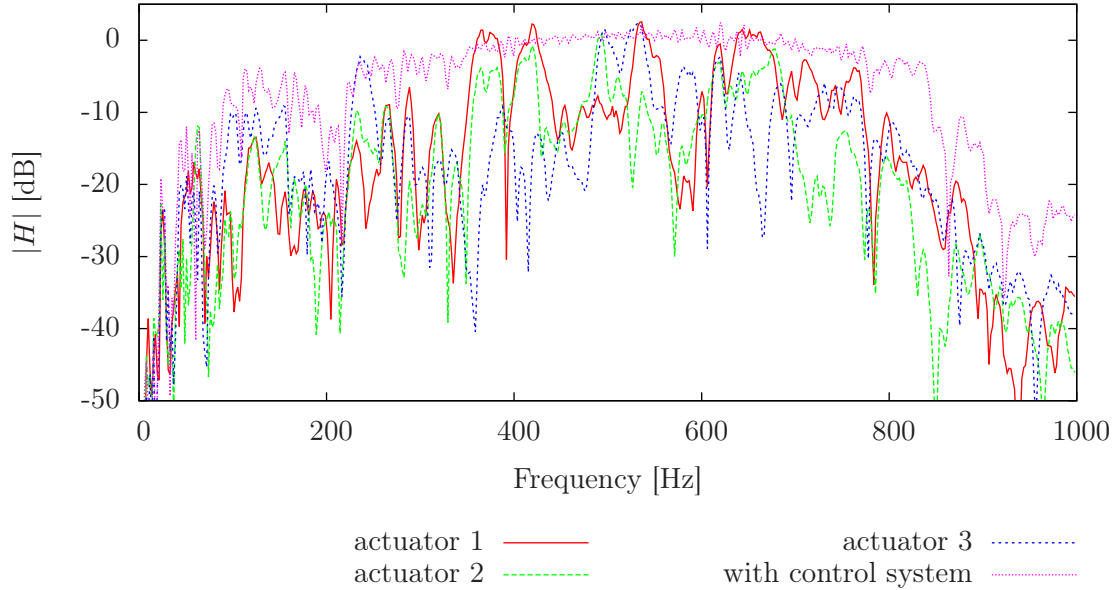


Figure 5.3: Amplitude response of secondary paths for different EX-1 actuators and the amplitude response of plate with sound radiation control system.

delay is controlled by the desired path model H . It might decrease performance of ANC system for broadband disturbances.

A-weighted results of noise control at the position of the error microphone, obtained with different systems are presented in Figure 5.5. The classical single-layer ANC system reduced the A-weighted noise pressure level by 8.5 dB compared to the case of plate passive isolation only. In case of the two-layer system the reduction was decreased to 7.1 dB. For this system, the distance between the reference microphone and the plate is too small and the anti-aliasing and reconstruction filters increase secondary path delay over the delay in the primary path. In such case, a small increase of the delay of the secondary path caused by the plate controller involves prediction action of the ANC filter, what degrades the noise reduction level. For the simple deterministic tonal and multi-tonal disturbances no differences in obtained reduction levels were observed.

5.3 Nonlinear ANC with plate controller

In Chapter 4, adaptive feed-forward systems with nonlinear control filters for plate control were investigated. Such systems are highly computationally demanding. In case of application for vibrating plates with multiple actuators separate control filters

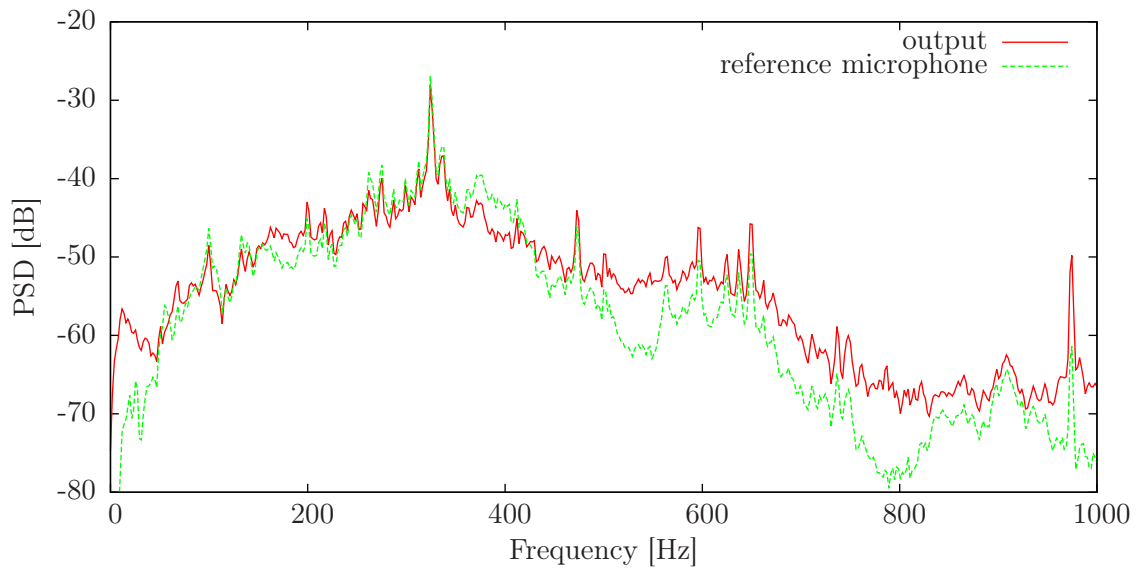


Figure 5.4: PSD of recorded pulverizer noise and the noise measured by reference microphone without ANC system.

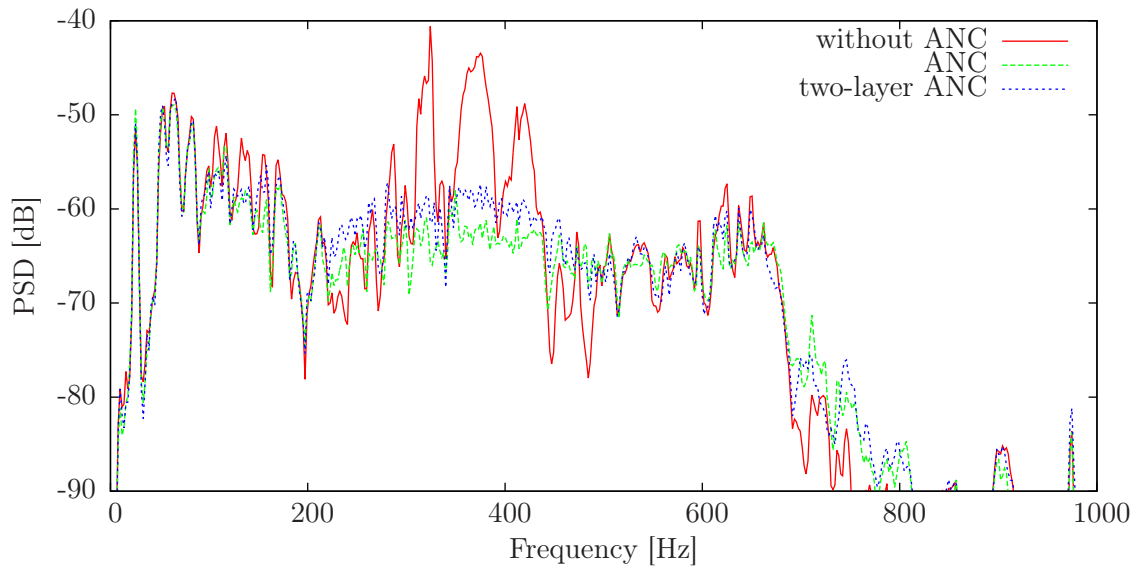


Figure 5.5: PSD of the error microphone signal for different control strategies for pulverizer noise.

were used for each actuator. This significantly increases computational cost. However, with the two-layer structure the nonlinear control can be used for a plate with control system. This allows for using a single nonlinear control filter.

The plate controller is required because of potential destructive interference of vibrations generated by different actuators when the same output signal is used to drive all actuators. Figure 5.6 shows the resulting structure (Mazur & Pawełczyk, 2013a,b). The output of nonlinear ANC control filter is filtered by the V_c filter dedicated for each actuator. Dependent of V_c filter choice, the filtration of the error signal by \hat{H}^* filter might be required. However, in the proposed system such filter is avoided, because the V_c filters are tuned to linearize the total secondary path phase response.

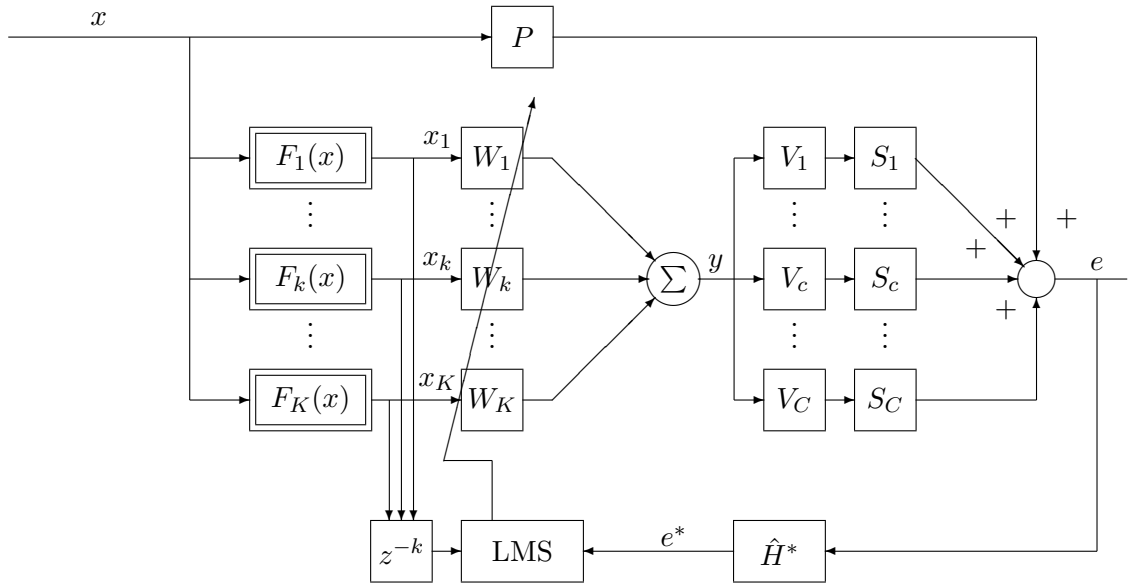


Figure 5.6: ANC system with Hammerstein nonlinear control filters using single nonlinear control filter.

Because the secondary path models may change in time (for instance they strongly depend on plate temperature (Mazur & Pawełczyk, 2011a)), V_c filters are made adaptive. This system compares the obtained actual response to the response of desired secondary path model H , and updates the weights appropriately. When the desired path have a linear phase response, filtration by \hat{H}^* is not needed, and delaying the reference signals by D steps, where D is the delay of the desired path H , is sufficient for convergence.

By using linear filters dedicated for each actuator bonded to a single plate, it is possible to use only one nonlinear control filter to efficiently drive all the actuators. The nonlinear filters are very computationally demanding, and reduction of their

number saves computational load, which can be spent for implementing more complex filters.

The per-actuator linear control filters were used also to linearize phase response of the secondary paths. That allowed for application of the FELMS, simplified even to the Delayed LMS algorithm for adaptation of nonlinear control filter weights. Such algorithm provides additional reduction of numerical operations. Efficiency of the proposed approach is particularly evident, when considering A-weighted noise reduction results.

5.3.1 Experimental verification

The system presented in Figure 5.6 was used as the nonlinear control system. The desired secondary path response H was equal to z^{-16} . The order of the V linear filters was set to $N_V = 256$. The order of control filter was set to $N = 256$. The parameters of NLMS adaptation algorithm were set to $\alpha = 1$, $\mu = 0.05$, $\zeta = 10^{-12}$. The first 5 functions of trigonometric expansion used in the FSLMS algorithm were used as the F_k functions:

$$\begin{aligned}
 F_1(x) &= x, \\
 F_2(x) &= \sin(\pi x), \\
 F_3(x) &= \cos(\pi x), \\
 F_4(x) &= \sin(2\pi x), \\
 F_5(x) &= \cos(2\pi x).
 \end{aligned} \tag{5.6}$$

The performance of the proposed nonlinear control system for a 155 Hz tone is shown in Figure 5.7. The FXLMS ANC achieves 18.9 dB reduction of the SPL. However, because the human hearing system is more sensitive to higher frequencies, the harmonics caused by the nonlinearity are even heard as louder. After A-weighting the SPL reduction of the FXLMS system is only 11.0 dB. The nonlinear feed-forward control system provides 28.3 dB reduction of the SPL, and even 30.6 dB, when A-weighted.

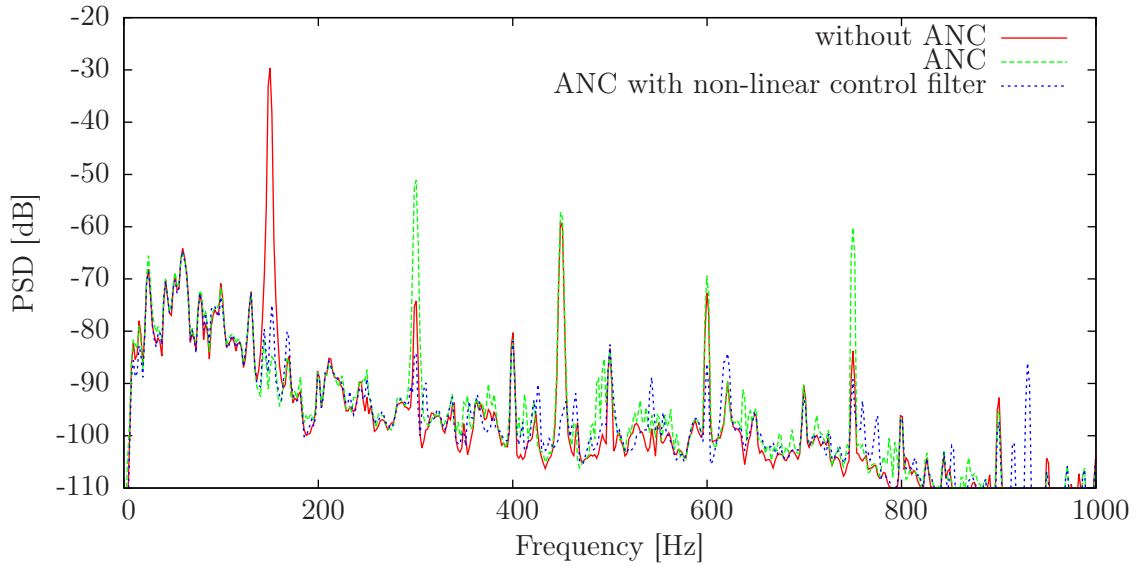


Figure 5.7: PSD of the error microphone signal for different control strategies for a 155 Hz tonal noise.

5.4 Computational complexity analysis

5.4.1 Nonlinear control

Table 5.1 shows asymptotic computational complexity of basic steps for the proposed algorithm and for the control system with separate per-actuator nonlinear filters, with the FXLMS and the FELMS adaptation algorithms. The order notion, O , is used. In case of per-actuator nonlinear filters with the FXLMS adaptation algorithm, each step has asymptotic computational complexity proportional to the number of channels multiplied by the number of nonlinear functions and the order of FIR filters. The FELMS adaptation algorithm reduces the computational complexity of the filtration by the secondary path model. In the proposed algorithm, there is only one nonlinear filter, and the computational complexity does not depend on the number of actuators. The computational complexity of added additional steps does not depend on the number of nonlinear functions, and the overall asymptotic computational complexity is reduced from $O(KCA)$ to $O(KA + CA)$, where $A = \max(N, M, N_V, N_K)$.

5.5 Summary

The two-layer control system structure presented in this chapter allows for reducing the number of control signals to be worked out by the ANC controller. This, in turn,

Table 5.1: Asymptotic computational complexity of presented algorithms.

Algorithm stage	NFXLMS	NFELMS	proposed algorithm
Nonlinear filter			
Output calculation	$O(KCN)$	$O(KCN)$	$O(KN)$
Reference/error filtration	$O(KCM)$	$O(CM)$	$O(M)$
Filter adaptation	$O(KCN)$	$O(KCN)$	$O(KN)$
Linear per-actuator filters			
Output calculation	-	-	$O(CN_V)$
Reference/error filtration	-	-	$O(CM_E)$
Filter adaptation	-	-	$O(CN_V)$

reduces complexity of the ANC system. It is especially important, when multiple reference signals, multiple error signals or multiple plates are used. The total number of adaptive filters is reduced from $N_P N_A N_X N_E$ to $N_P N_X N_E + 2N_P N_A$, when adaptive plate vibration controller is used, where N_A is the number of actuators signals per plate, N_P is the number of plates, N_X is the number of reference signals, and N_E is the number of error signals. Consequently, it reduces the computational load. This, however, comes with cost of an increased delay of the secondary path. This delay can decrease performance of the overall system for broadband disturbances, if the reference signal is not provided well in advance.

Additionally, the two-layer system can yield a faster convergence. The maximum LMS step coefficient in the higher-layer ANC controller for stable operation was higher than in case of the single-layer system. Obtained reduction of the number of ANC controller outputs reduces the number of ANC filters, and hence it reduces the number of adapted parameters. Equalization of the secondary path response also contributes to a faster adaptation of the ANC filters.

The two-layer structure can also be employed to reduce the computational complexity for adaptive feed-forward control with nonlinear filters. Instead of using a dedicated nonlinear filter for each actuators, single nonlinear filter in higher-level controller can be used.

The adaptive plate controller can also use plate vibration sensors, such as accelerometers, for adaptation (Mazur & Pawełczyk, 2012a). This eliminates the need

to place error microphones in the acoustic environment. The plate controller might also be used for reduction of nonlinear distortions (Mazur & Pawełczyk, 2011d,c).

Chapter 6

Temperature influence

6.1 Introduction

For potential applications of an ANC system its robust operation is required. The system must work properly for all possible environmental conditions. This is especially important for feedback systems and adaptive systems, where plant parameters changes can possibly destabilize the system.

One of important plate parameters is the temperature. The temperature of a plate depends on the ambient temperature, which in case of industrial environments, where ANC applications are targeted, may change in a wide range. The plate is additionally heated by the internal friction and heating of actuators. First reports on the influence of the temperature of the plate on the plate response and the performance of ANC systems were published in (Mazur & Pawełczyk, 2010a; Kochan, 2010), and later extended in (Mazur & Pawełczyk, 2011a).

6.2 Plate temperature control

To investigate the influence of the plate temperature, an additional control system was built. To be able to change the temperature in a wide range, both above and below the ambient temperature, six Peltier devices were mounted near plate edges (see Figure 6.1). Peltier devices allow for a very effective heating of the plate and a sufficient cooling.

Peltier device uses the Peltier effect to transfer heat between two sides (see Figure 6.2) (Heaton, 1963). The direction of the heat transfer can be changed by changing the direction of a current flow in the Peltier device. The amount of transferred heat

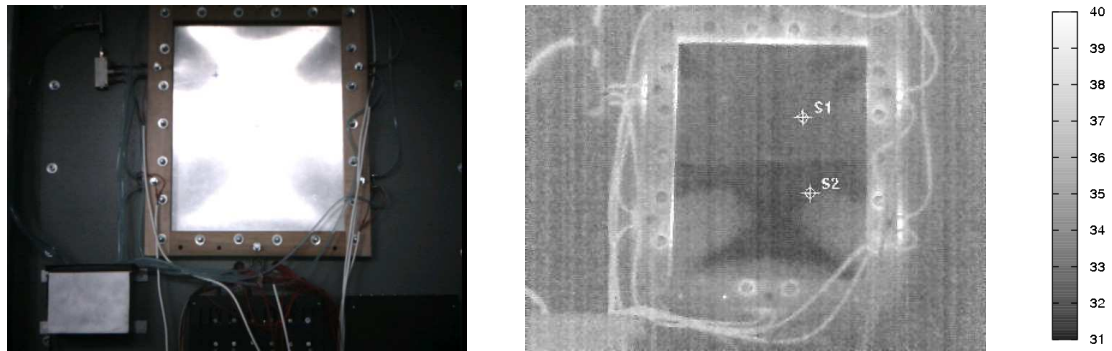


Figure 6.1: Plate at 32°C (left), and its infrared image converted to temperature estimation with position of temperature sensors (right).

by the Peltier effect is proportional to the electrical current. However, in real Peltier devices, two additional effects have also a significant influence on the heat transfer: the Joule heating and the thermal conductance. The Joule heating is proportional to the squared electrical current. This effect makes Peltier devices more effective in heating than in cooling. The second side-effect, the thermal conductance, is proportional to the temperature difference.

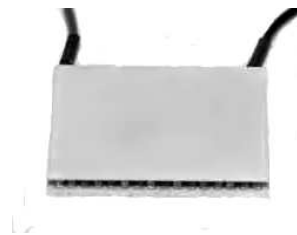


Figure 6.2: Peltier cell.

Because Peltier devices transfer the heat between two sides, one side of each Peltier device was connected to the plate. The temperature of the other side should be then stabilized. Otherwise, the temperature of the other side will change—will rise when the plate is cooled and drop when the plate is heated. The high difference of temperature will make the Peltier device ineffective, because the thermal conductance would be large. To avoid such problems the temperature of the second side was stabilized by a water circuit. The heat of the water was later exchanged with the air.

For controlling the temperature of the plate, its temperature was measured by two methods. First, a thermographic camera was used to visualize the temperature. For temperature measurement two LM35 (LM35, 2000) sensors were used. Positions of sensors were chosen based on infrared thermal images of the plate. An average of

two LM35 sensors was considered as the plate temperature (Figure 6.1).

The temperature of the plate was controlled by a single-channel PID controller. This control system was sufficient for good stabilization of the temperature and the results were later confirmed in (Kochan, 2010) with an improved three-channel PID temperature controller.

6.3 Temperature influence on the plate response

Figure 6.3 presents the amplitude response of secondary paths for different temperatures. It confirms that the response of any secondary path significantly depends on the plate temperature. The differences are even higher than 30 dB for some frequencies, mainly because of a plate bulge (Figure 6.1). However, fortunately the bulge improves the plate response for the 100 Hz to 200 Hz band, which was originally very poor and the sound power radiated was low.

6.4 Control algorithm

An adaptive multichannel FXLMS feed-forward control system described in Section 2.5 was used to investigate the temperature influence on the control system. The system consists of three MFC actuators mounted on the plate, one reference microphone and one error microphone.

6.4.1 FXLMS algorithm convergence

For the FXLMS algorithm without leakage to converge with probability one it suffices and it is necessary that the actual paths differ in phase from their models by less than $\pi/2$ for all frequencies, under some assumptions (Wang & Ren, 1999). One of the assumptions require that the reference signal is sufficiently exciting. To mitigate such requirement for deterministic noise the leakage factor less than one can be introduced (Elliott, 2001). It corresponds to introducing a trade-off to minimization of the instantaneous value of the squared error signal and suppressing excessive rise of control filter parameters. Therefore, the algorithm with leakage exhibits a potential to stabilize its operation even in case of larger phase errors between the paths and their models. This effect is found particularly useful for analysis of control system performance in case of plate temperature variation.

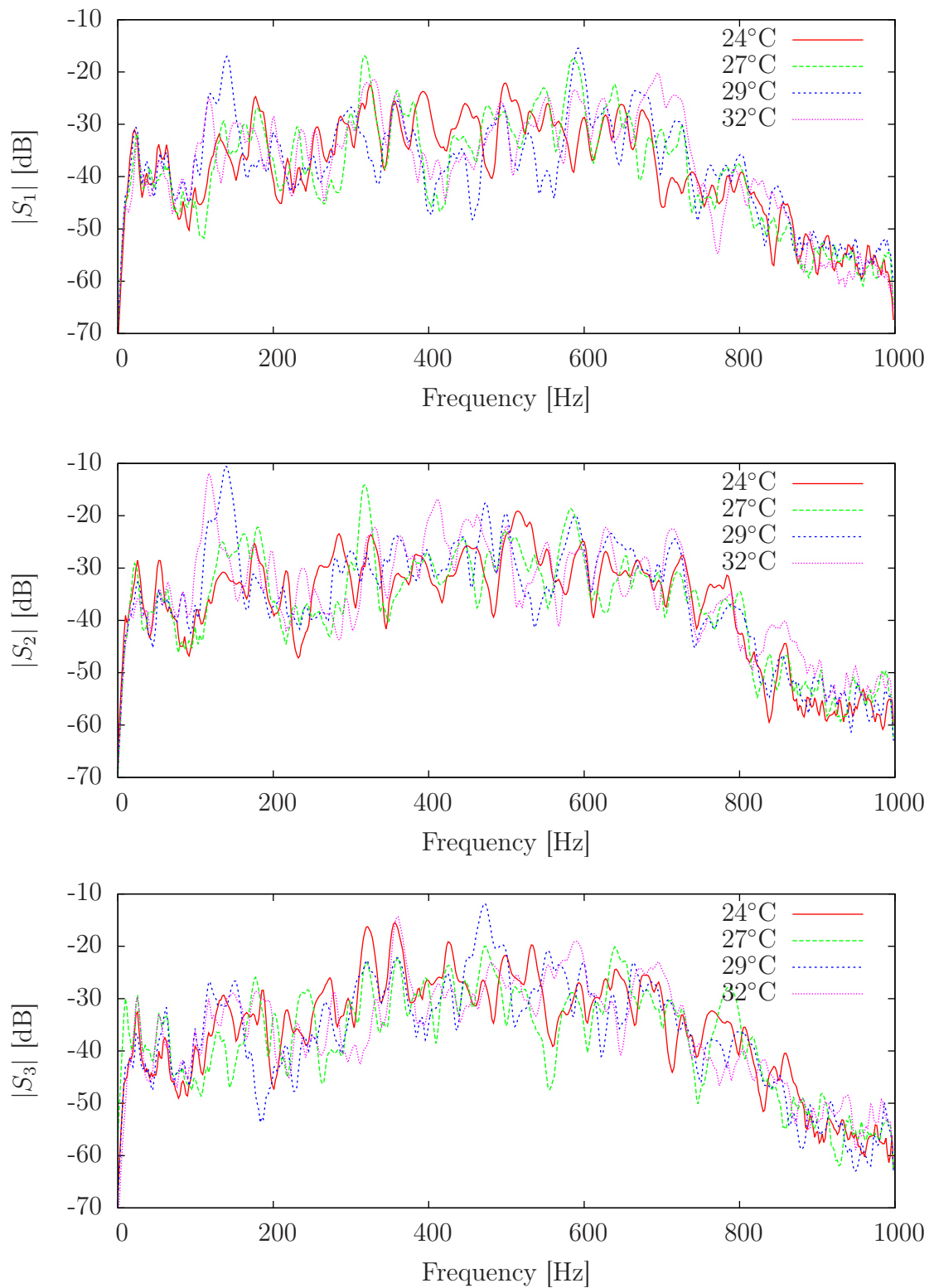


Figure 6.3: Amplitude frequency response of secondary paths for different temperatures.

There are also other ways to investigate convergence of the FXLMS algorithm, which include effect of the noise to be reduced (Larsson *et al.*, 2009a).

Figure 6.4 presents the plate amplitude response and phase response difference for different actuators, for two temperatures: 24°C and 28°C. This 4°C temperature change is sufficient to cause much higher differences in amplitude response than theoretically required for divergence of the Filtered-reference LMS algorithm without leakage. This conclusion was later confirmed experimentally.

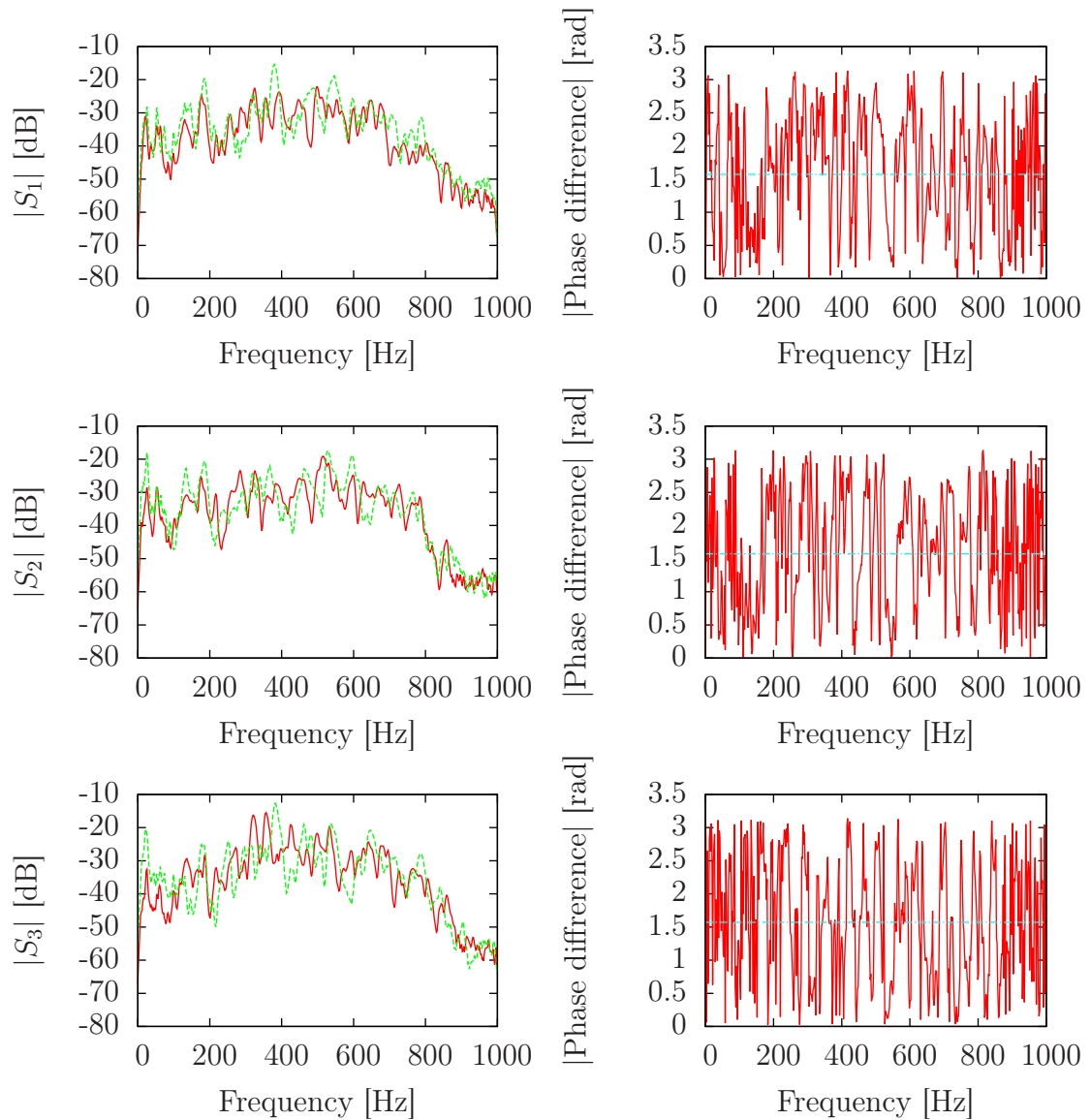


Figure 6.4: Amplitude frequency characteristics (left) of the secondary paths for 24°C (solid) and 28°C (dashed), and absolute phase difference (right; the horizontal line represents the phase error threshold at $\frac{\pi}{2}$).

6.5 Adaptation of secondary paths

Because differences in the phase response for different temperatures are higher than theoretically required to make the FXLMS algorithm divergent, an adaptation of secondary paths is needed. The need was also confirmed experimentally.

6.5.1 On-line secondary path identification

One of possible solutions to keep the FXLMS algorithm convergent is to use on-line secondary path identification widely discussed in case of ANC systems, where the expected quiet zone is moving (Michalczyk, 2008, 2010). Simultaneous identification of the secondary paths and adaptation of the control filter is, however, difficult and may cause stability problems. On the other hand, in most cases additional noise for identification must be generated, which deteriorates performance (Kuo & Morgan, 1996). There are also other methods such as the simultaneous equation method that could be used (Fujii *et al.*, 2010).

6.5.2 Temperature-based gain scheduling

Another possible method for adaptation of the secondary path, which is needed to keep the FXLMS algorithm convergent, is to use a simple gain scheduling approach (Mazur & Pawełczyk, 2011a). A set of models can be identified off-line for different plate temperatures and stored in a look-up table. Based on the temperature measurement as an indicator the appropriate triple S_1 – S_3 is chosen on-line (see Fig 6.5). Similarly, also other algorithm tuning parameters such as α , μ and ζ could be updated, if necessary. For instance, for typical well tested operating conditions the leak factor α and the step size μ can be increased to provide a faster adaptation.

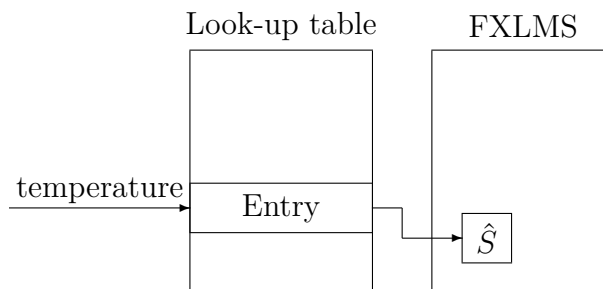


Figure 6.5: Gain scheduling scheme for secondary path model.

For a simple gain-scheduling with a lookup table indexed by the temperature, models of the secondary paths should be stored there as static functions of the temperature. The repeatability of the secondary path models for the same temperature was tested, by comparing identified models for the same temperature after colling and heating operations.

Figure 6.6 shows the differences of the secondary path responses for the same temperature 28°C. The first model was identified after heating the plate from the ambient temperature 24°C. The plate was later heated to 34°C and then cooled back to 28°C. Dynamical differences between those two secondary path responses are significant, although much smaller than differences between models for different temperatures.

The differences between models for the same temperature are still too high for some frequencies to guarantee convergence of the Filtered-reference LMS algorithm without leakage, but even a small leak set by $\alpha = 0.9999$ has sufficed for successful operation.

6.6 Experimental results

Three FXLMS ANC systems, discussed in the Chapter 2, were tested at temperature 28°C. Control systems used different secondary path models:

1. model identified for the ambient temperature of 24°C,
2. model identified after heating the plate to 28°C (this is the model that is used by gain-scheduling adaptation).
3. model identified just before the experiment (this model is close to the best possible model that can be used in the system with on-line secondary path adaptation).

After identification of the second model for temperature 28°C the plate was heated to 34°C, and then it was cooled to 28°C. Afterwards, the third model was identified.

6.6.1 Tonal noise reduction

The performance for tonal noise reduction was tested for individual tones of frequencies from 250 Hz to 500 Hz with 10 Hz steps. It has been found that a temperature

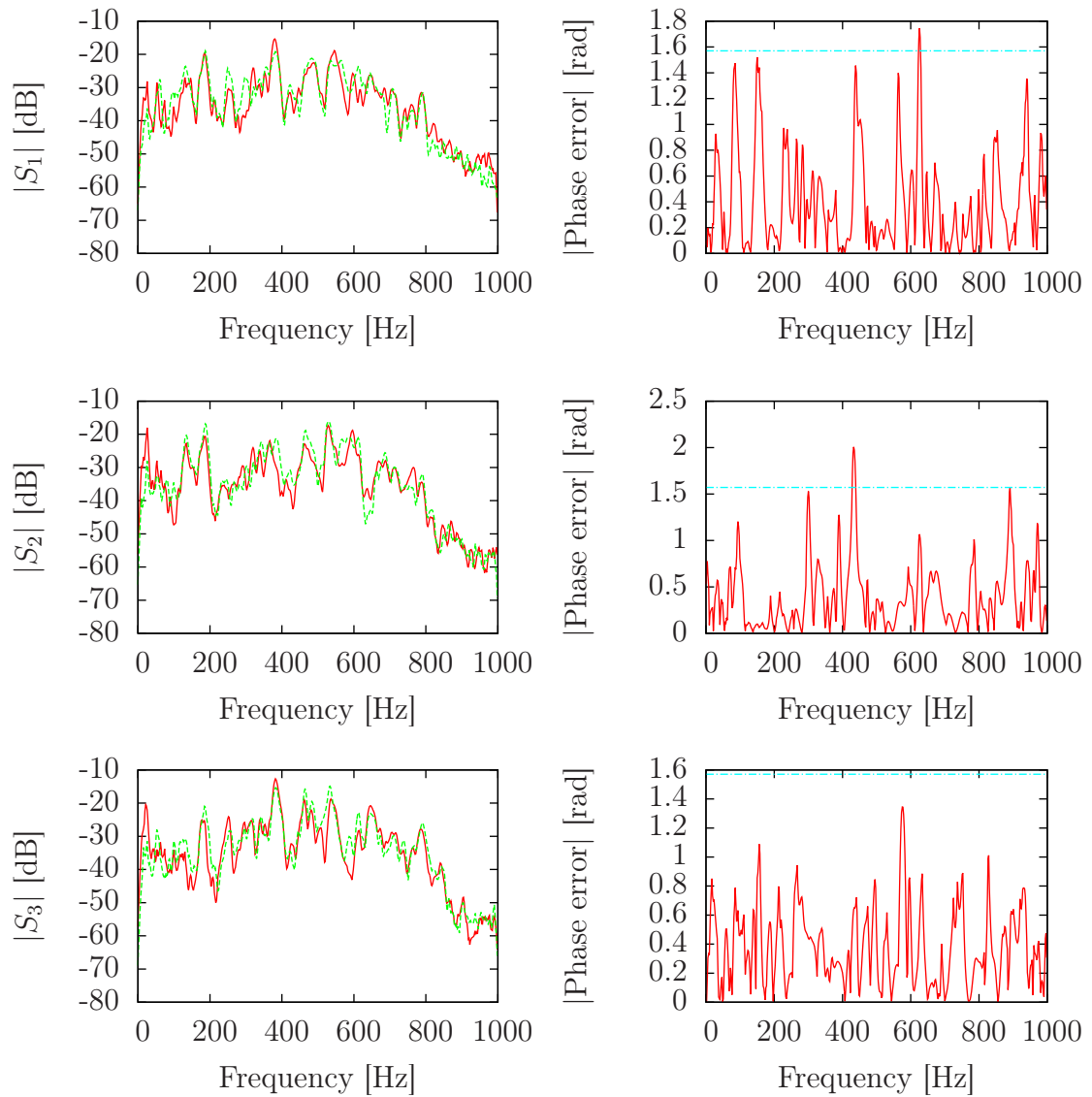


Figure 6.6: Amplitude frequency characteristics (left) of the secondary paths for 28°C after heating from 24°C (solid line) and for 28°C after cooling from 34°C (dashed line), and absolute phase difference (right; the horizontal line represents the phase error threshold at $\frac{\pi}{2}$).

change of 4°C suffices to cause stability problems for the Filtered-reference LMS algorithm without secondary path model adaptation, even with a leakage of $\alpha = 0.9999$ (Figure 6.7). The noise reduction level was limited mostly due to the leakage, resulting in a compromise between reduction of the mean square value of the error signal, and suppressing the filter gain. Without leakage, the noise reduction to the acoustic floor level has been achieved.

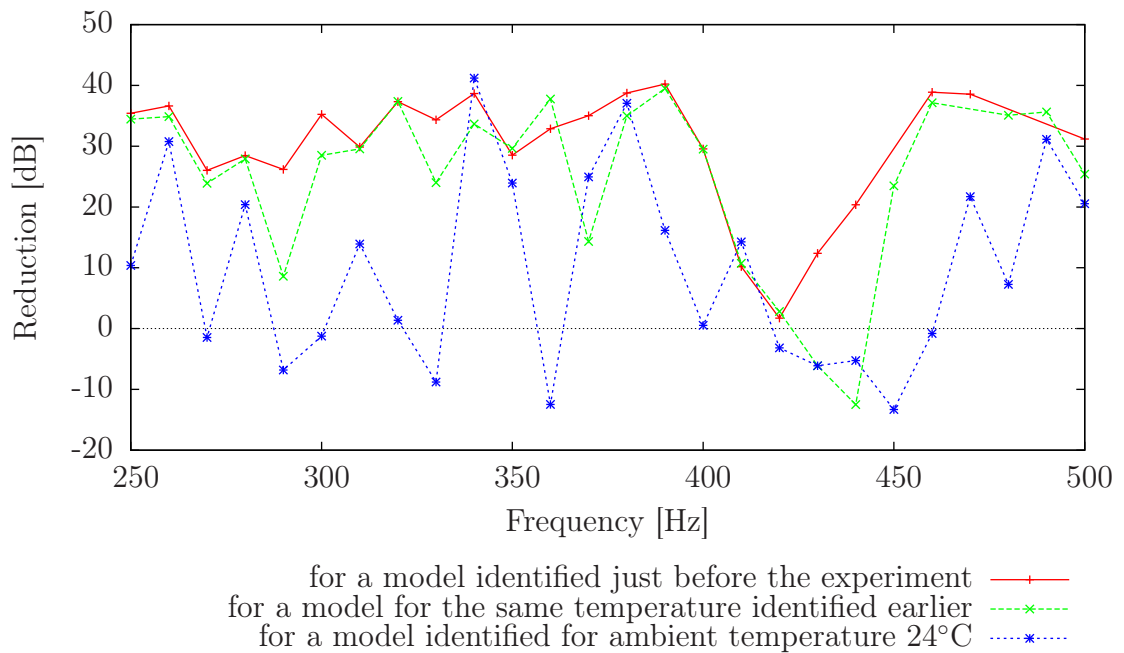


Figure 6.7: Results of tonal noise reduction for 28°C, $\alpha = 0.9999$, $\mu = 0.1$, $\zeta = 0.001$.

The system with gain-scheduling approach, except for 430 Hz and 440 Hz frequencies, provides stable operation. The lack of convergence for that frequencies can be theoretically explained. The phase difference for secondary path S_2 is higher than required (see 6.6). Also for those frequencies the gain of secondary paths is small, and the ANC system performance was limited by saturation of the control signal, even when appropriate model was used.

Figure 6.8 presents the PSD for a 300 Hz tone. Control system with a model for the ambient temperature of 24°C was unstable. The dominating tone was not reduced, and additional frequencies were generated. For models identified for 28°C temperature (both just before the experiment as well as after the heating and cooling), the primary noise was successfully reduced. Generation of harmonics of the 300 Hz frequency was caused by plate nonlinearity.

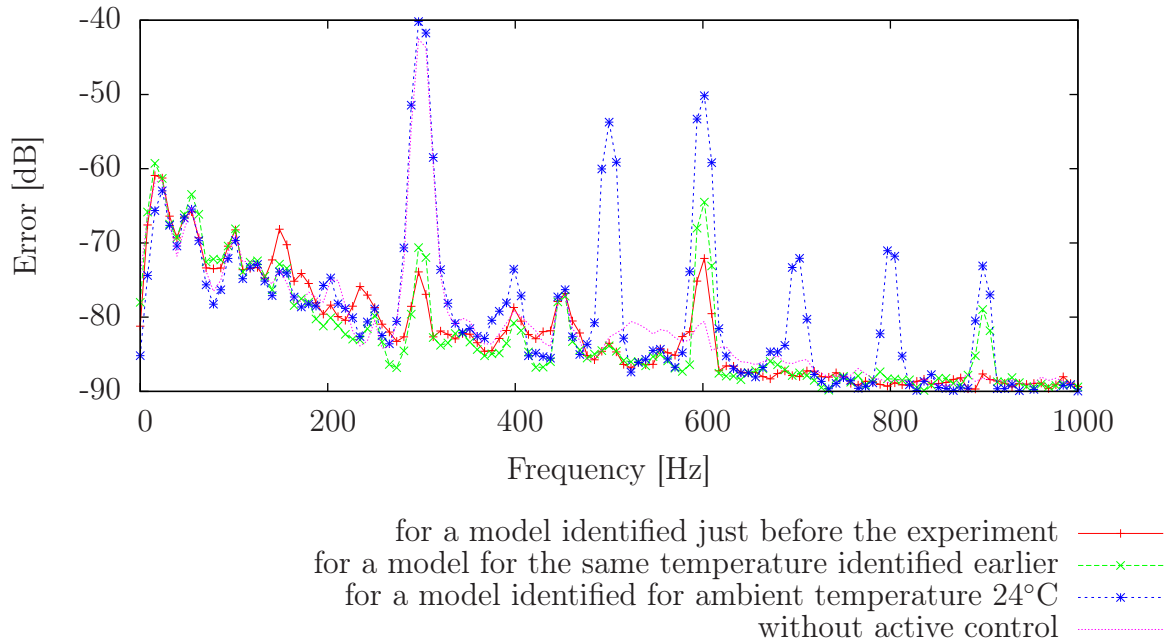


Figure 6.8: Power Spectrum Density for 300 Hz tonal noise for 28°C, $\alpha = 0.9999$, $\mu = 0.1$, $\zeta = 0.001$.

6.6.2 Coal mills noise reduction

The performance was also tested for a real-world noise recorded in the coal mills hall. This noise has a dominating tone of 330 Hz related to rotors, and a wideband component related to pulverizers (Figure 6.9).

For the system with the secondary path model for the ambient temperature of 24°C the leak factor of $\alpha = 0.9999$ has been required to provide reduction of the dominating tone.

For both $\alpha = 1.0$ and $\alpha = 0.9999$, exchanging secondary path models based on the temperature measurement has increased reduction of the dominating tone, but the wideband component has been reduced less. Noise reduction levels are shown in Table 6.1. For all cases, the control system without the secondary path model adaptation failed. That system was using the secondary path model identified before the experiment for the ambient temperature and the model was not appropriate for the temperature of 28°C. Results for the gain-scheduling system, which used the pre-identified model for 28°C, and the system that used the model identified just before experiments, are comparable, except wideband reduction for $\alpha = 1$, where results with the former model are worse.

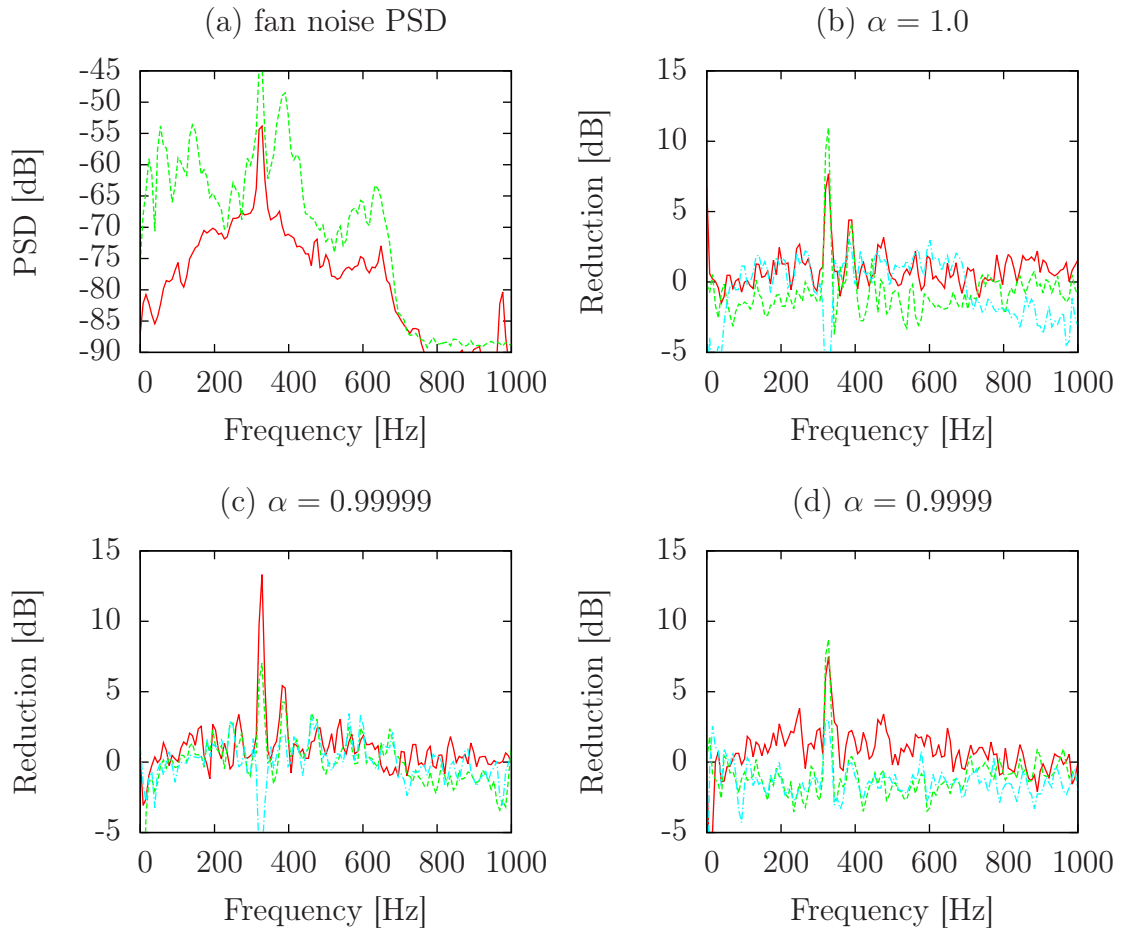


Figure 6.9: (a) — Power Spectral Density of the signal for the primary noise loudspeaker (solid) and the primary noise at error microphone (dashed); (b, c, d) — The results of coal mills hall noise reduction for 28°C for different values of parameter α for a model identified just before experiment (solid line), for the same temperature before heating and cooling (hashed line), for ambient temperature 24°C (dash-dotted).

6.7 Summary

For a typical fully clamped mounting of a vibrating plate, the secondary path response highly depends on the plate temperature. Differences higher than 30 dB for some frequencies in the amplitude response were observed. The plate temperature has been set with Peltier cells and it has been monitored with LM35 sensors.

The influence of plate temperature variation on the convergence and the performance of the feed-forward ANC system with the FXLMS algorithm has been tested. It has been shown that the some kind of adaptation of the secondary path is required for operation in different temperatures. Even the temperature change of 4°C may

Table 6.1: Noise reduction level for coal mills noise at 28°C

Model	$\alpha = \mathbf{0.9999}$	$\alpha = \mathbf{0.99999}$	$\alpha = \mathbf{1}$
Global noise reduction [dB]			
Model identified just before experiment	2.4	1.9	3.1
Pre-identified model for 28°C	1.9	3.1	1.2
Model for 24°C	-0.8	-2.7	-2.4
A-weighted global noise reduction [dB]			
Model identified just before experiment	2.6	2.3	3.7
Pre-identified model for 28°C	2.1	3.5	1.4
Model for 24°C	-1.0	-2.0	-2.2
310–340 Hz band noise reduction [dB]			
Model identified just before experiment	7.6	7.5	7.9
Pre-identified model for 28°C	7.5	6.8	7.5
Model for 24°C	-1.7	-6.6	-8.5

result in divergence of the FXLMS algorithm. The control system can be stabilized by using a leakage, but the needed leak is relatively large and the system performance is significantly reduced. Since the ambient temperature in typical industrial halls changes much more than 4°C, such system cannot be accepted.

It was found that the FXLMS algorithm with a simple gain-scheduling secondary path adaptation algorithm, which selects appropriate secondary path models based on the plate temperature, behaves satisfactorily.

So huge differences between secondary path responses for different temperatures can also lead to unexpected control signal saturation. The system might operate correctly at some temperature, but a temperature change results in the secondary path change, and the system might be not able to provide sufficient signal power required for effective control after that change.

Chapter 7

Summary

7.1 Conclusions

This dissertation is concerned with active control of sound with a vibrating plate. Although, it is focused on active noise control. The same algorithms can be used, when the desired sound is not silence, but a known input signal. As an example, control of sound radiation from a plate has been presented.

Firstly, the classic adaptive feed-forward algorithms were tested with various goals. The minimization of signals from error microphones or the VMC system, based on vibration sensors, provide better performance over a small area (zone of quiet) than the system minimizing plate vibrations.

It has been found that for a fully clamped plate, the plate temperature have a significant influence on the plate response. Changes in the plate response are sufficient for a divergence of the FXLMS algorithm. The secondary path adaptation is required for a stable operation of the system. A simplified gain-scheduling based secondary path adaptation has been proposed as a simpler alternative to commonly used on-line identification of the secondary path.

The performance of the feed-forward ANC system with linear control filters was much worse, than expected for simple tonal noise signals, due to harmonics generated by the plant nonlinearity. The ANC system performance can be improved by using IMC feedback control, but the best performance was obtained when nonlinear control filters in the feed-forward structure were employed. For more complex signals, i.e. stochastic signals or real-world wideband signals, the improvements were much smaller, because the performance was limited by other factors, e.g. causality problems.

A two-layer structure has been proposed to simplify the usage of vibrating plates in larger ANC systems. Each individual plate has a dedicated controller, which hides additional complexity, e.g. the existence of multiple actuators. It has been found that the two-layer ANC system structure has also advantages for a single plate, when the adaptive feed-forward control with nonlinear control filters is used. The combination of the single channel nonlinear active noise controller and the linear plate controller significantly reduces the computational complexity, because only one costly nonlinear control filter is used for a whole plate (not for each individual actuator). Such structure allows for application of more complex nonlinear ANC algorithms.

7.2 Author's contribution

The author believes that his contributions are the following:

- Developing the idea of using a leak in LMS-based algorithms for controlling distribution of power to multiple actuators.
- Application of the idea of Virtual Microphone Control to estimate acoustic pressure based on acceleration sensors.
- Application of the idea of Virtual Microphone Control for controlling sound radiation from a vibrating plate.
- Application of adaptive feed-forward control Active Noise Reduction structures for controlling sound radiation from a vibrating plate.
- Application of adaptive nonlinear feed-forward structures for controlling vibrating plates.
- Developing the idea of a two-layer Active Noise Control system, capable to shape frequency response of sound radiating plate, compensating for its nonlinearity and distributing power to multiple actuators.
- Investigating influence of plate temperature on Active Noise Control system, and proposing the idea of using gain-scheduling to compensate for the secondary path changes.

Appendix A

Definitions

A.1 Noise reduction level

A.1.1 Total noise reduction level

The total noise reduction level, J , is defined as:

$$J = P_{\text{off}} - P_{\text{on}}, \quad (\text{A.1})$$

where P_{off} and P_{on} are sound pressure levels, when the active control system is turned off and turned on, respectively.

The sound pressure level is estimated as:

$$P = 10 \log_{10} (\hat{\sigma}^2), \quad (\text{A.2})$$

where $\hat{\sigma}^2$ is a variance estimate of the sound pressure signal.

A.1.2 A-weighted total noise reduction level

The A-weighted total noise reduction level, J_A , is defined as:

$$J_A = P_{A,\text{off}} - P_{A,\text{on}}, \quad (\text{A.3})$$

where $P_{A,\text{off}}$ and $P_{A,\text{on}}$ are A-weighted noise levels, when the active control system is turned off and turned on, respectively.

The A-weighted sound pressure level P_A is estimated as:

$$\hat{P}_A = 10 \log_{10} \int_{\omega=0}^{\omega=\omega_N} A_w(j\omega) \hat{P}(j\omega) d\omega, \quad (\text{A.4})$$

where ω_N is the Nyquist pulsation, $\hat{P}(j\omega)$ is a PSD estimate of the signal, and $A_w(j\omega)$ is the A-weighting function defined as (Bao & Panahi, 2009)

$$A_w(j\omega) = 10^{1/10} R_A \left(\frac{1}{2\pi} \omega \right), \quad (\text{A.5})$$

where:

$$R_A(f) = \frac{12200^2 f^4}{(f^2 + 20.6^2) \sqrt{(f^2 + 107.7^2)(f^2 + 737.9^2)} (f^2 + 12200^2)}. \quad (\text{A.6})$$

A.1.3 Band limited noise reduction level

The band limited noise reduction level, J_B , is defined as:

$$J_B = P_{B,\text{off}} - P_{B,\text{on}}, \quad (\text{A.7})$$

where $P_{B,\text{off}}$ and $P_{B,\text{on}}$ are band limited noise levels, when the active control system is turned off and turned on, respectively.

The band limited sound pressure level P_B is estimated as:

$$\hat{P}_B = 10 \log_{10} \int_{\omega=\omega_1}^{\omega_1} \hat{P}(j\omega) d\omega, \quad (\text{A.8})$$

where ω_1 and ω_2 represent the lower and upper frequency band limit, respectively.

A.1.4 Total Harmonic Distortion

The THD_R(Total Harmonic Distortion) is defined for tonal signals as (Shmilovitz, 2005):

$$\text{THD}_R = \sqrt{\frac{\sum_{n=2}^{\infty} P_n}{\sum_{n=1}^{\infty} P_n}}, \quad (\text{A.9})$$

where P_n is the power of the n -th harmonic, assuming that the first harmonic ($n = 1$) is the fundamental frequency.

Bibliography

- [1] Athans, M. 1971. The Role and Use of the Stochastic Linear-Quadratic-Gaussian problem in Control System Design. *IEEE Transactions on Automatic Control*, **AC-16**(6), 529–552.
- [2] Bao, H., & Panahi, I. M. S. 2009. Using A-weighting for psychoacoustic active noise control. *Pages 5701–5704 of: Engineering in Medicine and Biology Society, 2009. EMBC 2009. Annual International Conference of the IEEE*.
- [3] Bauer, B. B., & Torick, E. L. 1996. Researches in Loudness Measurement. *IEEE Transactions on Audio and Electroacoustics*, **AV-14**(3).
- [4] Bismor, D. 1999. *Adaptive algorithms for active noise control in an acoustic duct*. Jacek Skalmierski Computer Studio, Gliwice.
- [5] Bismor, D. 2012. LMS Algorithm Step Size Adjustment for Fast Convergence. *Archives of Acoustics*, **37**(1), 31–40.
- [6] Brański, A., & Szela, S. 2008. Improvement of effectiveness in active triangular plate vibration reduction. *Archives of Acoustics*, **33**(4), 521–530.
- [7] Bullmore, A., Nelson, P., & Elliott, S. 1990. Theoretical studies of the active control of propeller-induced cabin noise. *Journal of Sound and Vibration*, **140**(2), 191–217.
- [8] Burgess, J. C. 1981. Active adaptive sound control in a duct: a computer simulation. *Journal of the Acoustical Society of America*, **70**(3), 715–726.
- [9] Carneal, J. P., Charette, F., & Fuller, C. R. 2004. Minimization of sound radiation from plates using adaptive tuned vibration absorbers. *Journal of Sound and Vibration*, **270**, 781–792.

- [10] Cieřlik, J., & Bochniak, W. 2010. Examination on the dependence of acoustic power radiation and the vibration energy flow in rectangular plates. *Pages 45–48 of: 57th Open Seminar on Acoustics 2010, Gliwice, September 20-24.*
- [11] Conover, W. B., & Ringlee, R. J. 1955. Recent contributions to transformer audible noise control. *AIEE Power Apparatus and Systems*, **74**(3), 77–90.
- [12] Das, D. P., & Panda, G. 2004. Active mitigation of nonlinear noise Processes using a novel filtered-s LMS algorithm. *IEEE Transactions on Speech and Audio Processing*, **12**(3), 313–322.
- [13] Elliott, S., Nelson, P., Stothers, I., & Boucher, C. 1990. In-flight experiments on the active control of propeller-induced cabin noise. *Journal of Sound and Vibration*, **140**(2), 219–238.
- [14] Elliott, S. E., Stothers, I. M., & Nelson, P. A. 1987. A Multiple Error LMS Algorithm and Its Application to the Active Control of Sound and Vibration. *IEEE Transactions on Acoustics, Speech and Signal Processing*, **ASSP-35**(10), 1423–1434.
- [15] Elliott, S. J. 2001. *Signal Processing for Active Control*. Academic Press, London.
- [16] Engel, Z. 1993. *Ochrona řrodowiska przed drganiem i hałasem (in Polish)*. PWN, Warszawa.
- [17] Engel, Z. 2010. From the History of the Noise Control Conference. *Archives of Acoustics*, **35**(2), 133–144.
- [18] Engel, Z., Makarewicz, G., Morzyński, L., & Zawieska, W. M. 2001. *Metody aktywne redukcji hałasu (in Polish)*. CIOP.
- [19] Fahy, F., & Gardonio, P. 2007. *Sound and Structural Vibration*. Second edition edn. Elsevier, Oxford.
- [20] Fujii, K., Kashihara, K., Muneyasu, M., & Morimoto, M. 2010. Study on application of cascade connection of recursive and non-recursive filters to noise control filter. *In: Proceedings of 17th International Congress of Sound and Vibration, Cairo.*
- [21] Gardonio, P., Bianchi, E., & Elliott, S. J. 2004. Smart panel with multiple decentralized units for the control of sound transmission. Part I: theoretical predictions. *Journal of Sound and Vibration*, **274**, 163–192.

- [22] George, N. V., & Panda, G. 2012. A robust filtered-s LMS algorithm for nonlinear active noise control. *Applied Acoustics*, **73**, 836–841.
- [23] George, N. V., & Panda, G. 2013. Advances in active noise control: A survey, with emphasis on recent nonlinear techniques. *Signal Processing*, **93**, 363–377.
- [24] Gil, A., Segura, J., & Temme, N. M. 2007. *Numerical Methods for Special Functions*. 1 edn. Philadelphia, PA, USA: Society for Industrial and Applied Mathematics.
- [25] Górski, P., & Kozupa, M. 2012. Variable Sound Insulation Structure with MFC Elements. *Archives of Acoustics*, **37**(1), 115–120.
- [26] Górski, P., & Morzyński, L. 2013. Active Noise Reduction Algorithm Based on NOTCH Filter and Genetic Algorithm. *Archives of Acoustics*, **38**(2), 185–190.
- [27] Halliday, D., Resnick, R., & Walker, J. 2010. *Fundamentals of Physics Extended*. John Wiley & Sons.
- [28] Hansen, C. H., & Snyder, S. D. 1997. *Active Control of Noise and Vibration*. E & FN Spon, London.
- [29] Haykin, S. S. 1994. *Neural networks: a comprehensive foundation*. Macmillan.
- [30] Heaton, A. G. 1963. Thermoelectrical cooling: Material characteristics and applications. *Proceedings of the Institution of Electrical Engineers.*, **110**(7), 1277–1287.
- [31] Hünecke, K. 1997. *Jet Engines: Fundamentals of Theory, Design, and Operation*. Motorbooks International.
- [32] Kadiri, M. El, Benamar, R., & White, R. G. 1999. The non-linear free vibration of fully clamped rectangular plates: second non-linear mode for various plate aspect ratios. *Journal of Sound and Vibration*, **228**(2), 333–358.
- [33] Kochan, A. 2010. *Badanie wpływu temperatury na własności układu aktywnego tłumienia hałasu z drgającą płytą (in Polish)*. M.Sc. thesis, Silesian University of Technology, Gliwice, Poland.
- [34] Konieczny, J., & Kowal, J. 2005. A pole placement controller for active vehicle suspension. *Archives of Control Sciences*, **15**(1), 97–116.

- [35] Kowal, J. 1990. *Aktywne i semiaktywne metody wibroizolacji układów mechanicznych (in Polish)*. AGH, Kraków.
- [36] Kowal, J., & Kot, A. 2007. Active vibration reduction system with energy regeneration. *Archives of Control Sciences*, **17**(3), 343–352.
- [37] Kowal, J., Pluta, J., Konieczny, J., & Kot, A. 2008. Energy recovering in active vibration isolation system—results of experimental research. *Journal of Vibration and Control*, **14**(7), 1075–1088.
- [38] Kuo, S. M., & Morgan, D. R. 1996. *Active Noise Control Systems: Algorithms and DSP Implementations*. Wiley, New York.
- [39] Kurczyk, S., & Pawełczyk, M. 2013. Active Noise Control Using a Fuzzy Inference System Without Secondary Path Modeling. *In: XVI International Conference on Noise Control NOISE CONTROL 2013, CD*.
- [40] Larsson, M., Johansson, S., Claesson, I., & Håkansson. 2009a. A Module Based Active Noise Control System for Ventilation Systems, Part I: Influence of Measurement Noise on the Performance and Convergence of the Filtered-x LMS Algorithm. *International Journal of Acoustics and Vibration*, **14**(4), 188–195.
- [41] Larsson, M., Johansson, S., Claesson, I., & Håkansson, L. 2009b. A Module Based Active Noise Control System for Ventilation Systems, Part II: Performance Evaluation. *International Journal of Acoustics and Vibration*, **14**(4), 196–206.
- [42] Latos, M. 2011. *Active noise reducing earplug with speech signal processing*. Ph.D. thesis, Silesian University of Technology, Gliwice, Poland.
- [43] Latos, M., & Pawełczyk, M. 2009. Feedforward vs. feedback fixed-parameter H2 control of non-stationary noise. *Archives of Acoustics*, **34**(4), 407–421.
- [44] Leniowska, L. 2005. Effect of plate vibration control by the use of piezoelectric actuators on its sound radiation attenuation. *Molecular and Quantum Acoustics*, **26**, 191–204.
- [45] Leniowska, L. 2006. Effect of active vibration control of a circular plate on sound radiation. *Archives of Acoustics*, **31**(1), 77–87.
- [46] Leniowska, L. 2011. An Adaptive Vibration Control Procedure Based on Symbolic Solution of Diophantine Equation. *Archives of Acoustics*, **36**(4), 901–912.

- [47] Leniowska, L., & Kos, P. 2009. Self-tuning control with regularized RLS algorithm for vibration cancellation of a circular plate. *Archives of Acoustics*, **34**(4), 613–624.
- [48] Liao, H., & Sethares, W. A. 1995. Suboptimal Identification of Nonlinear ARMA Models Using an Orthogonality Approach. *IEEE Transactions on Circuits and Systems—I Fundamental Theory and Applications*, **42**(1), 14–22.
- [49] Liu, C., Li, F., Fang, B., Zhao, Y., & Huang, W. 2010. Active control of power flow transmission in finite connected plate. *Journal of Sound and Vibration*, **329**, 4124–4135.
- [50] Lizhong, X., & Zhentong, W. 2009. Electromechanical Dynamics For Microplate. *International Journal of Acoustics and Vibration*, **14**(4), 12–23.
- [51] LM35. 2000. *LM35 Precision Centigrade Temperature Sensors*. National Semiconductors, <http://www.national.com/ds/LM/LM35.pdf>. Retrived October 14th, 2010.
- [52] Lueg, P. 1936. *Process of silencing sound oscillations*. U.S. Patent, No 2,043,416.
- [53] Makarewicz, G. 1993. *Problemy stabilności w układach aktywnej redukcji dźwięku (in Polish)*. Ph.D. thesis, AGH, Kraków, Poland.
- [54] Mao, Q., & Pietrzko, S. J. 2005. Control of sound transmission through double wall partitions using optimally tuned Helmholtz resonators. *Acta Acustica united with Acustica*, **95**, 723–731.
- [55] Material, Smart. 2010. *MFC*. <http://www.smart-material.com/Smart-choice.php?from=MFC>. Retrieved October 14th, 2010.
- [56] Mazur, K., & Pawełczyk, M. 2010a. Active structural acoustic control using the Filtered-Reference LMS algorithm with compensation of vibrating plate temperature variation. *In: XV International Conference on Noise Control „Noise Control 2010”, Książ, 6–9 June, CD-ROM*.
- [57] Mazur, K., & Pawełczyk, M. 2010b. Adaptive active noise control of sound transmitted through a plate with insufficient acoustic isolation. *In: 57th Open Seminar on Acoustics OSA 2010, 20-24 Sept., Gliwice*.

- [58] Mazur, K., & Pawełczyk, M. 2011a. Active noise-vibration control using the filtered-reference LMS algorithm with compensation of vibrating plate temperature variation. *Archives of Acoustics*, **36**(1), 65–76.
- [59] Mazur, K., & Pawełczyk, M. 2011b. Adaptive equalization of sound radiation from a plate using acceleration sensors. *Pages 49–56 of: Polish-German Structured Conference on Acoustics, Jurata, Poland 13-16.09.2011.*, vol. 2.
- [60] Mazur, K., & Pawełczyk, M. 2011c. Feed-forward compensation for nonlinearity of vibrating plate. *In: 10th Conference on Active Noise and Vibration Control Methods MARDiH, June 6–8.*
- [61] Mazur, K., & Pawełczyk, M. 2011d. Feed-forward compensation for nonlinearity of vibrating plate as the sound source for Active Noise Control. *Mechanics and Control*, **30**(3), 146–150.
- [62] Mazur, K., & Pawełczyk, M. 2011e. Feed-forward equalization of sound radiation from a vibrating plate. *In: 10th Conference on Active Noise and Vibration Control Methods MARDiH, June 6–8.*
- [63] Mazur, K., & Pawełczyk, M. 2012a. Aktywna Redukcja Hałasu przechodzącego przez płytę drgającą z mikrofonem wirtualnym (in Polish). *Pages 185–191 of: Materiały XL Zimowej Szkoły Zwalczania Zagrożeń Wibroakustycznych, Gliwice-Szczyrk, 27 Feb. to 2 Mar.*
- [64] Mazur, K., & Pawełczyk, M. 2012b. Feed-forward equalization of sound radiation from a vibrating plate. *Mechanics and Control*, **31**(1), 35–39.
- [65] Mazur, K., & Pawełczyk, M. 2012c. Nonlinear Active Noise Control of sound transmitted through a plate. *Pages 159–162 of: 59th Open Seminar on Acoustics joint with Workshop on Strategic Management of Noise including Aircraft Noise.*
- [66] Mazur, K., & Pawełczyk, M. 2013a. Active Noise Control with a single nonlinear control filter for a vibrating plate with multiple actuators. *Archives of Acoustics*, **38**(4).
- [67] Mazur, K., & Pawełczyk, M. 2013b. Active Noise Control with a single nonlinear control filter for a vibrating plate with multiple actuators. *In: XVI International Conference on Noise Control NOISE CONTROL 2013, CD.*

- [68] Mazur, K., & Pawełczyk, M. 2013c. Hammerstein nonlinear active noise control with the Filtered-Error LMS algorithm. *Archives of Acoustics*, **38**(2), 197–203.
- [69] MEAS. 2008. *Piezo Film Sensors Technical Manual*. Measurement Specialties, Inc.
- [70] Michalczyk, M. I. 2004. *Adaptive control algorithms for three-dimensional zones of quiet*. Skalmierski Computer Studio, Gliwice.
- [71] Michalczyk, M. I. 2008. Active Noise Control with Moving Error Microphone. *Mechanics*, **27**(3), 113–119.
- [72] Michalczyk, M. I. 2010. Active Noise Control systems with time varying sound sensor position. *Pages 59–62 of: Proc. 10th IFAC Workshop on Programmable Devices and Embedded Systems, Pszczyna, Poland*.
- [73] Michalczyk, M. I., & Wieczorek, M. 2011. Parameterization of adaptive control algorithms for multi-channel active noise control system. *Pages 73–78 of: 58th Open Seminar on Acoustics joint with 2nd Polish-German Structured Conference on Acoustics. OSA '11, Gdańsk - Jurata*, vol. 2. Polskie Towarzystwo Akustyczne. Oddział Gdański.
- [74] Morgan, D. R. 1980. An analysis of multiple correlation cancellation loops with a filter in the auxiliary path. *IEEE Transactions on Acoustics Speech, and Signal Processing*, **28**(4), 454–467.
- [75] Nelson, P. A., & Elliott, S. J. 1993. *Active Control of Sound*. Academic Press, Cambridge.
- [76] Niederliński, A., Mościński, J., & Ogonowski, Z. 1995. *Regulacja adaptacyjna (in Polish)*. PWN, Warszawa.
- [77] Northern, J. L., & Downs, M. P. 2002. *Hearing in Children*. Lippincott Williams & Wilkins.
- [78] Olson, H. F., & May, E. G. 1953. Electronic sound absorber. *Journal of the Acoustical society of America*, **25**, 1130–1136.
- [79] Pawełczyk, M. 2004. Adaptive noise control algorithms for active headrest system. *Control Engineering Practice*, **12**, 1101–1112.

- [80] Pawełczyk, M. 2005. *Feedback Control of Acoustic Noise at Desired Locations*. Silesian University of Technology, Gliwice.
- [81] Pawełczyk, M. 2008. Active noise control — a review of control-related problems. *Archives of Acoustics*, **33**(4), 509–520.
- [82] Pawełczyk, M. 2012. Active noise control in large industrial halls. *In: Proc. IASTED Asian Conference Modelling, Identification, and Control — AsiaMIC, 2–4 April, Phuket, Thailand*.
- [83] Pawełczyk, M. 2013. *Application-Oriented Design of Active Noise Control Systems*. Academic Publishing House EXIT, Warsaw.
- [84] Pawełczyk, M., & Watras, P. 2011. Enlarging and spatially equalizing a zone of quiet by using active control of sound at virtual microphones. *In: inter-noise 2011, Osaka Japan, September CD Proceedings*.
- [85] Pawełczyk, M., Michalczyk, M. I., Czyż, K., Latos, M., & Mazur, K. 2011a. An Efficient Communication System for Noisy Environments. *In: 2011 International Conference on Modelling, Identification and Control, June 26–29 2011, Shanghai, China*.
- [86] Pawełczyk, M., Michalczyk, M. I., Czyż, K., Latos, M., & Mazur, K. 2011b. Integrating noise control, speech enhancement and wireless communication in an active earplug. *In: 18th International Congress on Sound & Vibration, ICSV 18 Rio de Janeiro, July 10–14 2011*.
- [87] Pawełczyk, M., Michalczyk, M. I., Czyż, K., Latos, M., & Mazur, K. 2011c. Signal processing in an active noise reducing earplug with improved communication features. *In: 10th Conference on Active Noise and Vibration Control Methods MARDiH 2011, June 6–8 2011*.
- [88] Petitjean, B., & Legrain, I. 1996. Feedback controllers for active vibration suppression. *Journal of Structural Control*, **3**(1-2), 111–127.
- [89] Pietrzko, S. J. 2009. *Contributions to Noise and Vibration Control Technology*. AGH—University of Science and Technology Press, Kraków.
- [90] Rdzanek, W. P. 2000. *Promieniowanie dźwięku przez drgającą płaską płytę pierścieniową (in Polish)*. Ph.D. thesis, AGH, Kraków, Poland.

- [91] Rdzanek, W. P., & Zawieska, W. M. 2003. Vibroacoustic analysis of a simply supported rectangular plate of a power transformer casing. *Archives of Acoustics*, **28**(2), 117–125.
- [92] Rdzanek, W. P., Szemela, K., & Pieczonka, D. 2011. Acoustic Pressure Radiated by a Circular Membrane Into the Quarter-Space. *Archives of Acoustics*, **36**(1), 121–139.
- [93] Ringwelski, S., Luft, T., & Gabbert, U. 2011a. Computational design and experimental testing of a smart car engine for active noise reduction. *Pages 435–444 of: Polish-German Structured Conference on Acoustics, Jurata, Poland 13-16.09.2011.*, vol. 2.
- [94] Ringwelski, S., Luft, T., & Gabbert, U. 2011b. Piezoelectric controlled noise attenuation of engineering systems. *Journal of theoretical and applied mechanics*, **49**(3), 859–878.
- [95] Saha, K. N., Misra, D., Ghosal, S., & Pohit, G. 2005. Nonlinear free vibration analysis of square plates with various boundary conditions. *Journal of Sound and Vibration*, **287**, 1031–1044.
- [96] Schetzen, M. 1980. *The Volterra and Wiener theories of nonlinear systems*. Wiley, New York.
- [97] Shmilovitz, D. 2005. On the definition of total harmonic distortion and its effect on measurement interpretation. *IEEE Transactions on Power Delivery*, **20**(1), 526–528.
- [98] Sicuranza, G. L., & Carini, A. 2011. A generalized FLANN filter for nonlinear active noise control. *IEEE Transactions on Audio, Speech, and Language Processing*, **19**(8), 2412–2417.
- [99] Snyder, S. D., & Tanaka, N. 1995. Active control of vibration using a neural network. *IEEE Transactions on Neural Networks*, **6**(4), 819–828.
- [100] Staniek, J., & Pawełczyk, M. 2008. Zastosowanie elementów MFC do aktywnej redukcji hałasu (In Polish). *Pages 131–139 of: Proc. XXXVI Winter Workshop on Active Noise and Vibration Control Wisła, Poland.*

- [101] Stuebner, M., Smith, R. C., Hays, M., & Oates, W. S. 2009. Modeling the nonlinear behavior of Macro Fiber Composite actuators. *Behavior and Mechanics of Multifunctional Materials and Composites 2009, Proceedings of the SPIE*, **7289**, 728913–728918.
- [102] Tadeu, A. J. B., & Mateus, D. M. R. 2001. Sound transmission through single, double and triple glazing. Experimental evaluation. *Applied Acoustics*, **62**, 307–325.
- [103] Talbot-Smith, M. 2001. *Audio Engineer's Reference Book*. Taylor & Francis.
- [104] Tan, L., & Jiang, J. 2001. Adaptive Volterra filters for active control of nonlinear noise processes. *IEEE Transactions on Signal Processing*, **49**(8), 1667–1676.
- [105] Tan, L. Z., & Jiang, J. 1997. Filtered-X second-order Volterra adaptive algorithms. *Electronics Letters*, **33**(8), 671–672.
- [106] Tanaka, N. 2009. Cluster Control of Distributed-Parameter Structures. *International Journal of Acoustics and Vibration*, **14**(1), 24–34.
- [107] Tawfik, M., & Baz, A. 2004. Experimental and Spectral Finite Element Study of Plates with Shunted Piezoelectric Patches. *International Journal of Acoustics and Vibration*, **9**(2), 87–97.
- [108] Thompson, E. 1995. Machines, Music, and the Quest for Fidelity: Marketing the Edison Phonograph in America, 1877-1925. *The Musical Quarterly*, **79**(1), 131–171.
- [109] Tu, Y., & Fuller, C. R. 2000. Multiple reference feedforward Active Noise Control part II: reference preprocessing and experimental results. *Journal of Sound and Vibration*, **233**(5), 761–774.
- [110] Wang, A. Kuo, & Ren, W. 1999. Convergence Analysis of the filtered-U Algorithm for Active Noise Control. *Signal Process.*, **73**(3), 255–266.
- [111] Watras, P., & Pawełczyk, M. 2011a. Active noise control based on potential and kinetic acoustic energy estimates. In: *Proc. Active Noise and Vibration Control Methods MARDiH, Wojanów, Poland*.
- [112] Watras, P., & Pawełczyk, M. 2011b. Feedforward adaptive active noise control system with time-varying of zones of quiet. In: *Polish-German Structured Conference on Acoustics, Jurata, Poland 13–16.09.2011*.

- [113] Weyna., S. 2010. Acoustic Intensity Imaging Methods for in-situ Wave Propagation. *Archives of Acoustics*, **35**(2), 265–273.
- [114] Weyna., S., Mickiewicz, W., Pyła, M., & Jabłoński, M. 2013. Experimental Acoustic Flow Analysis Inside a Section of an Acoustic Waveguide. *Archives of Acoustics*, **38**(2), 211–216.
- [115] Wiciak, J. 2008. Sound radiation by set of L-jointed plates with four pairs of piezoelectric elements. *The European Physical Journal Special Topics*, **154**(1), 229–233.
- [116] Wiciak, J., Borkowski, B., & Czopek, D. 2013. A System for Determination of Areas Hazardous for Blind People Using Wave-vibration Markers — Final Conclusions and Technical Application. *ACTA PHYSICA POLONICA A*, **123**(6), 1101–1105.
- [117] Widrow, B., & Stearns, S. D. 1985. *Adaptive Signal Processing*. Prentice-Hall, Englewood Cliffs, NJ.
- [118] Wrona, S., & Pawełczyk, M. 2013a. Controllability-oriented placement of actuators for active noise-vibration control of rectangular plates using a memetic algorithm. *Archives of Acoustics*, **38**(4).
- [119] Wrona, S., & Pawełczyk, M. 2013b. Observability-oriented placement of sensors for active noise-vibration control of flexible structures using a memetic algorithm. *In: Proc. Active Noise and Vibration Control Methods MARDiH, Kraków-Rytro, Poland*.
- [120] Zawieska, W. M. 1991. *Analiza i synteza układu aktywnej redukcji hałasu w falowodzie*. Ph.D. thesis, AGH, Kraków, Poland.
- [121] Zawieska, W. M., & Rdzanek, W. P. 2007. The influence of a vibrating rectangular piston on the acoustic power radiated by a rectangular plate. *Archives of Acoustics*, **32**(2), 405–415.
- [122] Zawieska, W. M., Rdzanek, W. P., Rdzanek, W. J., & Engel, Z. 2007. Low frequency estimation for the sound radiation efficiency of some simply supported flat plates. *Acta Acustica United with Acustica*, **93**(3), 353–363.

Glossary

t	continuous-time variable
i	discrete-time variable
l, j, m, n	index, integer number
z^{-1}	inverse of Z-transform variable, backward time-shift operator
α	leakage coefficient in the LMS algorithm
μ	step size of the LMS algorithm
ζ	denominator bias for Normalized LMS
$d(i)$	disturbance signal
$e(i)$	error signal
$r(i)$	filtered-reference signal
$u(i)$	control signal
$x(i)$	reference signal, filter input signal
$y(i)$	general output signal
C	number of control signals
D	delay in desired path model
H	desired response of secondary path
K	additional filter in the VMC system
L	number of error signals
M	number of plant model parameters
N	number of control filter coefficients
N_V	number of V filter parameters
N_K	number of K filter parameters
P	primary path
S	secondary path
\hat{S}	model of the secondary path
W	ANC control filter
V	plate control filter

ASAC	Active Structural Acoustic Control
ADC	Analog-to-Digital Converter
ANC	Active Noise Control
ANN	Artificial Neural Network
ANVC	Active Noise/Vibration Control
AVC	Active Vibration Control
DAC	Digital-to-Analog converter
FELMS	Filtered-Error LMS
FIR	Finite Impulse Response
FLANN	Functional Link Artificial Neural Network
FSLMS	Filtered-s LMS
FXLMS	Filtered-Reference LMS (Filtered-x LMS)
IIR	Infinite Impulse Response
IMC	Internal Model Control
LMS	Least Mean Squares
MFC	Macro Fiber Composite
MIMO	Multi-Input Multi-Output
PSD	Power Spectral Density
RLS	Recursive Least Squares
SISO	Single-Input Single-Output
SPL	Sound Pressure Level
VMC	Virtual Microphone Control

Other symbols or acronyms used in this dissertation have only a local character.

Index

- acoustic feedback, 18
- Active Noise Control, 7
- active noise control, 3, 4
- active noise-vibration control, 4
- Active Noise/Vibration Control, 7
- active structural acoustic control, 4
- Active Vibration Control, 7
- ADC, 23
- ADC conversion, 24
- ANC, 3, 7
- ANN, 59, 62
- anti-aliasing filter, 23
- ANVC, 7
- artificial neural network, 59
- artificial neural networks, 62
- ASAC, 4
- AVC, 7, 35

- control filter, 16
- control signal, 8
- convergence coefficient, 17

- DAC, 23
- Diophantine equation, 12

- error signal, 8, 16, 29

- feedback path, 18
- filtered-reference, 16
- Filtered-reference Least Mean Squares, 3
- FLANN, 62

- FSLMS, 62
- functional expansion, 62
- FXLMS, 16
- FXLMS convergence, 88

- gain scheduling, 91

- Hammerstein model, 61
- heat transfer, 86
- Heating, Ventilation and Air Conditioning, 3
- HVAC, 3

- IMC, 57
- Internal Model Control, 10
- internal model control, 57

- Joule heating, 87

- leakage coefficient, 18
- Leaky LMS, 17
- Linear-Quadratic-Gaussian, 9
- LQG, 9

- MFC, 6
- MIMO, 10
- Minimal Variance Control, 12
- multiple actuators, 19
- multiple errors, 27
- Multiple-Input Multiple-Output, 10

- NARMA, 58
- NLMS, 17

- nonlinear FIR, 60
- Normalized LMS, 17
- Peltier device, 86
- Peltier effect, 86
- phon, 1
- plate temperature, 86
- Pole Placement, 12
- Pole-Zero Placement, 12
- polynomial, 65
- primary noise, 8
- primary path, 8

- reconstruction filter, 24
- reference microphone, 8
- reference signal, 16

- secondary path, 8
- secondary path adaptation, 91
- Single-Input Single-Output, 10
- SISO, 10
- smart panels, 10
- sound generation, 69
- Sound Pressure Level, 1
- sound radiation, 40
- SPL, 1

- temperature control, 86
- thermal conductance, 87
- total noise reduction, 100

- Variable Step LMS, 17
- virtual microphone, 32
- Virtual Microphone Control, 14
- VMC, 14, 32
- Volterra FXLMS, 62
- Volterra series, 62

- VS-LMS, 17
- zone of quiet, 34